

# **D R A F T**

**Texas Commission on Environmental Quality  
PGA No. 582-8-862-45-FY09-04  
Tracking No. 2008-81  
with  
Supplemental Support from the  
Air Quality Research Program  
TCEQ Grant No. 582-10-94300**

## **2010 TCEQ Flare Study Project Final Report**

**Prepared by**

**David T. Allen, Ph.D.  
Principal Investigator**

**Vincent M. Torres  
Project Manager**



**The University of Texas at Austin  
The Center for Energy and Environmental Resources**

**May 23, 2011**

# DRAFT

## Executive Summary

In May 2009, the TCEQ contracted with The University of Texas at Austin (UT Austin) to conduct the Comprehensive Flare Study project (PGA No. 582-8-86245-fy09-04, Tracking Number 2008-81) (TCEQ, 2009). In August 2010, the project was provided supplemental funding by the Air Quality Research Program (TCEQ Grant No. 582-10-94300). The purpose of this project was to conduct field tests to measure flare emissions and collect process and operational data in a semi-controlled environment to determine the relationship between flare design, operation, vent gas lower heating value (LHV) and flow rate, destruction and removal efficiency (DRE), and combustion efficiency (CE). The TCEQ's primary objectives for this study in order of decreasing priority were:

- Assess the potential impact of vent gas flow rate turndown on flare CE and VOC DRE;
- Assess the potential impact of steam/air assist on flare CE and Volatile Organic Compound (VOC) DRE at various operating conditions, including low vent gas flow rates;
- Determine whether flares operating over the range of requirements stated in 40 Code of Federal Regulations (CFR) § 60.18 achieve the assumed hydrocarbon DRE of 98 percent at varying vent gas flow rate turndown, assist ratios and vent gas heat content; and
- Identify and quantify the hydrocarbon species in flare plumes visualized with passive infrared cameras.

In this report, the term vent gas will be used to represent the waste gas stream that would be sent to the flare for destruction in an industrial facility. The terms flare plume and plume will always refer to the total stream of gases that leave the flare and change composition due to some level of combustion.

This final report is submitted to fulfill the requirements of PGA No. 582-8-86245-fy09-04, Tracking Number 2008-81, Task 10 and Task Order No. UTA10-000924-LOAT-RP9, Task 1 and presents the results for this project and the data collected to address the Study Objectives.

### **Project Scope and Design**

Extensive research has been conducted in controlled environments on devices that are not full-scale flares, i.e., with diameters less than three inches as opposed to industrial scale flares, which are typically on the order of multiple feet in diameter and can be as large as ten feet in diameter. To make the results of this study most directly applicable to industrial scale operations, the field tests performed for this study were conducted on full-scale industrial design flares. Specifically, the flare designs selected were the John Zink Models EE-QSC-36" Flare Tip (36-inch diameter) with (3) EEP-503 pilots (steam assist) and the LHTS-24/60 Flare Tip (24-inch diameter) with (3) Pilots (air assist), with maximum capacities of 937,000 lb/hr and 144,000, respectively. These sizes and design configurations were selected as they represent a large number of flare models currently in the field and the results will be applicable to these and similar flare designs when operated under similar conditions to those used in this study.

### *Controlled Environment Laboratory*

To measure flare emissions on full-scale flares in a semi-controlled environment (i.e., controlled flare operations but uncontrolled ambient conditions), the study was conducted at the outdoor

# DRAFT

flare test facility of the John Zink Company, LLC (Zink), in Tulsa, Oklahoma. Zink is a flare tip manufacturer whose flare test facility is capable of accommodating a wide range of flare tips, test configurations and operating conditions.

## *Measurement of Flare Emissions*

A core element of UT Austin's study approach was to directly measure flare emissions at the end of the flare plume, and calculate DRE and CE based on those measurements. To measure these emissions, UT Austin selected Aerodyne Research, Inc., (ARI) due to their extensive experience in ambient air quality studies and their unique capability to make continuous (1 Hz frequency, i.e., 1 measurement per second) measurements of the chemical species expected to be present in the flare plume. These direct measurements of the flare emissions serve as the primary data used to address the study objectives.



Figure ES-1. Flare Plume Sampling System. Flare Plume Sampling System making measurements of flare plume from the steam assist flare while the sampling system is held in position by crane and ground crew [4-7]\*

\* Numbers in brackets at the end of Tables and Figures are the table or figure number for the same Table or Figure in the main body of the report.

# DRAFT

## *Compare Remote Sensing Technologies*

Remote sensing technologies were also included in the study and a comparison of their performance is included in the study results. The following remote sensing measurement methods were included:

1. Infrared Hyper-Spectral Imaging Technology (Contractor: Telops Inc.)  
Identify flare hydrocarbon plume species and determine plume species concentrations.
2. Passive and Active Fourier Transform Infrared (PFTIR, AFTIR) Spectroscopy (Contractor: Industrial Monitor and Control Corporation)  
Collect the required data to determine flare combustion efficiency.
3. FLIR GasFindIR Passive Infrared (IR) Cameras (Contractor: Leak Surveys Inc.)  
Provide a visual comparison of IR images to the infrared hyper-spectral imaging technology results, and assist other remote sensing tools to take measurements.

A single blind approach was used to compare the remote sensing technology measurements, i.e., the only information provided to the contractors performing remote sensing measurements was that which would be provided to them if they were engaged to measure combustion efficiencies at an industrial facility. The results of the CE and DRE measurements made by ARI were not made available to the remote sensing teams until this report was released to the public.

## *Performance and Comparison Metrics*

VOC DRE was selected as the primary metric for assessing flare performance because of the critical role VOCs play in contributing to the formation of ozone. CE was selected as a secondary metric because the remote sensing technologies included in the study can only measure CE. DRE (hydrocarbon species X) is the percentage of species X that is destroyed relative to the quantity of species X entering the flare. Numerically, this is represented as

$$DRE (\%) = \left(1 - \frac{X_{plume}}{X_{in}}\right) \times 100 \quad \text{Eq. ES.1}$$

where

DRE (%) = destruction and removal efficiency (%)

$X_{plume}$  = flow rate of species X found in the flare plume

$X_{in}$  = flow rate of species X in the vent gas entering the flare

CE is the percentage of the total hydrocarbon stream entering the flare that burns completely to form only carbon dioxide and water. Numerically, this is represented as

$$CE (\%) = \left(\frac{CO_2 (plume)}{CO_2 (plume) + CO (plume) + \sum \text{hydrocarbons} (plume)}\right) \times 100 \quad \text{Eq. ES.2}$$

where

CE (%) = combustion efficiency (%)

# DRAFT

CO<sub>2</sub> (plume) = volume concentration of carbon dioxide in the plume (ppmv)

CO (plume) = volume concentration of carbon monoxide in the plume (ppmv)

Σ hydrocarbons (plume) = volume concentration of all the unburned hydrocarbons in the plume multiplied by the number of carbons in the hydrocarbon (ppmCv)

## *Vent Gas Composition and Flow Rates*

For this study, the vent gas composition was a mixture of natural gas, propylene and nitrogen. The ratio of natural gas to propylene was 1:4 by volume. Nitrogen was used as the diluent to achieve the desired lower heating value (LHV) for the vent gas. This study focused on vent gases with low LHV (350 Btu/scf and 600 Btu/scf) and low flow rates because this range of LHV is close to the minimum (300 Btu/scf) LHV allowed for a vent gas in an assisted flare that complies with 40 CFR § 60.18. The range of vent gas flow rates was 0.1% to 0.65% of the flare's design capacity. These vent gas flow rates were selected as they are in the range of operation for typical flow rates (less than 0.5%) used in industry. In the case of a steam-assisted flare, these flow rates introduce the greatest probability for over-assisted steam operation because of minimum levels of steam assist recommended to industry by flare manufacturers, 500 lb/hr center, 750 lb/hr upper, for the 36 inch diameter steam assisted flare used in this study.

## *Quality Assurance*

UT Austin prepared a Category 2 Quality Assurance Project Plan (The University of Texas at Austin, 2010) for this project that complied with the requirements of the Environmental Protection Agency's (EPA) *Requirements for Quality Assurance Project Plans*, EPA QA/R-5, and *Guidance for Quality Assurance Project Plans*, EPA QA/G-5. This QAPP was posted for public comment by the TCEQ and was reviewed by the EPA.

## **Test Plan**

A summary of the test series is shown in Table 1, where steam flare tests begin with the letter "S" in the designation of the test series and air flare tests begin with the letter "A". The test plan consisted of multiple flare test series conducted on the air-assisted flare tip and multiple test series conducted on the steam-assisted flare tip. The designation used to identify each test point and run was: S[number 1].[number 2]R[number 3], where the number 1 is the test series number and number 2 designates the level of assist (air or steam) used in the test series. Number 3 is the run or repetition number for the test point. So, for example, S3.2R2 is steam flare test series number 3, the second set of assist conditions, repetition number 2.

To focus on low LHV vent gas streams and still comply with 40 CFR § 60.18, a LHV of 350 Btu/scf ± 50 Btu/scf was selected as the lowest target LHV for the vent gases used in the Test Plan. To obtain additional data on the effect of LHV on DRE and CE, a second LHV of 600 Btu/scf ± 80 Btu/scf was also included in the Test Plan.

# DRAFT

**Table ES-1. Summary of Flare Test Plan [3-1]**

## Steam Flare Tests

Test Series	Vent Gas (Nominal)			Target (Nominal) Steam Assist (lb/hr)	
	Flow Rate lb/hr	LHV Btu/scf	Composition %	Center	Upper
S1	2342	2149	100% Propylene	500	ISP to <Snuff
S2	937	2149	100% Propylene	500	ISP to <Snuff
S3	937	350	20:80 TNG to Propylene Ratio Diluted to Target LHV	500	ISP to <Snuff
S3	937	350	20:80 TNG to Propylene Ratio Diluted to Target LHV	100	230
S3	937	350	20:80 TNG to Propylene Ratio Diluted to Target LHV	0	230
S3	937	350	20:80 TNG to Propylene Ratio Diluted to Target LHV	0	0
S4	2342	350	20:80 TNG to Propylene Ratio Diluted to Target LHV	500	ISP to <Snuff
S4	2342	350	20:80 TNG to Propylene Ratio Diluted to Target LHV	330	110
S4	2342	350	20:80 TNG to Propylene Ratio Diluted to Target LHV	0	330
S5	937	600	20:80 TNG to Propylene Ratio Diluted to Target LHV	500	ISP to <Snuff
S6	2342	600	20:80 TNG to Propylene Ratio Diluted to Target LHV	500	ISP to <Snuff
S7	2342 - 937	350	20:80 TNG to Propylene Ratio Diluted to Target LHV	500	525
S8	2342 - 937	350	20:80 TNG to Propylene Ratio Diluted to Target LHV	0	500
S9	2342 - 937	350	20:80 TNG to Propylene Ratio Diluted to Target LHV	0	1025
S10	2342 - 937	350	20:80 TNG to Propylene Ratio Diluted to Target LHV	0	825
S11	2342 - 937	350	20:80 TNG to Propylene Ratio Diluted to Target LHV	300	525
S12	2342 - 937	350	20:80 TNG to Propane Ratio Diluted to Target LHV	500	525
S13	2342 - 937	350	20:80 TNG to Propane Ratio Diluted to Target LHV	325	525
S14	2342 - 937	350	20:80 TNG to Propane Ratio Diluted to Target LHV	0	525

TNG = Tulsa Natural Gas  
 Snuff = Visible flame extinguished  
 ISP = Incipient Smoke Point  
 LHV = Lower Heating Value

## Air Flare Test Tests

Test Series	Vent Gas (Targets)			Target (Nominal) Air Assist (lb/hr)
	Flow Rate lb/hr	LHV Btu/scf	Composition %	
A1	937	2149	100 % Propylene	ISP to <Snuff
A2	359	2149	100 % Propylene	ISP to <Snuff
A3	937	350	20:80 TNG to Propylene Ratio Diluted to Target LHV	ISP to <Snuff
A4	937	600	20:80 TNG to Propylene Ratio Diluted to Target LHV	ISP to <Snuff
A5	359	350	20:80 TNG to Propylene Ratio Diluted to Target LHV	ISP to <Snuff
A6	359	600	20:80 TNG to Propylene Ratio Diluted to Target LHV	ISP to <Snuff
A7	359	350	20:80 TNG to Propane Ratio Diluted to Target LHV	ISP to <Snuff

TNG = Tulsa Natural Gas  
 Snuff = Visible flame extinguished  
 ISP = Incipient Smoke Point  
 LHV = Lower Heating Value

# DRAFT

The steam flare burner used for this study had a design capacity of 937,000 lb/hr for use with propylene. Therefore the 0.1% and 0.25% of design capacity vent gas flow rates for this flare are 937 lb/hr and 2,342 lb/hr, respectively. The air flare burner used for this study had a design capacity of 144,000 lb/hr for use with propylene. The 0.1% of design capacity vent gas flow rate for this flare was thought to be too low, so values of 0.25% and 0.65% of design capacity were selected for the air flare. These vent gas flow rates were 359 lb/hr and 937 lb/hr, respectively.

## Summary of Flare Tests Results

Figures ES-2a and ES-2b show DRE (propylene) versus steam assist rate and CE versus steam assist rate, respectively, for the two nominal steam flare vent gas flow rates, 937 lb/hr and 2,342 lb/hr at a nominal LHV of 350 Btu/scf. At this LHV, the 937 lb/hr vent gas flow rate (Test Series S3) was only able to achieve a DRE (propylene) > 99% at a steam-to-vent gas (S/VG) ratio of 0.25 or less, 230 lb/hr total steam assist rate (center = 0 lb/hr). The 2,342 lb/hr vent gas flow rate (Test Series S4) was able to sustain a 99% DRE (propylene) up to a S/VG = 0.29, 670 lb/hr total steam assist (center = 560 lb/hr) before the DRE and CE fell below 99% DRE. These levels of steam assist are lower than the minimum levels of steam assist (500 lb/hr center, 750 lb/hr upper) recommended to industry by flare manufacturers as reported to the TCEQ by industry representatives for the 36-inch diameter steam flare model used in this study with center and upper steam assist.

Figures ES-3a and ES-3b show DRE (propylene) versus S/VG ratio and CE versus S/VG ratio, respectively, for all of tests series S3 and S4 on one graph. Figures ES-4a and ES-4b are the same graphs focusing on the range DRE (propylene)  $\geq$  84%. It can be seen from Figures ES-4a and ES-4b that in this range of S/VG ratios there can be multiple DREs. This is due in part to the fact that, in this range of S/VG ratios, steam added at the center has a different effect on DRE than steam added at the upper nozzles.

Figures ES-5a and ES-5b show DRE (propylene) versus steam assist rate and CE versus steam assist rate, respectively, for the two nominal steam flare vent gas flow rates, 937 lb/hr and 2,342 lb/hr at a nominal LHV of 600 Btu/scf. For a nominal 937 lb/hr vent gas flow rate (Test Series S5), a DRE (propylene)  $\geq$  98% was achieved at a S/VG = 0.82, 770 lb/hr total steam assist (center = 490 lb/hr). A lower S/VG would have been required to achieve a DRE (propylene)  $\geq$  99%. The 2,342 lb/hr vent gas flow rate (Test Series S6) was able to sustain a 99% DRE (propylene) up to a S/VG = 0.84, 2,000 lb/hr total steam assist (center = 520 lb/hr) before the DRE and CE fell below 99% DRE. This LHV and vent gas flow rate did achieve a DRE (propylene)  $\geq$  99% with a level of steam assist greater than the minimum levels of steam assist (500 lb/hr center, 750 lb/hr upper) recommended to industry by flare manufacturers as reported to the TCEQ by industry representatives for the 36-inch diameter stream flare model used in this study with center and upper steam assist.

# DRAFT

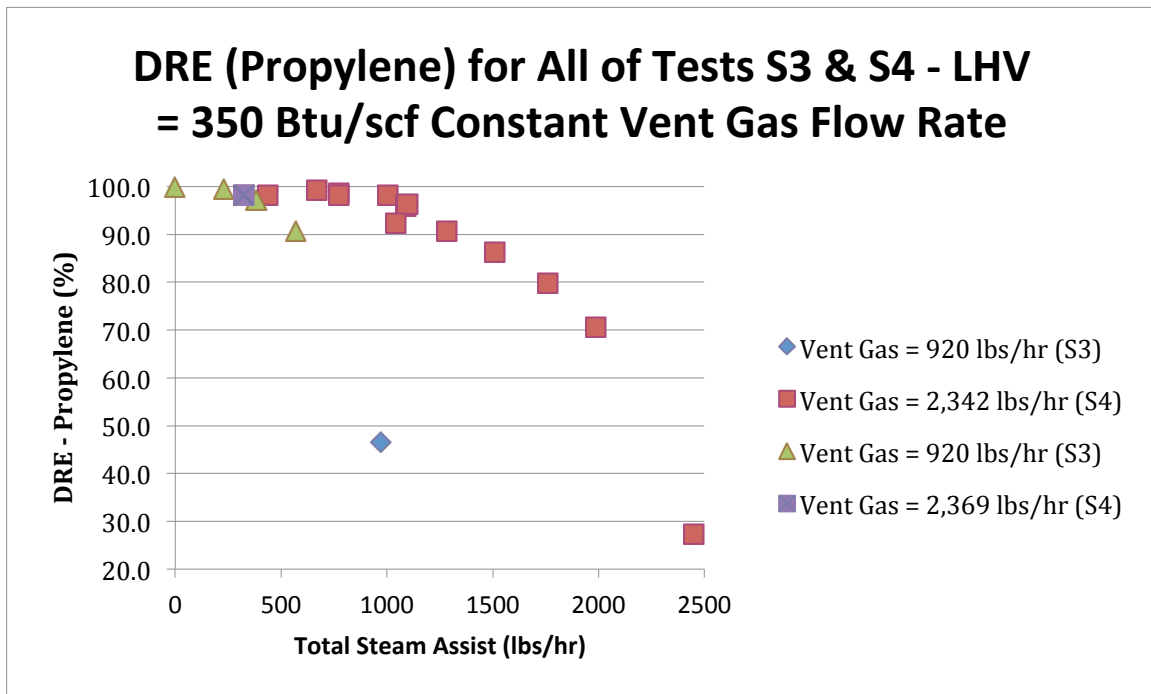


Figure ES-2a. DRE vs Steam Assist for All Test Series S3 and S4 [5-12a]

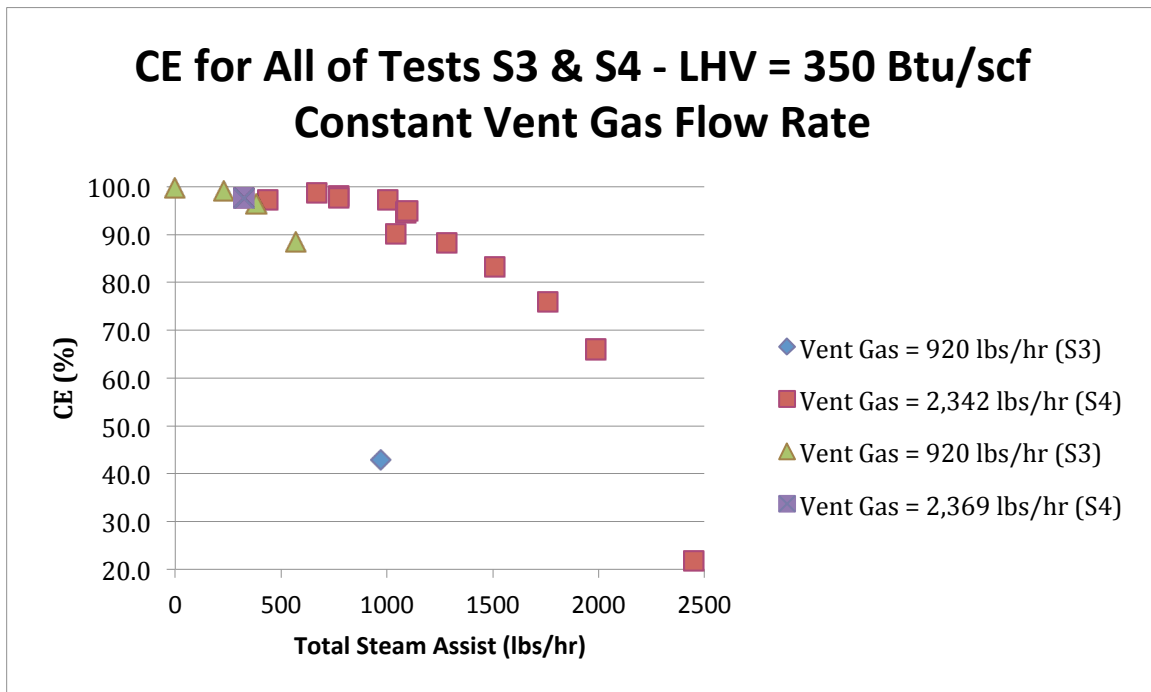


Figure ES-2b. CE vs Steam Assist for All Test Series S3 and S4 [5-12b]

# DRAFT

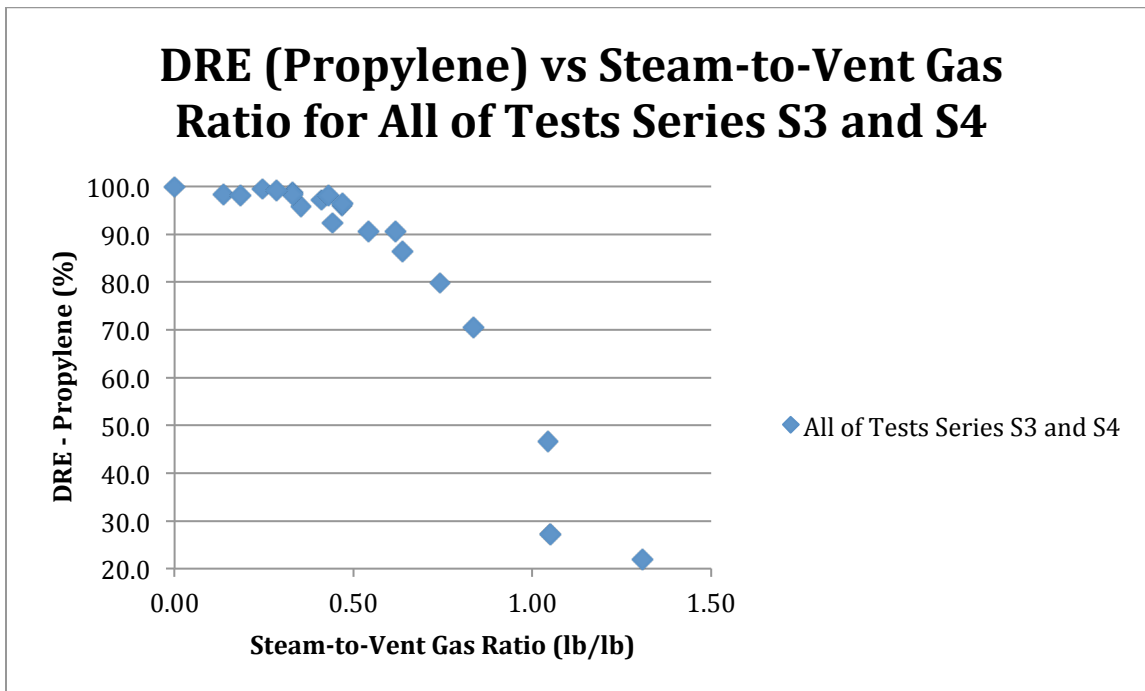


Figure ES-3a. DRE vs Steam-to-Vent Gas Ratio for All Test Series S3 and S4 [5-14a]

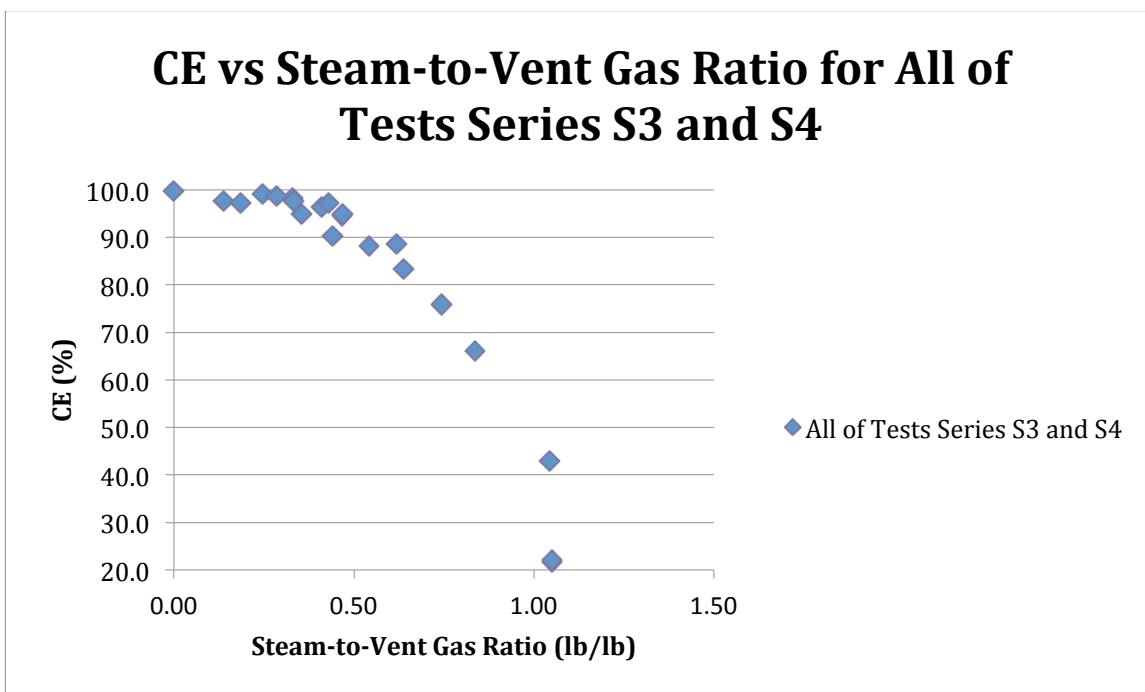


Figure ES-3b. CE vs Steam-to-Vent Gas Ratio for All Test Series S3 and S4 [5-14b]

# DRAFT

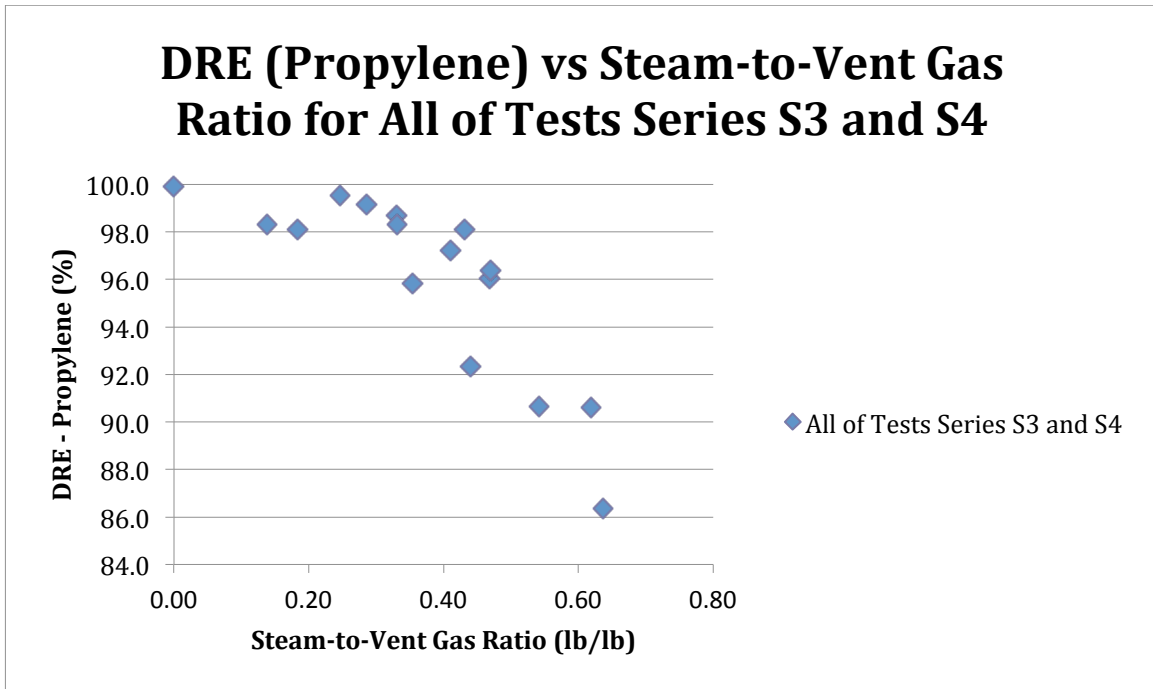


Figure ES-4a. DRE vs Steam-to-Vent Gas Ratio for All Test Series S3 and S4 [5-15a]

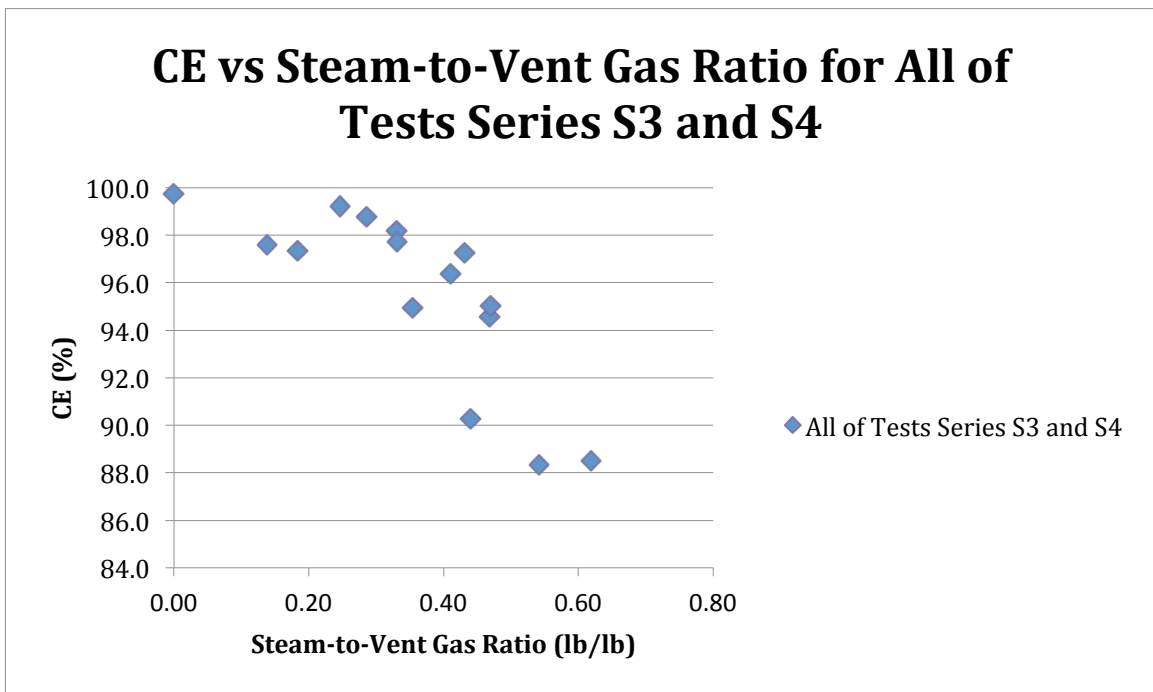


Figure ES-4b. CE vs Steam-to-Vent Gas Ratio for All Test Series S3 and S4 [5-15b]

# DRAFT

## DRE (Propylene) for Tests S5 & S6 - LHV = 600 Btu/scf, Constant Vent Gas Flow Rate

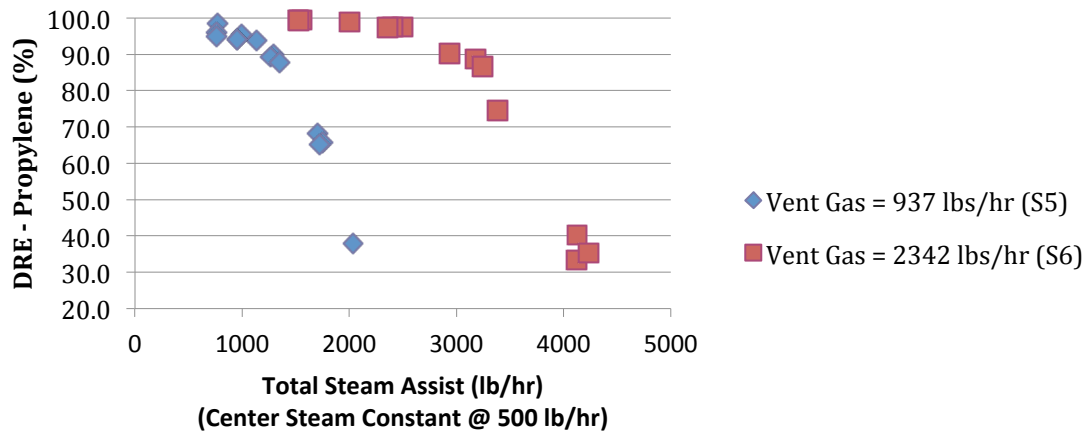


Figure ES-5a. DRE vs Steam Assist for Test Series S5 and S6 [5-13a]

## CE for Tests S5 & S6 - LHV = 600 Btu/scf, Constant Vent Gas Flow Rate

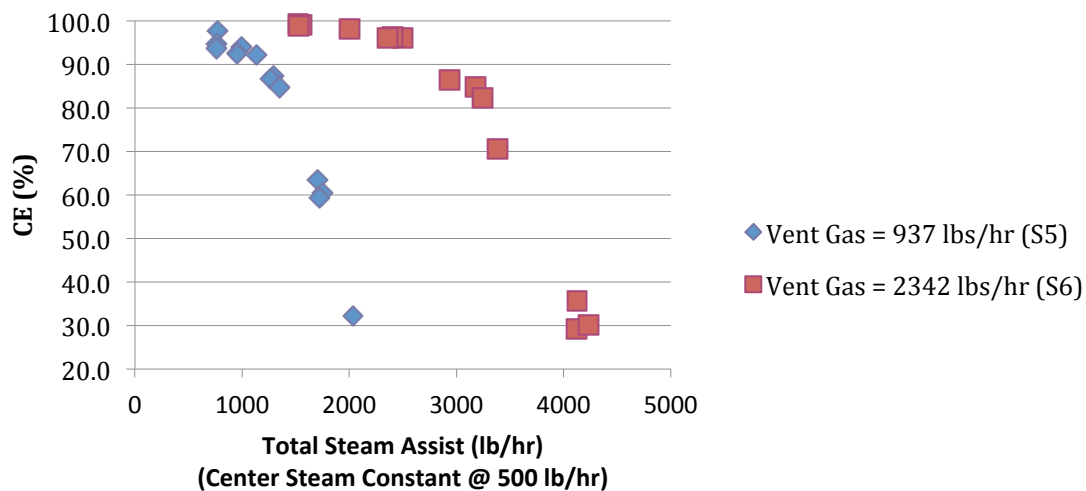


Figure ES-5b. DRE vs Steam Assist for Test Series S5 and S6 [5-13b]

# DRAFT

Figures ES-6a and ES-6b show DRE (propylene) versus S/VG ratio and CE versus S/VG ratio, respectively, for all of tests series S5 and S6 on one graph. Figures ES-7a and ES-7b are the same graphs focusing on the range DRE (propylene)  $\geq$  84%. It can be seen from Figures ES-7a and ES-7b that in this range of S/VG ratios there can be multiple DREs.

The previous graphs have illustrated the effect of varying steam assist on a vent gas of constant flow rate and constant LHV. Figures ES-8a and ES-8b show how DRE and CE vary as the vent gas flow rate is varied for five different steam assist combinations that were held constant as the vent gas flow rate was varied. The LHV was held constant at 350 Btu/scf for all tests shown in these two figures. Note that the horizontal axis (vent gas flow rate) is reversed and decreases from left to right. These graphs show the significant effect center and total steam have on DRE at low vent gas flow rates. The flare performance curves with small negative slopes are those with the lowest level of center steam (center = 0 lb/hr) followed by low levels (500 lb/hr and 835 lb/hr) of upper steam assist (Test Series S8 and S10). The graph with the larger negative slopes (Test Series S7) has the highest center steam (500 lb/hr). For all graphs, if steam assist is held constant, as vent gas flow rate increases, DRE increases.

Figures ES-9a and ES-9b show the relationship between DRE (propylene) and combustion zone gas net heat value (CZG NHV) for Test Series S3 to S6. Figures ES-10a and ES-10b provide the same information for Test Series S7 to S11. Note that the horizontal axis (CZG NHV) in Figures ES-9b and ES-10b has been reversed and decreases from left to right. Figures ES-9b and ES-10b focus on the range of DRE  $\geq$  84 % to better examine the relationship between these two parameters. There can be multiple DREs for CZG NHVs up to at least 250 Btu/scf and perhaps as high as 300 Btu/scf. Once again, this is due in part to the fact that, in this range of S/VG ratios, steam added at the center has a different effect on DRE than steam added at the upper nozzles.

# DRAFT

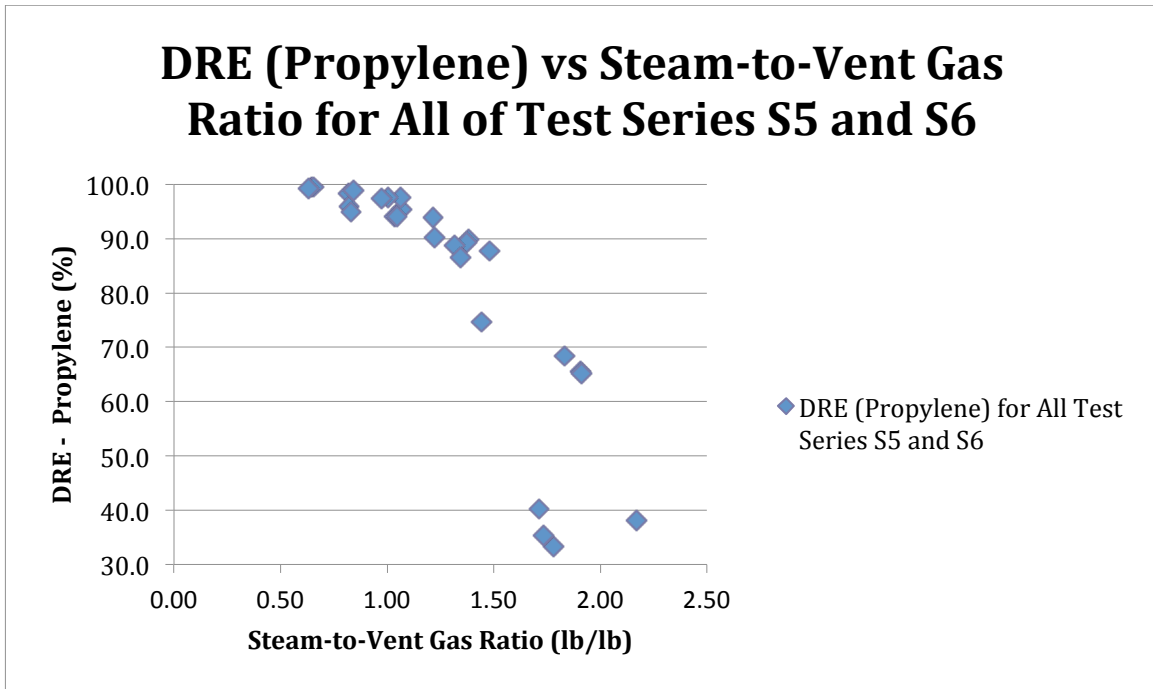


Figure ES-6a. DRE vs Steam-to-Vent Gas Ratio for All Test Series S5 and S6 [5-16a]

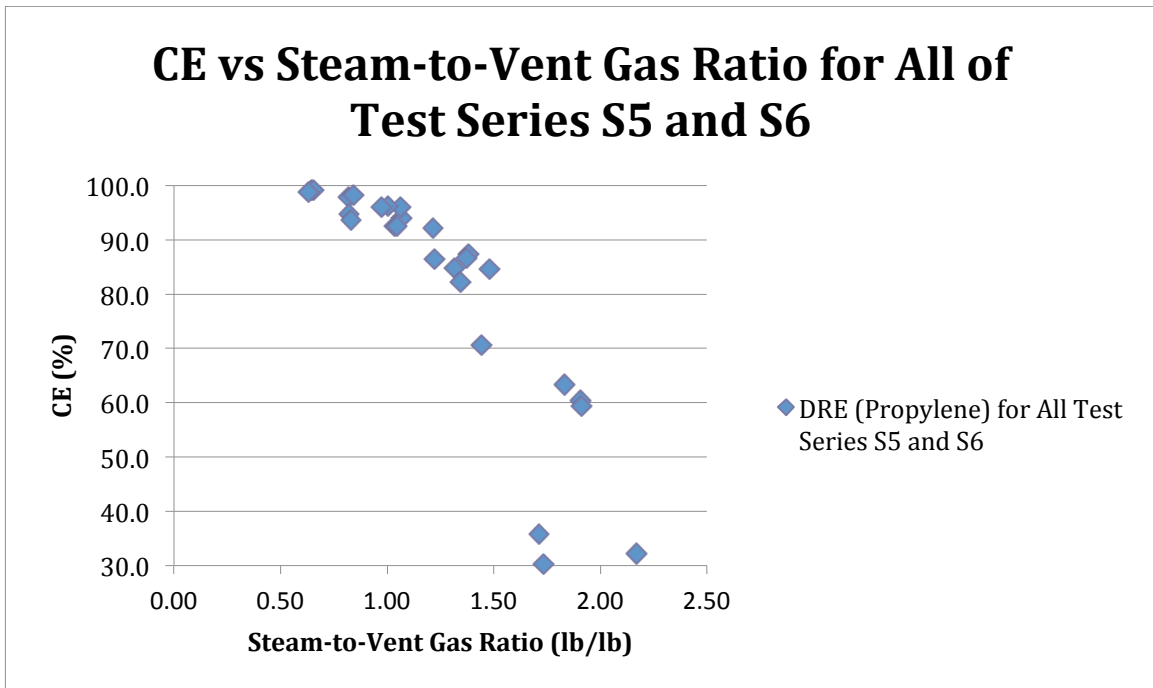


Figure ES-6b. CE vs Steam-to-Vent Gas Ratio for All Test Series S5 and S6 [5-16b]

# DRAFT

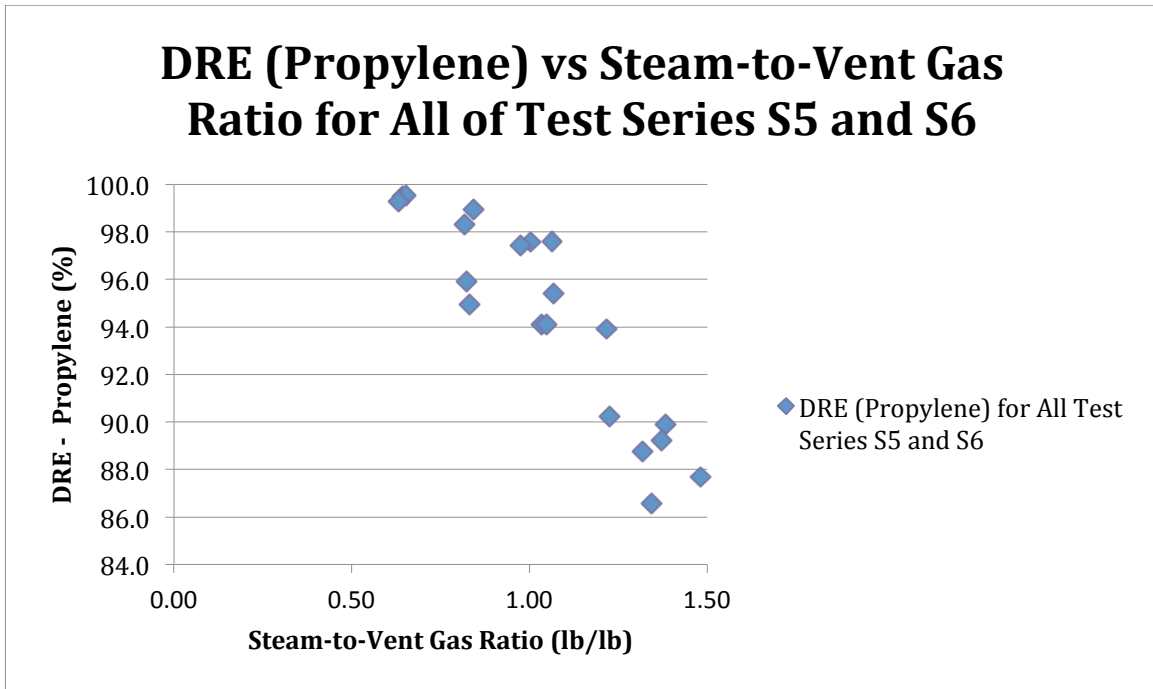


Figure ES-7a. DRE vs Steam-to-Vent Gas Ratio for All Test Series S5 and S6 [5-17a]

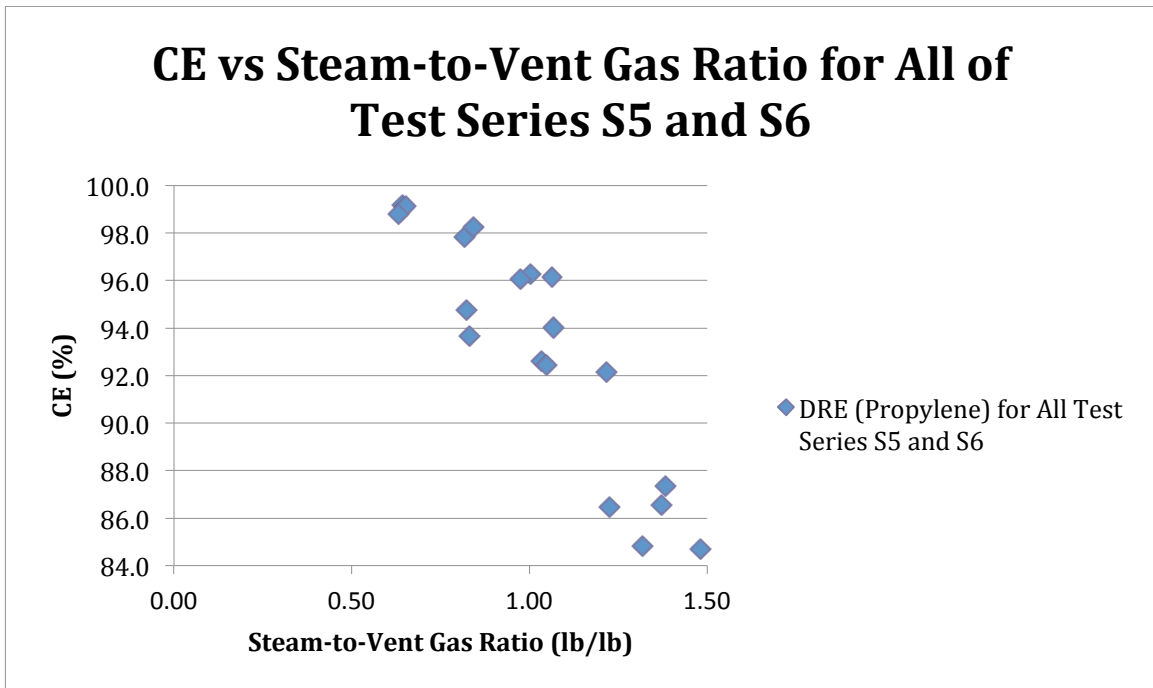


Figure ES-7b. CE vs Steam-to-Vent Gas Ratio for All Test Series S5 and S6 [5-17b]

# D R A F T

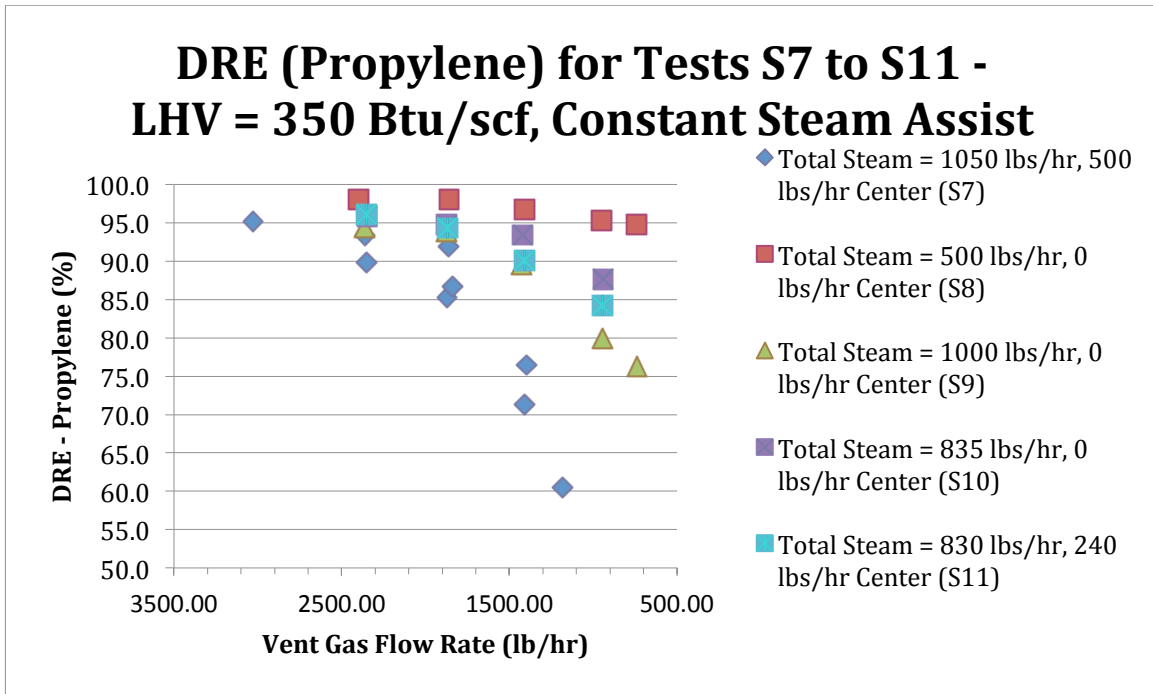


Figure ES-8a. DRE vs Vent Gas Flow Rate for Test Series S7, S8, S9, S10 and S11 [5-19a]

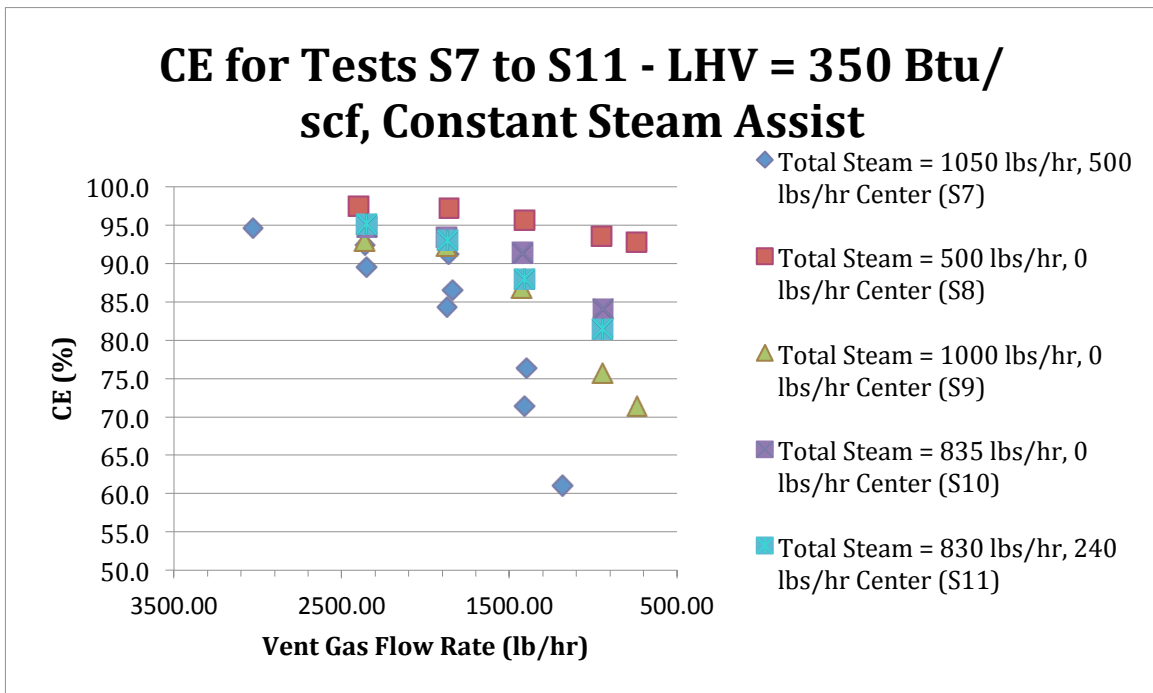


Figure ES-8b. CE vs Vent Gas Flow Rate for Test Series S7, S8, S9, S10 and S11 [5-19b]

# DRAFT

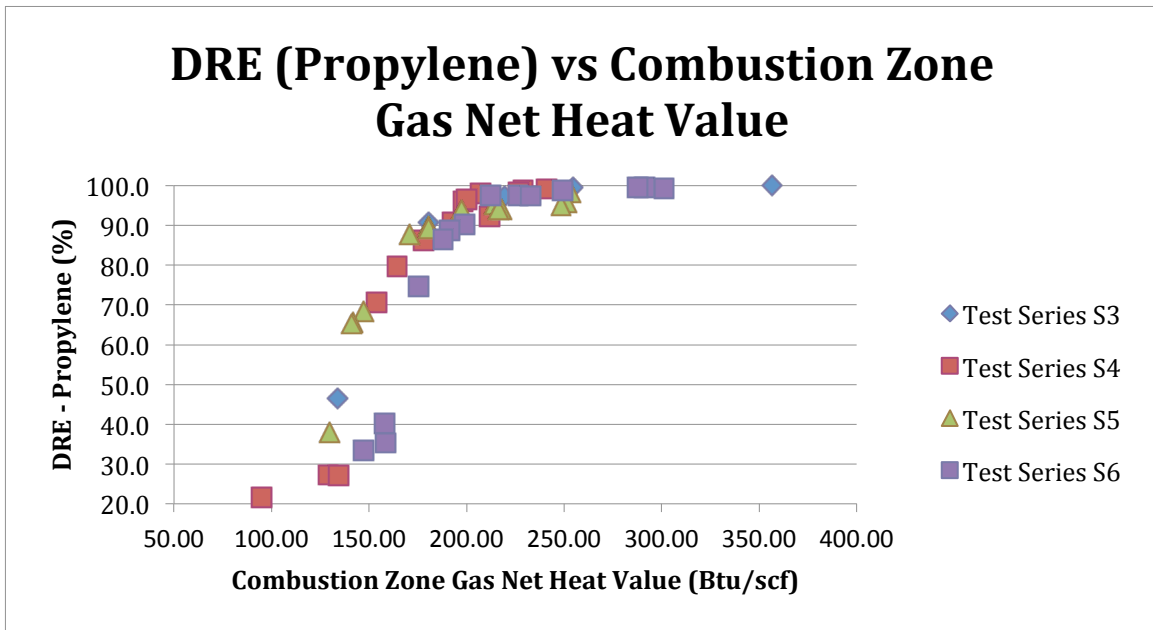


Figure ES-9a. DRE vs CZG NHV for Test Series S3, S4, S5 and S6 [5-20a]

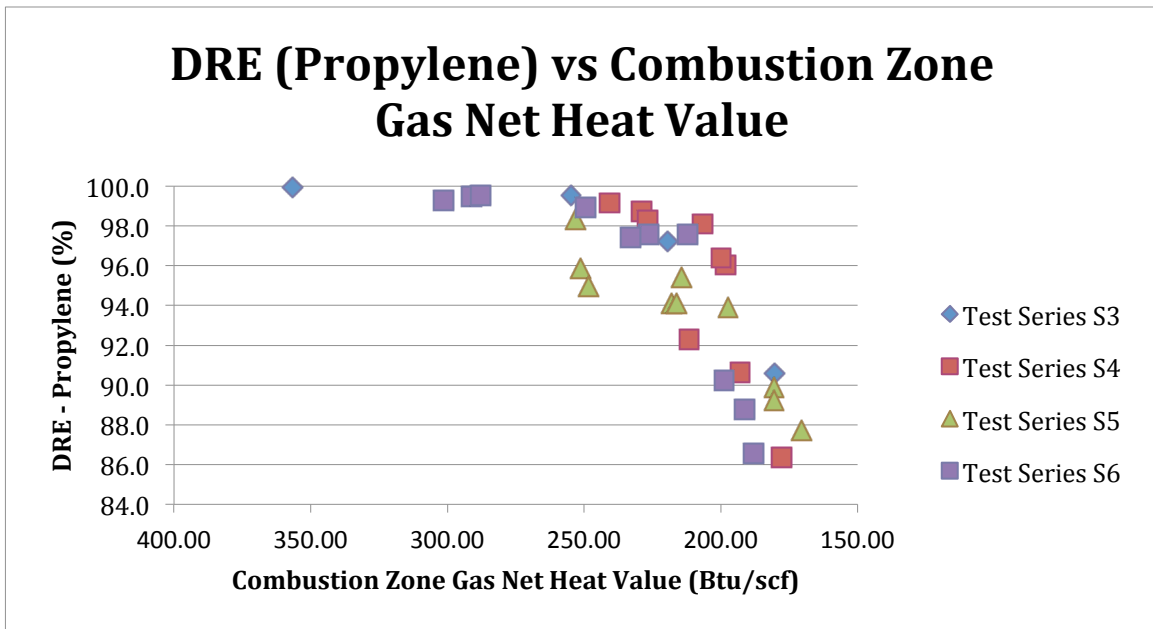


Figure ES-9b. DRE vs CZG NHV for Test Series S3, S4, S5 and S6 [5-20b]

# DRAFT

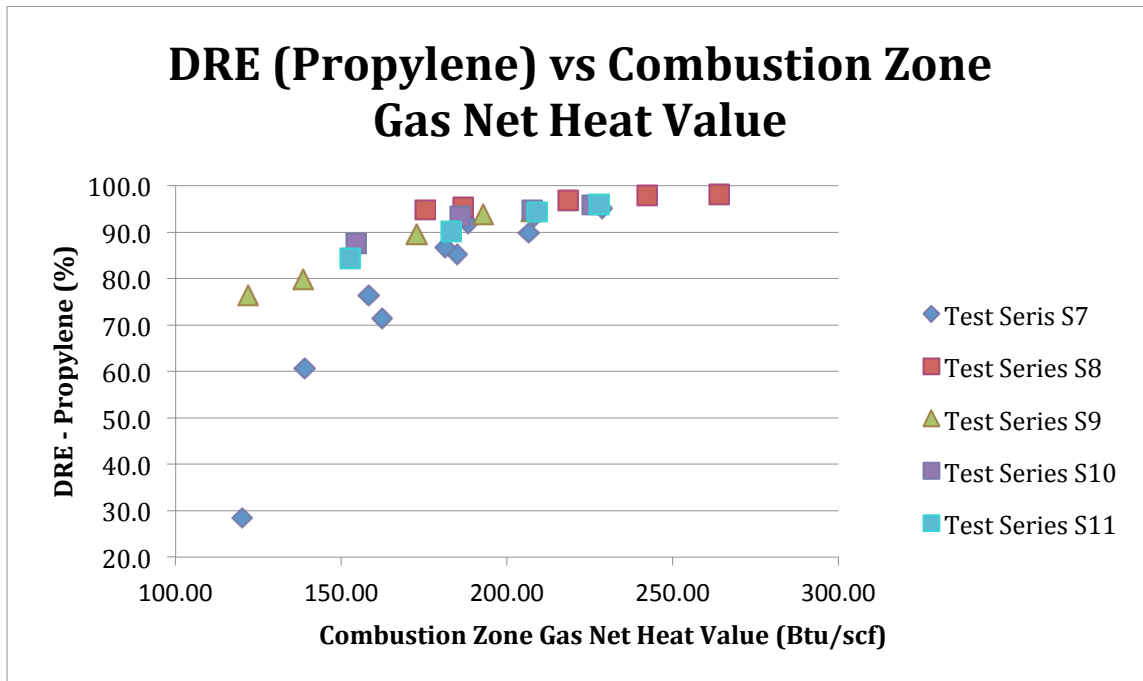


Figure ES-10a. DRE vs CZG NHV for Test Series S7, S8, S9, S10 and S11 [5-21a]

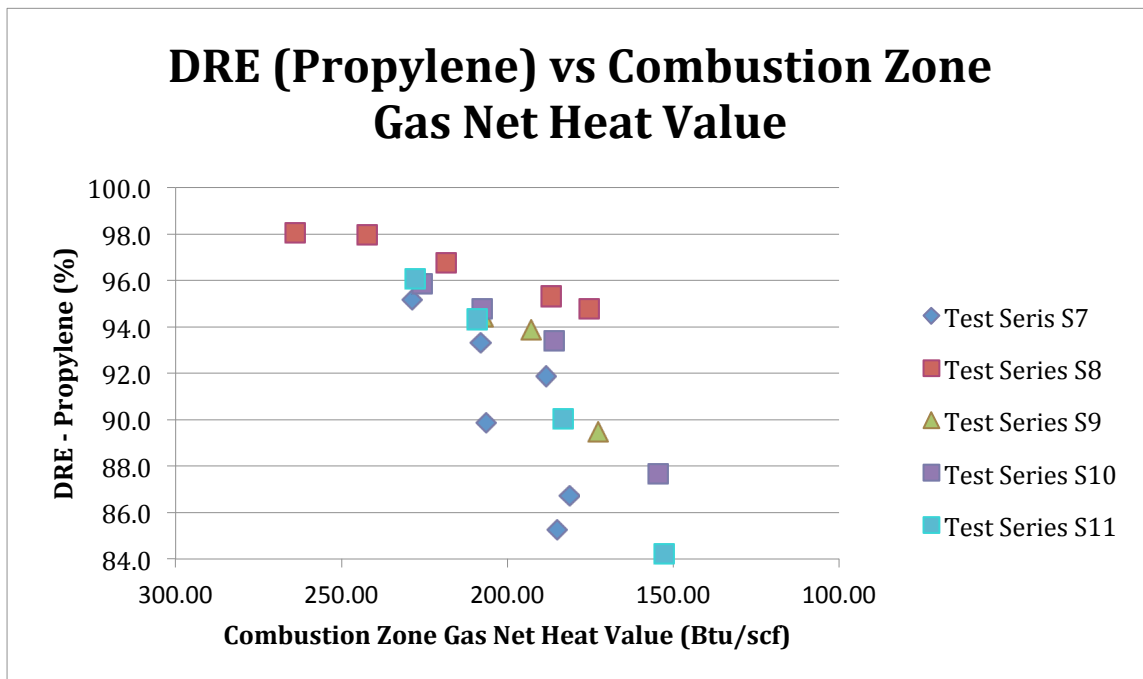


Figure ES-10b. DRE vs CZG NHV for Test Series S7, S8, S9, S10 and S11 [5-21b]

# DRAFT

Figures ES-11a and ES-11b show DRE (propylene) versus air assist and CE versus air assist for the nominal LHV = 350 Btu/scf and the two nominal vent gas flow rates, 359 lb/hr and 937 lb/hr. Figures ES-12a and ES-12b show DRE (propylene) versus air assist and CE versus air assist for the nominal LHV = 600 Btu/scf and the two nominal vent gas flow rates, 359 lb/hr and 937 lb/hr. These show an almost linear decline in DRE and CE as air assist increases. The S4 and S6 test series with a vent gas flow rate with an LHV = 600 Btu/scf has a slope that is not as steep but falling below DRE = 99 % at air assist levels that equal approximately 6 times the quantity of air required theoretically for stoichiometric combustion. As air assist is increased beyond this quantity, the DRE decreases almost linearly for both of the nominal LHVs used in this study.

Figures ES-13a and ES-13b show DRE (propane) versus vent gas flow rate and CE versus vent gas flow rate for three different steam assist combinations that were held constant as the vent gas flow rate was varied. The LHV was held constant at the nominal 350 Btu/scf for all tests shown in these two figures. As with propylene, the highest DREs (99.1%) are achieved in test series (S14) with the lowest center steam (0 lb/hr) and 540 lb/hr upper steam, while test series S12 with the highest center (490 lb/hr) and upper (560 lb/hr) steam assist only achieved a DRE = 97.4% (CE = 99.1%).

Figures ES-14a and ES-14b show DRE (propane) versus air assist and CE versus air assist. The LHV was held constant at the nominal 350 Btu/scf for all tests shown in these two figures. As with propylene, at air assist levels that equal approximately 6 times the quantity of air required theoretically for stoichiometric combustion, DRE (propane) = 99.3% (CE = 99.7%).

# DRAFT

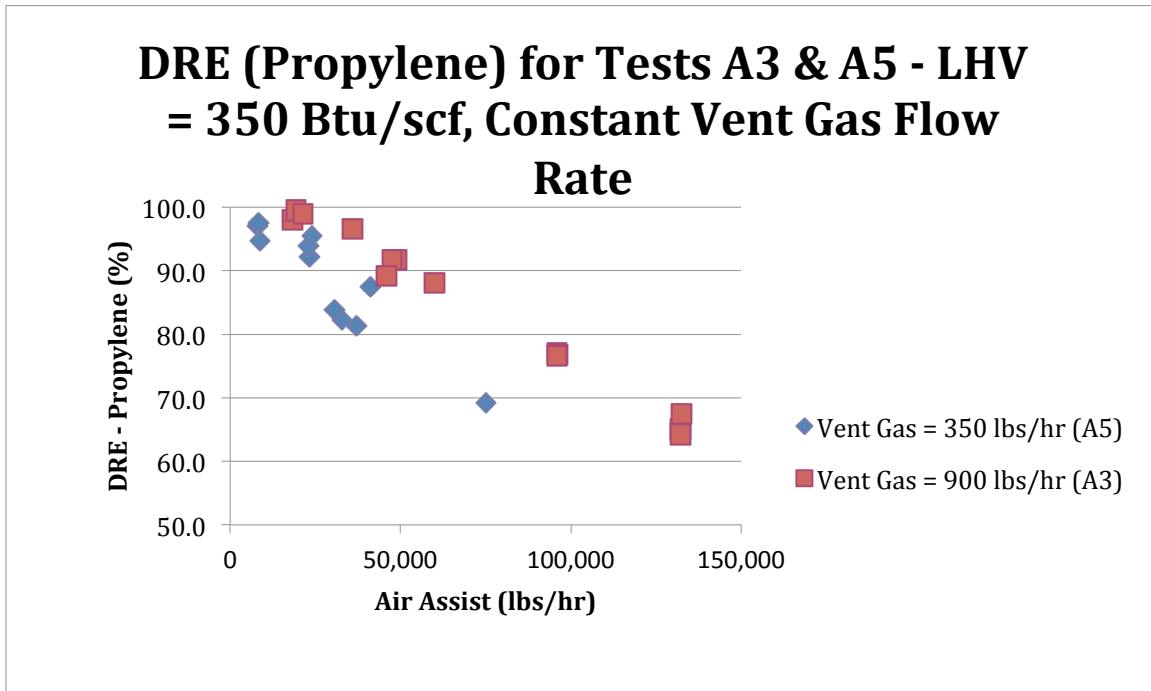


Figure ES-11a. DRE vs Air Assist for Test Series A3 and A5 [5-22a]

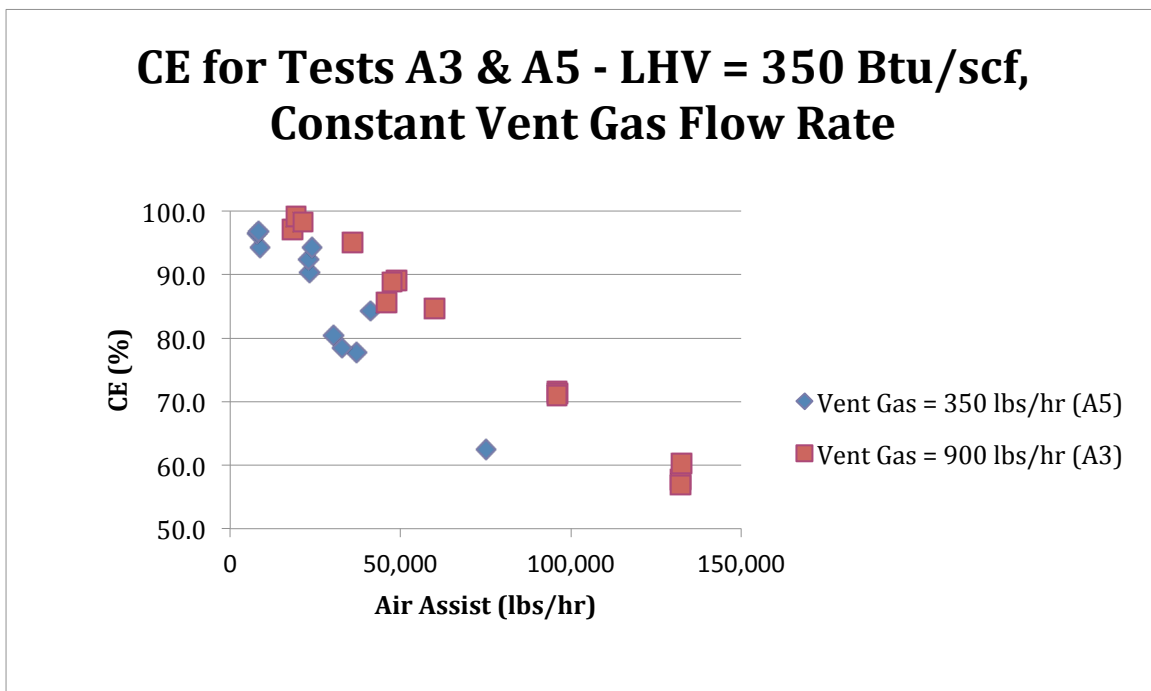


Figure ES-11b. CE vs Air Assist for Test Series A3 and A5 [5-22b]

# DRAFT

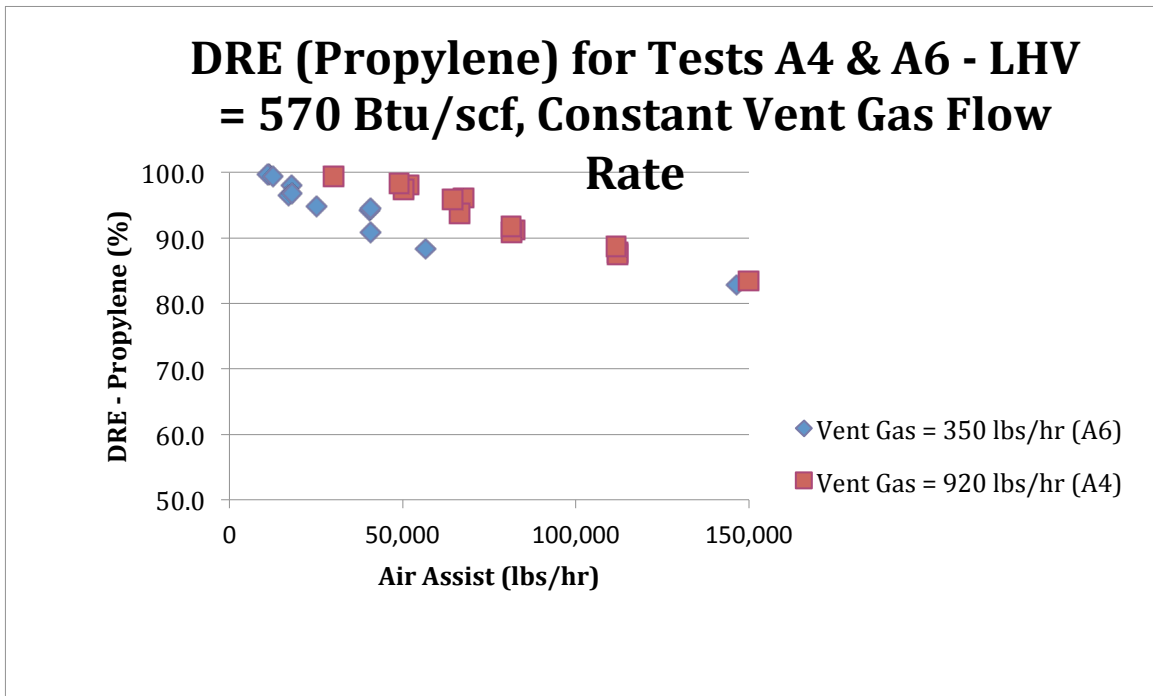


Figure ES-12a. DRE vs Air Assist for Test Series A4 and A6 [5-23a]

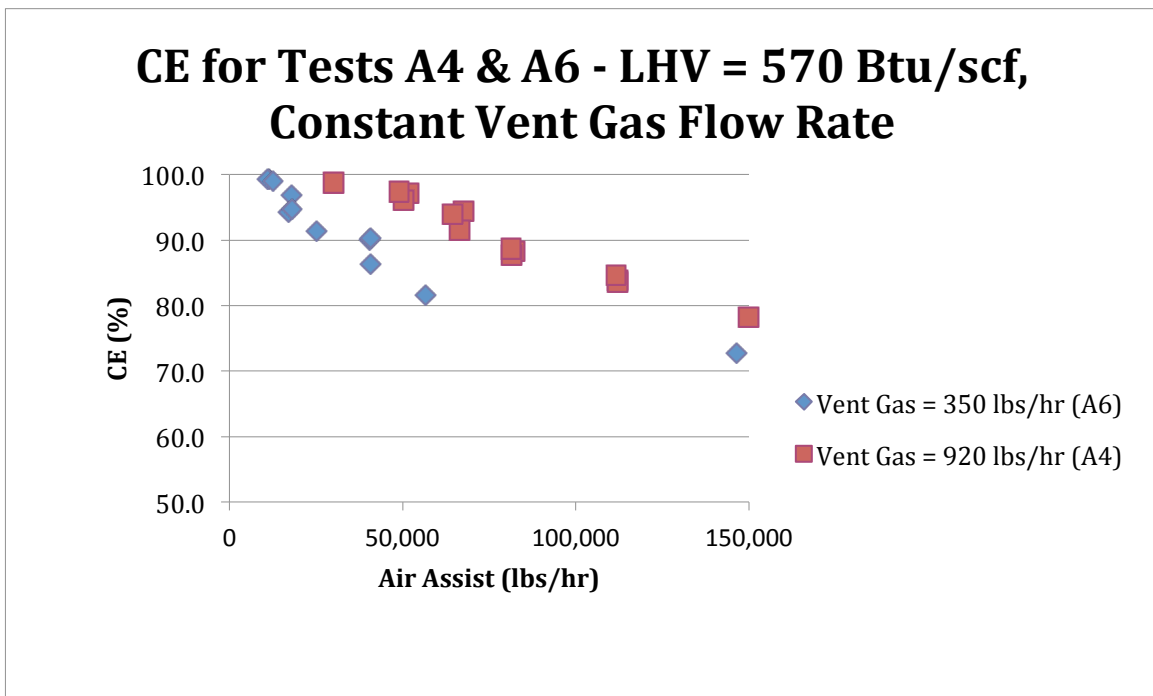


Figure ES-12b. CE vs Air Assist for Test Series A4 and A6 [5-23b]

# DRAFT

## DRE (Propane) for Tests S12 to S14 (Propane) - LHV = 340 Btu/scf, Constant Steam Assist

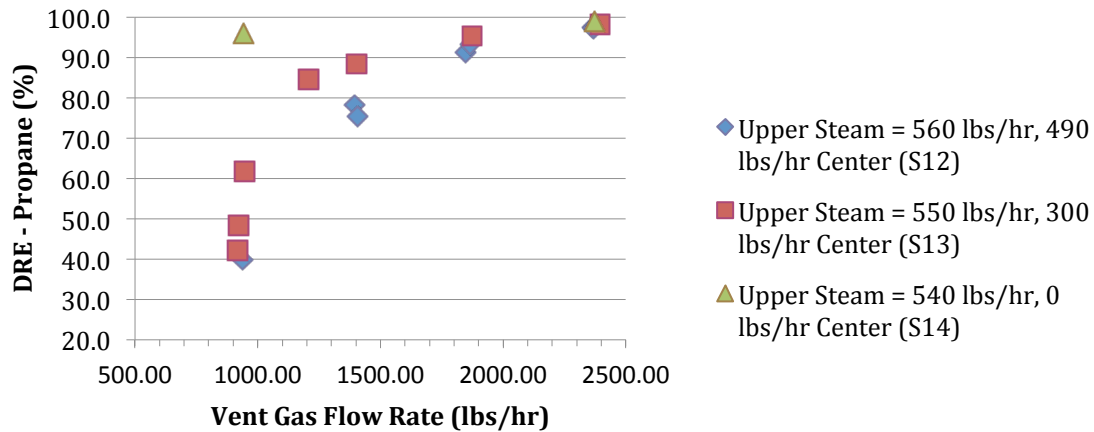


Figure ES-13a. DRE vs Vent Gas Flow Rate for Test Series S12, S13 and S14 [5-24a]

## CE for Tests S12 to S14 (Propane) - LHV = 340 Btu/scf, Constant Steam Assist

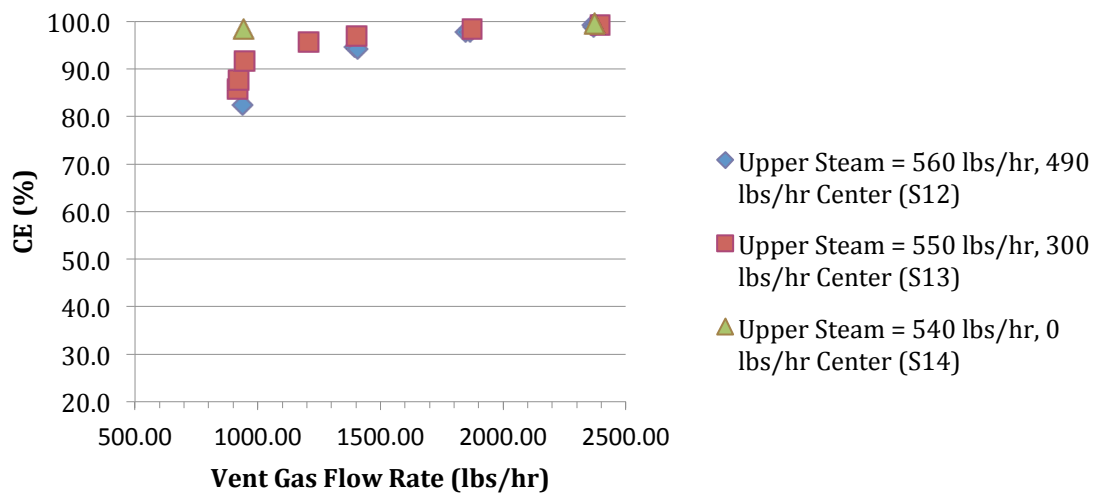


Figure ES-13b. CE vs Vent Gas Flow Rate for Test Series S12, S13 and S14 [5-24b]

# DRAFT

## DRE (Propane) for Test A7 (Propane) - LHV = 350 Btu/scf, Constant Vent Gas Flow Rate

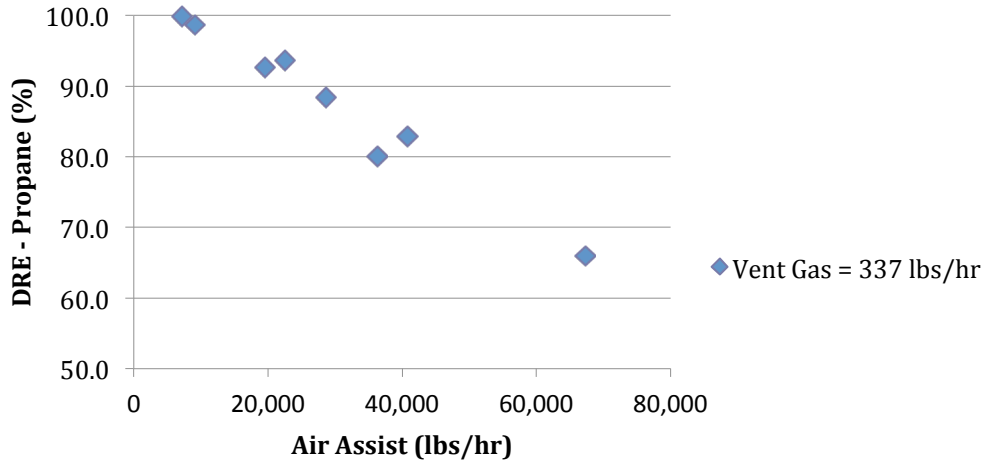


Figure ES-14a. DRE vs Air Assist for Test Series A7 [5-25a]

## CE for Test A7 (Propane) - LHV = 350 Btu/scf, Constant Vent Gas Flow Rate

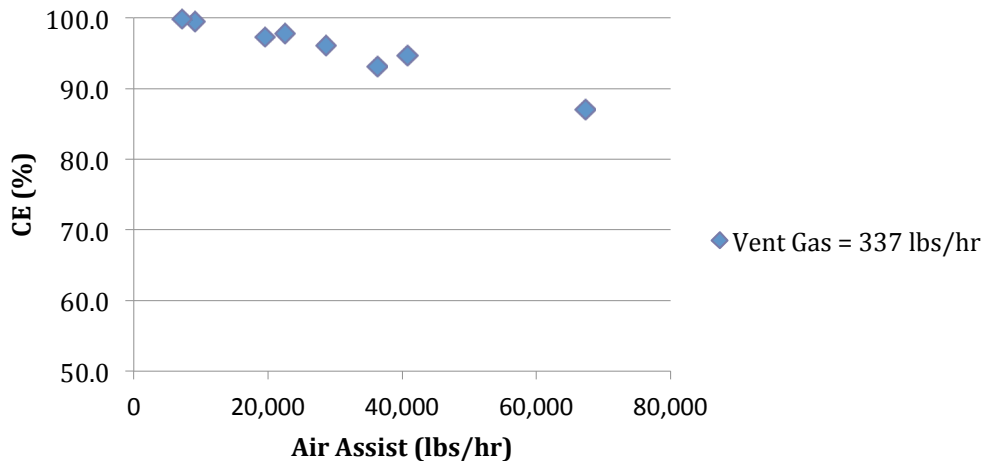


Figure ES-14b. CE vs Air Assist for Test Series A7 [25b]

# DRAFT

## Comparison with Remote Sensing Technology Measurements with Test Results

There were three remote sensing technologies participating in the study: IMACC PFTIR and AFTIR spectrometers, Telops Hyper-cam passive imaging radiometric spectrometer, and LSI FLIR GasFindIR and thermal IR cameras. The LSI cameras provide visual images of hydrocarbons in the gas phase and are useful in detection of these gases but were not used for quantitative assessment of flare combustion. The discussion in this section will focus on the IMACC and Telops instruments, which can measure the combustion efficiency of the flare. Telops can also make mass flow rate measurements of hydrocarbons in the plume. However, these results were provided so late in the preparation of this report that the comparison of the Telops mass flow rate results will be provided as an addendum to this report at a later date.

As summarized in Section 3, the measurement of emissions in samples extracted from the plume and analyzed by ARI provided the baseline or reference DRE and CE values against which the remote sensing technologies would be compared. The results of the analyses of the extractive samples and determination of DRE and CE by ARI were not provided to IMACC or Telops. Subsequent to the field tests, IMACC and Telops submitted their CE measurements for each test run, including their standard deviation ( $\sigma$ ) for their measurements.

Three statistical criteria were selected to compare the measurements of IMACC and Telops with the ARI values. The first two are the mean difference and the standard deviation of the difference. These terms are defined numerically as follows.

$$\text{mean difference} = \frac{\sum_{i=1}^N \text{ABS}(CE_{RS} - CE_{ARI})_i}{N} \quad \text{Eq. ES.3}$$

$$\text{standard deviation} = \sqrt{\frac{\sum_{i=1}^N [(CE_{RS} - CE_{ARI})_i]^2}{N - 1}} \quad \text{Eq. ES.4}$$

where

mean difference = average of the absolute values of the difference between the CE determined by the remote sensing contractor and the CE determined by ARI for test point  $i$

standard deviation = standard deviation of the differences between the CE determined by the remote sensing contractor and the CE determined by ARI for the test point  $i$

$CE_{RS}$  = combustion efficiency determined by the remote sensing contractor for the test point  $i$

$CE_{ARI}$  = combustion efficiency determined by ARI for the test point  $i$

$N$  = total number of test points in the subset

# DRAFT

The third criterion is data return. Data return is the percentage of the total number of possible test points for which data were reported. It is defined numerically as follows.

$$\text{data return} = \frac{\text{Number of test points for which data were reported}}{\text{Total number of test points}} \times 100 \quad \text{Eq. ES.5}$$

To more easily compare IMACC's and Telops' data with ARI's, the CE data sorted by ARI CE ( $CE_{ARI}$ ) value in descending order for the range  $100\% \geq CE \leq 80\%$ . On the assumption that the accuracy of the CE values may not be constant across this entire range, the data have been divided as follows:  $CE_{ARI} \geq 95\%$ ;  $90\% \geq CE_{ARI} < 95\%$ ;  $85\% \geq CE_{ARI} < 90\%$ ; and  $80\% \geq CE_{ARI} < 85\%$ . The difference between the IMACC's and Telops's CE values and the  $CE_{ARI}$  values are shown in each table. The CE mean differences and the standard deviation of the CE differences are calculated using Eqs. ES-3 and ES-4. These two criteria are summarized in Table ES-2, with data return.

### *Steam Flare Tests*

As shown in Table ES-2, the mean difference and the standard deviation of the CE differences for the IMACC AFTIR and PFTIR increase as the  $CE_{ARI}$  decreases. The mean difference and the standard deviation of the CE differences for the Telops CE values do not have a clear trend. In examining the differences in CE values in Table D-2, the inaccuracies in the IMACC AFTIR and PFTIR do not appear to have a bias relative to  $CE_{ARI}$ , while the Telops values tend to be biased lower than the  $CE_{ARI}$  values.

In examining the data return in Table 10-1, the IMACC AFTIR was 100% in all four ranges, while the PFTIR was 100% in all ranges except  $90\% \leq CE_{ARI} < 95\%$ , where it was 95%. Data return for the Telops CE values was less than 45% for all ranges except  $80\% \leq CE_{ARI} < 85\%$ , where it was 88%.

### *Air Flare Tests*

As shown in Table ES-2, the mean difference and the standard deviation of the CE differences for the IMACC PFTIR increase as the  $CE_{ARI}$  decreases. The IMACC AFTIR was not deployed for any of the air flare tests. In examining the CE differences in Table ES-2, the inaccuracies in these data tend to be biased low relative to the  $CE_{ARI}$  values.

The number of Telops data points, five, for all four ranges of the air flare tests are too few to statistically develop trend data. Additionally, the data return for these four  $CE_{ARI}$  ranges did not exceed 15%. Therefore, no additional analyses will be performed on the Telops air flare data.

# D R A F T

**Table ES-2. Summary of Comparison Criteria for Remote Sensing CE Values  
for CE<sub>ARI</sub> > 80% [10-1]**

Steam					
Range	Criterion	Telops	AFTIR	PFTIR	ARI
CE <sub>ARI</sub> ≥ 95%	Mean Difference (% pts)	17.2	1.7	1.4	40
	Standard Deviation (% pts)	29.6	2.4	2.2	
	Data Return (%)	45	100	100	
	Number of Test points	17	23*	40	
90% ≤ CE <sub>ARI</sub> < 95%	Mean Difference (% pts)	22.5	3.3	2.2	22
	Standard Deviation (% pts)	86.0	4.0	3.1	
	Data Return (%)	32	100*	95	
	Number of Test points	7	8	21	
85% ≤ CE <sub>ARI</sub> < 90%	Mean Difference (% pts)	5.1	10.2	6.4	12
	Standard Deviation (% pts)	7.4	12.4	10.6	
	Data Return (%)	17	100*	100	
	Number of Test points	3	6	12	
80% ≤ CE <sub>ARI</sub> < 85%	Mean Difference (% pts)	17.1	14.8	6.9	8
	Standard Deviation (% pts)	23.8	19.4	13.3	
	Data Return (%)	88	100*	100	
	Number of Test points	7	4	8	
Air					
Range	Criterion	Telops	AFTIR	PFTIR	ARI
CE <sub>ARI</sub> ≥ 95%	Mean Difference (% pts)	0.4	-	1.8	22
	Standard Deviation (% pts)	0.4		2.5	
	Data Return (%)	5		100	
	Number of Test points	1		22	
90% ≤ CE <sub>ARI</sub> < 95%	Mean Difference (% pts)	4.0	-	2.7	20
	Standard Deviation (% pts)	5.1		3.3	
	Data Return (%)	15		100	
	Number of Test points	3		20	
85% ≤ CE <sub>ARI</sub> < 90%	Mean Difference (% pts)	NMR	-	4.8	10
	Standard Deviation (% pts)	NMR		5.7	
	Data Return (%)	0		100	
	Number of Test points	0		10	
80% ≤ CE <sub>ARI</sub> < 85%	Mean Difference (% pts)	9.7	-	7.1	7
	Standard Deviation (% pts)	9.7		8.3	
	Data Return (%)	14		100	
	Number of Test points	1		7	

NMR = No CE values were reported for these tests.

\*Instrument not on site to obtain measurements during some of these test points.

# DRAFT

In summary, the IMACC PFTIR mean differences for the range  $CE_{ARI} \geq 90\%$  for both the air and steam flare tests averaged 2.0 percentage points, with an average standard deviation of the CE differences of 2.8 percentage points and average data return of 99%.

The IMACC AFTIR mean difference for the range  $CE_{ARI} \geq 90\%$  for the steam flare tests averaged 2.5 percentage points, with an average standard deviation of the CE differences of 3.2 percentage points and an average data return of 100%.

The Telops Hyper-Cam mean difference for the range  $CE_{ARI} \geq 90\%$  for the steam flare tests averaged 19.9 percentage points, with an average standard deviation of the CE differences of 57.8 percentage points and an average data return of 39%.

It is important to note that the difference in some of the values between the IMACC and Telops instruments and the ARI measurements may be due to less than ideal aiming due to interference of the plume sampling system. In a few instances, the remote sensing operators indicated that the position of the plume sampling system had restricted their ability to aim their instruments.

All participants were required to submit their preliminary data within six weeks of completion of the field campaign. Telops was unable to do so. Their report explains some of the challenges they had in making measurements and processing the large volume of data generated by their sensor and the number of test points conducted in this study.

## **Comparison of Conventional Emission Estimation Methods with Actual Emissions Measured**

Conventional methods for calculating emission rates as prescribed by the TCEQ (Air Permit Division's *Technical Guidance for Flares and Vapor Oxidizers*, RG-109 Dated October 2000) and EPA's AP-42 (Table 13.5-1) assume a constant DRE for smokeless flares that are operated in compliance with 40 Code of Federal Regulations (CFR) § 60.18, i.e., greater than a minimum LHV of 300 Btu/scf and not in excess of the exit velocity criterion.

The tests in this study were conducted in compliance with all criteria of 40 CFR § 60.18. For propylene and propane, a DRE of 99% would be used to predict emissions for all the tests. As can be seen from the data, it was possible to achieve a 99% DRE for many conditions tested.

However, as can also be seen in the data, many operating conditions produced actual DREs of less than 99%. These operating conditions resulted in the production of propylene emissions multiple times greater than that that would be calculated using the above prescribed conventional estimation methods. Using the procedures from the TCEQ and EPA noted above, estimates of emissions for each test point were calculated. These methods consider only the vent gas constituents and flow rate used and assume a constant emission factor (for NO<sub>x</sub>, CO and THC emissions) or DRE (methane, ethane, and VOCs) in estimating the emissions. Consequently, for actual DREs less than those assumed, the estimates of emissions will be low. Also, the TCEQ conventional method for estimating speciated VOCs assumes the products of combustion to be

# DRAFT

the same as the vent gas constituents in calculating the mass of emissions, i.e., 99% DRE for propylene results in 1% propylene emissions, when in reality the complex combustion process can result in propylene and other emissions. As an example, for the flare tests conducted Table ES-3 lists the hydrocarbon species typically found during any propylene flare tests.

Table ES-3. List of Hydrocarbons Typically Found in Plume During Propylene Flare Tests [6-1]

Propylene  
Methane  
Formaldehyde  
Ethylene  
Acetaldehyde  
Acrolein  
Acetylene  
Ethane  
Propylene-oxide  
Methanol  
Acetone  
Propanol  
Butene isomers

In Table ES-4, the emissions (lb/hr) for propylene, methane, total VOCs and total hydrocarbons (THC) are tabularized by method along with the measured emissions for five steam and five air tests with DREs above 90%. As points of reference, the Test Point, Run Number and propylene flow rate (lb/hr) in the vent gas along with the DRE for the test point are also included with the estimates. The values in the table show that as the DRE decreases from 99.9% to 90%, the difference between the conventional estimates and the measured emissions increases. This is true for both the air and steam tests.

As an example, for test point S3.6R1, the conventional method estimated 1.89 lb/hr propylene and 1.89 lb/hr total VOCs, where the measured emissions were 0.13 lb/hr and 0.15 lb/hr, respectively. Measured emissions averaged only 7.4% of the amount estimated by the conventional method. At a DRE of 96.0% (S4.1R2), the conventional method estimated 4.84 lb/hr propylene and 4.85 lb/hr total VOCs, where the measured emissions were 19.21 lb/hr and 21.78 lb/hr, respectively. Measured emissions averaged 420% of the amount estimated by the conventional method. And finally at 90% DRE (S11.3R1), the conventional method estimated 2.97 lb/hr propylene and 2.98 lb/hr total VOCs where the measured emissions were 29.61 lb/hr and 32.46 lb/hr, respectively. Measured emissions averaged 1,043% of the amount estimated by the conventional method, more than 10 times the amount estimated. This trend is similar for the air flare.

# D R A F T

Table ES-4. Summary of Selected Emissions Estimated Using Conventional TCEQ and EPA Methods and Emissions Measured During the Flare Tests [6-2]

Test Point	Run Number	Vent Gas Propylene lb/hr	TCEQ Conventional			EPA	Measured				ARI
			Propylene (99% DRE)	Methane (99% DRE)	Total VOCs	THC	Propylene	Methane	TVOC	THC	DRE
			lb/hr	lb/hr	lb/hr	lb/hr	lb/hr	lb/hr	lb/hr	lb/hr	lb/hr
S3.6	1	189.1	1.89	0.16	1.89	0.57	0.13	0.02	0.15	0.17	99.9
S8.1	1	509.9	5.10	0.45	5.11	1.55	9.92	1.31	11.25	12.66	98.1
S4.1	2	483.9	4.84	0.39	4.85	1.46	19.21	2.53	21.78	24.51	96.0
S5.6	2	312.2	3.12	0.28	3.13	0.95	18.43	2.43	20.20	22.82	94.1
S11.3	1	297.0	2.97	0.26	2.98	0.90	29.61	3.90	32.46	36.67	90.0
A6.1	1	117.8	1.18	0.10	1.18	0.36	0.34	0.05	0.41	0.46	99.7
A6.3	1	117.9	1.18	0.11	1.18	0.36	2.34	0.31	2.80	3.13	98.0
A4.3	3	297.7	2.98	0.27	2.98	0.91	12.23	1.61	13.88	15.61	95.9
A5.5	2	71.5	0.71	0.07	0.72	0.22	4.28	0.56	4.77	5.38	94.0
A6.4	1	118.1	1.18	0.11	1.18	0.36	10.84	1.43	12.09	13.63	90.8

The differences noted in the examples above are largely due to the difference in assumed DRE and the actual DRE. It is also important to note that the species included in the estimate of total VOCs for the conventional method is based on the components in the natural gas and not the actual products of combustion. Table ES-3 lists the species actually measured during the actual flare tests. The actual VOCs produced are the result of the combustion chemistry and the flare operating conditions so an analysis attributing the VOCs to one or more of the constituents in the vent gas is beyond the scope of this project. It is simply important to note that if the specific VOCs that will be produced is important or the attribution of total VOCs produced to the vent gas components is desired, conventional estimation methods do not provide the information needed.

# DRAFT

Major findings of the study were:

1. At a vent gas LHV = 350 Btu/scf and flow rates of 0.1% and 0.25% of rated design capacity (propylene) for the John Zink Models EE-QSC-36" steam and LHTS-24/60 air flares, these flare models were able to achieve DREs (propylene) of > 99% and CE > 99%.
2. The most efficient operation, as measured by the DRE and CE, for the flare operating conditions tested, was achieved at or near the incipient smoke point (ISP). Higher efficiencies could have been achieved with steam or air assist slightly less than the ISP assist value but this condition, i.e., a smoking flare, would not have been in compliance with 40 CFR § 60.18.
3. At LHV = 350 Btu/scf and a nominal vent gas flow rate 937 lb/hr, the recommended steam-assist rates of center = 500 lb/hr and upper = 750 lb/hr did not achieve a DRE (propylene) > 99%. At these conditions, a S/VG = 0.25 or less was required to achieve a DRE (propylene) > 99%. The addition of only 100 lb/hr of center steam changed the DRE from 99.5% to 95.8%.
4. At these low vent gas flow rates (nominally 937 lb/hr and 2,342 lb/hr) and low LHVs (nominally 350 Btu/scf and 600 Btu/scf), the flare performance curve of DRE vs steam assist has a very short to non-existent "shelf" before the DRE falls off to less than 98%. Beyond this point, the DRE and CE decrease almost linearly as steam assist increases.
5. For nominal LHVs of 350 Btu/scf and 600 Btu/scf and vent gas flow rates of 359 lb/hr and 937 lb/hr, air flare test data showed that an air assist quantity of 6 times the stoichiometric air-to-fuel ratio (lb/lb) produced a DRE > 99%. Higher levels of air assist produced lower DREs in an almost linearly decreasing manner.
6. Conventional emission estimation methods provide good estimates of emissions for DRE (propylene) = 99%. However, flare performance was less than DRE (propylene) = 99% for many flare operating conditions tested during this study. For these operating conditions, conventional methods would have assumed DRE (propylene) = 99% and the actual emissions measured were greater than that estimated by the conventional methods.
7. The IMACC PFTIR and AFTIR mean differences between their values of CE and the ARI values of CE averaged 2.0 and 2.5 percentage points, respectively, and had average standard deviations of the CE differences of 2.8 and 3.2 percentage points in the range  $CE_{ARI} \geq 90\%$  for the air and steam flare tests. The PFTIR and AFTIR had average data returns of 99% and 100% in this range.
8. The Telops Hyper-Cam mean differences between their values of CE and the ARI values of CE averaged 19.9 percentage points, with an average standard deviation of the CE differences of 57.8 percentage points in the range  $CE_{ARI} \geq 90\%$ . The Telops Hyper-Cam had average data return of 39% in this range.

# DRAFT

## Table of Contents

Executive Summary	2
List of Figures	32
List of Tables	35
List of Acronyms, Abbreviations and Symbols	36
Acknowledgments	39
1.0 Introduction and Background	40
2.0 Project Scope and Design	41
3.0 Test Plan	46
4.0 Overview of Flare Test Facility and Instrumentation	50
5.0 Results of Flare Tests	66
6.0 Discussion of Test Results	89
7.0 Accuracy and Precision of Plume Sampling System Measurements	95
8.0 Measurements Made by Remote Sensing Technology Instruments	108
9.0 Comparison of Measured Emissions and Conventional Methods for Estimating Emissions	117
10.0 Quality Assurance	120
11.0 Conclusions	125
References	126
Appendices	129
Appendix A – Test Plan	
Appendix B – Flare Tests Facility Description	
Appendix C – Data Quality Objectives	

# DRAFT

Appendix D – Summary of Steam-Assisted Flare Test Data

Appendix E – Summary of Air-Assisted Flare Test Data

Appendix F – Measured and Estimated Flare Emissions Using Conventional Estimation Methods

Appendix G – Method for Determining Vent Gas Composition and Flow Rate

Appendix H – Tulsa Natural Gas Analyses

Appendix I – Method of Determining Destruction Removal Efficiency and Combustion Efficiency Using the Flare Plume Extractive Sampling System and Quality Assurance Procedures Employed During Field Tests

Appendix J – Wind Speed and Direction Variation for Test Series S3, S4, S5, S6, A3, A4, A5, and A6

Appendix K – Quality Assurance Documentation for Test Systems and Instrumentation Used During Field Tests (This Appendix is included on the digital media section of the report. It is available only upon request.)

Appendix L – Video Image and Raw Data Files (This Appendix is included on the digital media section of the report. Due to the size of the electronic files, it is available only upon request.)

# DRAFT

## List of Figures

<b>Figure</b>	<b>Title</b>	<b>Page</b>
ES-1	Flare Plume Sampling System	3
ES-2a	DRE vs Steam Assist for All Test Series S3 and S4	8
ES-2b	CE vs Steam Assist for All Test Series S3 and S4	8
ES-3a	DRE vs Steam-to-Vent Gas Ratio for All Test Series S3 and S4	9
ES-3b	CE vs Steam-to-Vent Gas Ratio for All Test Series S3 and S4	9
ES-4a	DRE vs Steam-to-Vent Gas Ratio for All Test Series S3 and S4	10
ES-4b	CE vs Steam-to-Vent Gas Ratio for All Test Series S3 and S4	10
ES-5a	DRE vs Steam Assist for All Test Series S5 and S6	11
ES-5b	CE vs Steam Assist for All Test Series S5 and S6	11
ES-6a	DRE vs Steam-to-Vent Gas Ratio for All Test Series S5 and S6	13
ES-6b	CE vs Steam-to-Vent Gas Ratio for All Test Series S5 and S6	13
ES-7a	DRE vs Steam-to-Vent Gas Ratio for All Test Series S5 and S6	14
ES-7b	CE vs Steam-to-Vent Gas Ratio for All Test Series S5 and S6	14
ES-8a	DRE vs Vent Gas Flow Rate for Test Series S7, S8, S9, S10 and S11	15
ES-8b	CE vs Vent Gas Flow Rate for Test Series S7, S8, S9, S10 and S11	15
ES-9a	DRE vs CZG NHV for Test Series S3, S4, S5 and S6	16
ES-9b	DRE vs CZG NHV for Test Series S3, S4, S5 and S6	16
ES-10a	DRE vs CZG NHV for Test Series S7, S8, S9, S10 and S11	17
ES-10b	DRE vs CZG NHV for Test Series S7, S8, S9, S10 and S11	17
ES-11a	DRE vs Air Assist for Test Series A3 and A5	19
ES-11b	CE vs Air Assist for Test Series A3 and A5	19
ES-12a	DRE vs Air Assist for Test Series A4 and A6	20
ES-12b	CE vs Air Assist for Test Series A4 and A6	20
ES-13a	DRE vs Vent Gas Flow Rate for Test Series S12, S13 and S14	21
ES-13b	CE vs Vent Gas Flow Rate for Test Series S12, S13 and S14	21
ES-14a	DRE vs Air Assist for Test Series A7	22
ES-14b	CE vs Air Assist for Test Series A7	22
2-1	Flare Burners Used in Study	42
4-1	Overall View of Flare Test Facility	50
4-2	Flare Plume Sampling System During Morning Steam Only Start-up Routine	51
4-3	Flare Burners	52
4-4	Vent Gas Supply	52
4-5	Control Room for the Flare Test System	53
4-6	Control Room Display	53
4-7	Flare Plume Sampling System	54
4-8	Sample Collector at Near Ground Level	55
4-9	Meteorology System	57
4-10	Time Series of Sample Collector Inlet Thermocouples and CO <sub>2</sub> Concentration for Test Point S4.1R1	59
4-11	Sample Collector Location and Wind Data	60
4-12	Time Series of S4.1R1 of CO <sub>2</sub> , CO and Propylene Concentrations of the Dilution Probe	61

# DRAFT

## List of Figures (continued)

<b>Figure</b>	<b>Title</b>	<b>Page</b>
4-13	Propylene and CO <sub>2</sub> Concentrations Relative to CO Concentration in Combustion-Associated Plume Intercept	62
4-14	Time Series for the CO Concentrations and Other Trace Selected Hydrocarbon Species	63
4-15	Correlations of Trace Hydrocarbon Concentration with CO Concentration for S4.1R1	64
5-10a	DRE vs Steam Assist for Test Series S3 and S4	67
5-10b	CE vs Steam Assist for Test Series S3 and S4	67
5-11a	DRE vs Steam Assist for Test Series S3 and S4 Special	68
5-11b	CE vs Steam Assist for Test Series S3 and S4 Special	68
5-12a	DRE vs Steam Assist for All Test Series S3 and S4	70
5-12b	CE vs Steam Assist for All Test Series S3 and S4	70
5-13a	DRE vs Steam Assist for Test Series S5 and S6	72
5-13b	CE vs Steam Assist for Test Series S5 and S6	72
5-14a	DRE vs Steam-to-Vent Gas Ratio for All Test Series S5 and S6	73
5-14b	CE vs Steam-to-Vent Gas Ratio for All Test Series S5 and S6	73
5-15a	DRE vs Steam-to-Vent Gas Ratio for All Test Series S3 and S4	74
5-15b	CE vs Steam-to-Vent Gas Ratio for All Test Series S3 and S4	74
5-16a	DRE vs Steam-to-Vent Gas Ratio for All Test Series S5 and S6	75
5-16b	CE vs Steam-to-Vent Gas Ratio for All Test Series S5 and S6	75
5-17a	DRE vs Steam-to-Vent Gas Ratio for All Test Series S5 and S6	76
5-17b	CE vs Steam-to-Vent Gas Ratio for All Test Series S5 and S6	76
5-18a	DRE vs Vent Gas Flow Rate for Test Series S7, S8, S9, S10 and S11	78
5-18b	CE vs Vent Gas Flow Rate for Test Series S7, S8, S9, S10 and S11	78
5-19a	DRE vs Vent Gas Flow Rate for Test Series S7, S8, S9, S10 and S11	79
5-19b	CE vs Vent Gas Flow Rate for Test Series S7, S8, S9, S10 and S11	79
5-20a	DRE vs CZG NHV for Test Series S3, S4, S5 and S6	81
5-20b	CE vs CZG NHV for Test Series S3, S4, S5 and S6	81
5-21a	DRE vs CZG NHV for Test Series S7, S8, S9, S10 and S11	82
5-21b	CE vs CZG NHV for Test Series S7, S8, S9, S10 and S11	82
5-22a	DRE vs Air Assist for Test Series A3 and A5	84
5-22b	CE vs Air Assist for Test Series A3 and A5	84
5-23a	DRE vs Air Assist for Test Series A4 and A6	85
5-23b	CE vs Air Assist for Test Series A4 and A6	85
5-24a	DRE vs Vent Gas Flow Rate for Test Series S12, S13 and S14	87
5-24b	CE vs Vent Gas Flow Rate for Test Series S12, S13 and S14	87
5-25a	DRE vs Air Assist for Test Series A7	88
5-25b	CE vs Air Assist for Test Series A7	88
7-1	Time Series during Air Flare Tests A5.5R2 and A5.3R2	95
7-2	DRE Instrument Span Error for the 80/20 Propylene/TNG Gas Conditions	99

# DRAFT

## List of Figures (continued)

<b>Figure</b>	<b>Title</b>	<b>Page</b>
7-3	Carbon Fraction of Propylene in the Vent Gas for the 80/20 Propylene/TNG Composition	101
7-4	DRE Variability Analysis for S4.6R1	103
7-5	Grouping by Sample Collector Height (z)	104
7-6	Histogram of Second-by-Second DRE Grouped by Sample Collector Height	105
8-1	Comparison of All Remote Sensing Measurements Made To ARI Steam Flare CE Measurements	110
8-2	Comparison of All Remote Sensing Measurements Made To ARI Air Flare CE Measurements	110
8-3	Comparison of All Remote Sensing Measurements Made To ARI Steam Flare CE Measurements $\geq 95\%$	112
8-4	Comparison of All Remote Sensing Measurements Made To ARI Steam Flare CE Measurements $90\% \leq CE_{ARI} < 95\%$	112
8-5	Comparison of All Remote Sensing Measurements Made To ARI Steam Flare CE Measurements $85\% \leq CE_{ARI} < 90\%$	113
8-6	Comparison of All Remote Sensing Measurements Made To ARI Steam Flare CE Measurements $80\% \leq CE_{ARI} < 85\%$	113
8-7	Comparison of All Remote Sensing Measurements Made To ARI Air Flare CE Measurements $\geq 95\%$	115
8-8	Comparison of All Remote Sensing Measurements Made To ARI Air Flare CE Measurements $90\% \leq CE_{ARI} < 95\%$	115
8-9	Comparison of All Remote Sensing Measurements Made To ARI Air Flare CE Measurements $85\% \leq CE_{ARI} < 90\%$	116
8-10	Comparison of All Remote Sensing Measurements Made To ARI Air Flare CE Measurements $80\% \leq CE_{ARI} < 85\%$	116
10-1	LSI Four-Way Video Images	122

# DRAFT

## List of Tables

<b>Table</b>	<b>Title</b>	<b>Page</b>
ES-1	Summary of Flare Test Plan	6
ES-2	Summary of Comparison Criteria for Remote Sensing CE Values for $CE_{ARI} > 80\%$	25
ES-3	List of Hydrocarbons Typically Found in Plume During Propylene Flare Tests	27
ES-4	Summary of Selected Emissions Estimated Using Conventional TCEQ and EPA Methods and Emissions Measured During the Flare Tests	28
3-1	Summary of Flare Test Plan	47
4-1	Fit Parameters for Selected Trace Hydrocarbons for S4.1R1	64
7-1	Measurement Accuracy and Calibration Checks for Selected Species	98
7-2	Instrument Precision Specifications	100
7-3	Summary of Second-by-Second DRE by Sample Collector Height Groups	106
7-4	Estimated DRE Based on Slope Approach for Each Sample Collector Height Group	106
8-1	Summary of Comparison Criteria for Remote Sensing CE Values for $CE_{ARI} > 80\%$	111
9-1	List of Hydrocarbons Typically Found in Plume During Propylene Flare Tests	118
9-2	Summary of Selected Emissions Estimated Using Conventional TCEQ and EPA Methods and Emissions Measured During the Flare Tests	119
10-1	Repeatability of Test Results	124

# DRAFT

## List Acronyms, Abbreviations and Symbols

### A

A/F	Theoretical stoichiometric air-to-fuel ratio, mass basis (lb/lb)
ARI	Aerodyne Research, Inc.
AFTIR	Active Fourier Transform Infrared

### B

Btu	British thermal unit
-----	----------------------

### C

CE	Combustion efficiency
CEER	Center for Energy and Environmental Resources
CFD	Computational Fluid Dynamics
CFR	Code of Federal Regulations
CH <sub>3</sub> CHO	Acetaldehyde
CH <sub>4</sub>	Methane
C <sub>2</sub> H <sub>4</sub>	Ethylene, ethene
C <sub>3</sub> H <sub>6</sub>	Propylene, propene
CO	Carbon monoxide
CO <sub>2</sub>	Carbon dioxide

### D

°	Degree of temperature
°F	Degree Fahrenheit
DQO	Data Quality Objective
DRE	Destruction and removal efficiency

### E

EPA	U.S. Environmental Protection Agency
-----	--------------------------------------

### F

FLIR	Forward Looking Infrared
fps	Feet per second
ft <sup>2</sup>	Feet squared

### G

GC	Gas Chromatograph
GPS	Global Positioning System

### H

HCHO	Formaldehyde
HCOOH	Formic acid

# DRAFT

## I

IMACC	Industrial Monitor and Control Corporation
in	Inch
IR	Infrared
ISP	Incipient smoke point

## J

JZ	John Zink Company, LLC
----	------------------------

## L

lb/hr	Pounds per hour
LHV	Lower Heating Value
LL	Lower Limits
LSI	Leak Surveys, Inc.

## M

MPH	Miles per hour
mm/Hg	Millimeters of mercury
min	Minutes

## N

NA	Not Applicable
NO	Nitric oxide
NO <sub>2</sub>	Nitrogen dioxide
No.	Number

## O

O <sub>3</sub>	Ozone
----------------	-------

## P

%	Percent
PFTIR	Passive Fourier Transforms Infrared
PGA	Proposal for Grant Activities
ppbC	Parts per billion carbon
ppbv	Parts per billion volume
ppm	Parts per million
ppmC	Parts per million carbon
ppmv	Parts per million volume
pptv	Parts per trillion volume
psia	Pounds per square inch absolute
±	Plus or minus

# DRAFT

## Q

QA	Quality Assurance
QAPP	Quality Assurance Project Plan
QC	Quality Control

## S

sec	Seconds
scf	Standard cubic feet
scfm	Standard cubic feet per minute
SO <sub>2</sub>	Sulfur dioxide
ó	Standard deviation
SA	Stoichiometric air

## T

TCEQ	Texas Commission on Environmental Quality
THC	Total hydrocarbons
TRC	TRC Company
TNG	Tulsa Natural Gas

## U

UT Austin	The University of Texas at Austin
-----------	-----------------------------------

## V

VOC	Volatile organic compound
vs	Versus

## W

WD	Wind direction
WS	Wind speed

## Z

ZINK	John Zink Company, LLC
------	------------------------

# DRAFT

## Acknowledgements

The 2010 TCEQ Flare Study Project Team express their appreciation to the project sponsors: the Texas Commission on Environmental Quality and the State of Texas Air Quality Research Program for their financial and technical support. In particular, we express our appreciation to Ms. Danielle Nesvacil and Mr. Russ Nettles, TCEQ Project Managers, whose input, support and guidance have been greatly appreciated.

We also express our appreciation to the TCEQ's Technical Review Panel:

Peter E. G. Gogolek, Ph.D., CanmetENERGY, Canada  
John Pohl, SC.D., Virginia Polytechnic Institute and State University  
Eben Thoma, Ph.D., U.S. Environmental Protection Agency,

for their technical input and review of the QAPP and preliminary and final project reports.

We want to thank those who visited and observed the tests at the John Zink Test Facility and the organizations they represented: Lucy Randel, Industry Professionals for Clean Air; Bruce Davis, Texas Chemical Council; Scot Evans and Steve Smith, Texas Oil and Gas Association; and Brian Dickens, Eben Thoma, and Edgar Thompson, US EPA.

Finally, we express our thanks to the John Zink, LLC flare test facility team:

Scott Fox	Vice President, Flare Systems Division
Robert Schwartz	Project Representative / Project Director
Wes Bussman	Project Quality Assurance Officer
Zachary Kodesh	Project Operations Officer
Richard Lawhead	Test Center Technician, steam / fuel control
Clifford Pugh	Test Center Technician, steam / fuel control
Garrett Spaulding	Test Center Technician, steam / fuel control
	Test Center Technician, chain gang lead, Instrumentation
Charlie Crown	Test Center Technician, chain gang
Michael Bryant	Test Center Technician, chain gang
Chris Patrick	Test Center Technician, instrumentation
Craig Skaggs	Test Center Supervisor, fuel supply coordinator
Leon Longacre	Test Center Safety Manager
Dan Doss	Test Center Manager
Jerry Buhler	
Crane Operator	
Joe Potter	Belger Cartage Service, Inc.

whose hard work, cooperation and support helped make the flare testing a success.

# DRAFT

## 1.0 Introduction and Background

The results of previous research funded by and work performed for the Texas Commission on Environmental Quality (TCEQ) indicated a need to conduct a study to determine the relationship between flare design, operation and destruction and removal efficiency (DRE) (NPL 2008, URS 2004). In May 2009, the TCEQ contracted with The University of Texas at Austin (UT Austin) to conduct the 2010 TCEQ Flare Study project (PGA No. 582-8-86245-fy09-04, Tracking Number 2008-81) (TCEQ, 2009). The purpose of the 2010 TCEQ Flare Study project was to conduct field tests to measure flare emissions and collect process and operational data in a semi-controlled environment to determine the relationship between flare design, operation, vent gas lower heating value (LHV) and flow rate, DRE, and combustion efficiency (CE). Because the study was conducted outdoors, in a full-scale test facility, there was no attempt to control ambient conditions, i.e., temperature, humidity and wind speed and direction. It was anticipated that the results of these field tests would provide insight into operational conditions that may impact flare volatile organic compound (VOC) DRE and flare CE, such as assist rates or vent gas volumetric flow rates. In August 2010, the Air Quality Research Program funded a project (Task Order No. UTA10-000924-LOAT-RP9) that supplemented funding for this study.

This final report is submitted to fulfill the requirements of PGA No. 582-8-86245-fy09-04, Tracking Number 2008-81, Task 10 and Task Order No. UTA10-000924-LOAT-RP9, Task 1 and presents the results for this project and the data collected to address the Study Objectives (see Section 2.0), as defined by the TCEQ.

During this study and, in particular the field tests, data were collected that provided the information needed to address the Study Objectives. Due to excellent weather conditions, no major equipment problems that affected data quality, and efficient planning of the test series, the study team was able to collect data on almost 96% more test runs on the steam-assisted test flare and 27% more test runs on the air-assisted test flare than originally planned. The data collected are a valuable resource for addressing many questions related to flare operation and performance; however, work to date has focused on addressing the Study Objectives. The Study team recognizes that follow-on work with the data collected in this project would be valuable and looks forward to the opportunity to participate in those analyses.

# DRAFT

## 2.0 Project Scope and Design

UT Austin was contracted to measure flare emissions in a semi-controlled environment and collect and analyze process and operational data to fulfill TCEQ's study objectives for the project. The TCEQ's primary study objectives, in order of decreasing priority, were:

- Assess the potential impact of high vent gas flow rate turndown on flare CE and VOC DRE;
- Assess the potential impact of steam and air assist on flare CE and VOC DRE at various operating conditions, including low vent gas flow rates, i.e., high vent gas flow rate turndown;
- Determine whether flares operating over the range of requirements stated in 40 Code of Federal Regulations (CFR) § 60.18 achieve the assumed hydrocarbon DRE of 98% at varying vent gas flow rate turndown, assist ratios, and waste stream heat content; and
- Identify and quantify the hydrocarbon species in flare plumes visualized with passive infrared cameras.

In this study, the term vent gas will be used to represent the waste gas stream that would be sent to the flare for destruction in an industrial facility. The terms flare plume and plume will always refer to the total stream of gas that leaves the flare tip and changes composition due to some level of combustion.

### Industrial Scale Flares

Extensive research has been conducted in controlled environments on devices that are not full-scale flares, i.e., with diameters less than three inches as opposed to industrial scale flares, which are typically on the order of multiple feet in diameter and can be as large as ten feet in diameter. To make the results of this study most directly applicable to industrial scale operations, the TCEQ required that the field tests performed for this study be conducted on full-scale industrial design flares. Specifically, the TCEQ required that both air-and steam-assisted flares be included in the study and that the minimum design capacity and diameter of the flare burners be one million lb/hr and 36 inches, respectively. While these minimum specifications were appropriate for steam-assisted flares, a comparable design capacity for an air-assisted flare would mean the nominal diameter of the air flare would need to be about 4 feet to comply with the maximum exit velocity limitation of 40 CFR § 60.18, which was also a requirement of the study. This diameter for an air-assisted flare would not typically represent the size of flares currently found in the field as reported by John Zink Company, LLC (Zink) representatives (email from Z. Kodesh to V. Torres, UT Austin, February 15, 2010). So, this specification was modified to include an air-assisted flare burner representative of a design and size typically found in the field.

There are multiple flare manufacturers who have a wide range of proprietary flare burner designs. It was not within the scope of this project to attempt to test representative samples of every different flare design each with its own set of design options. Instead, the decision was made to select one design of an air flare and one design of a steam flare that would represent a large number of flare burners currently in the field. Zink was asked to identify models of flares, based on their market data, which satisfied this criterion. Additionally, the TCEQ required that

# DRAFT

the steam flare design selected have both center and upper steam assist. Based on these requirements for the flare burners, the John Zink Models EE-QSC-36" Flare Tip with (3) EEP-503 pilots and the LHTS-24/60 with (3) Pilots were selected for the steam flare and air flares, respectively.



Figure 2-1. Flare Burners Used in Study. Air Flare John Zink Model LHTS-24/60 (left) and Steam Flare John Zink Model EE-QSC-36" Flare Tip (right) used in the study

## **Controlled Environment Laboratory**

To measure flare emissions on full-scale flares in a semi-controlled environment (i.e., controlled flare operations but uncontrolled ambient conditions), UT Austin decided to conduct the study at the outdoor flare test facility of Zink in Tulsa, Oklahoma. Zink is a flare tip manufacturer whose flare test facility is capable of accommodating a wide range of flare tips, test configurations and operating conditions. Once the flare test configurations were made at their facility and approved by UT Austin, Zink dedicated their flare test facility exclusively to this project with uninterrupted operation for the duration of the study, which lasted almost three weeks.

# DRAFT

## Measurement of Flare Emissions

A core element of UT Austin's study approach was to directly measure flare emissions at the end of the flare plume, and calculate DRE and CE based on those measurements. To measure these emissions, UT Austin selected Aerodyne Research, Inc., (ARI) due to their extensive experience in ambient air quality studies and their unique capability to make continuous (1 Hz frequency) measurements of the chemical species expected to be present in the flare plume. These direct measurements of the flare emissions serve as the primary data used to address the study objectives.

## Compare Remote Sensing Technologies

The TCEQ also required that remote sensing technologies be included in the study and a comparison of their performance be included in the study results. The following remote sensing measurement methods were specified by the TCEQ for inclusion in this study (TCEQ, 2009):

1. Infrared Hyper-Spectral Imaging Technology (Contractor: Telops Inc.)  
Identify flare hydrocarbon plume species and determine plume species concentrations.
2. Passive Fourier Transform Infrared (PFTIR) Spectroscopy (Contractor: Industrial Monitor and Control Corporation)  
Collect the required data to determine flare combustion efficiency.
3. FLIR GasFindIR Passive Infrared (IR) Cameras (Contractor: Leak Surveys Inc.) Provide a visual comparison of IR images to the infrared hyper-spectral imaging technology results, and assist other remote sensing tools to take measurements.

During the course of the study planning, UT Austin recommended that Active Fourier Transform Infrared (AFTIR) spectroscopy also be considered for comparison with these remote sensing technologies as this instrument is reported to be able to detect all organics and have better performance (Hashmonay 2010) in minimum detection levels and data quality than the PFTIR, thereby having greater precision in the determination of CE than the PFTIR systems (email from R. Spellicy, IMACC to E. Michel, UT Austin May 19, 2010).

It was also decided by the UT Team that a single blind approach should be used to compare the remote sensing technology measurements, i.e., the only information provided to the contractors performing remote sensing measurements was that which would be provided to them if they were engaged to measure combustion efficiencies at an industrial facility. The results of the CE and DRE measurements made by ARI were not made available to the remote sensing teams until this report was released to the public.

## Performance and Comparison Metrics

VOC DRE was selected by the TCEQ to be the primary metric for assessing flare performance. TCEQ selected this metric because of the critical role VOCs play in contributing to the formation of ozone. CE was selected as a secondary metric because the remote sensing technologies included in the study can only measure CE. DRE (hydrocarbon species X) is the percentage of species X that is destroyed relative to the quantity of species X entering the flare. Numerically, this is represented as

# DRAFT

$$DRE (\%) = \left(1 - \frac{X_{plume}}{X_{in}}\right) \times 100 \quad \text{Eq. 1.1}$$

where

DRE (%) = destruction and removal efficiency (%)

$X_{plume}$  = flow rate of hydrocarbon species X found in the flare plume after combustion has ceased

$X_{in}$  = flow rate of hydrocarbon species X entering the flare

CE is the percentage of the total hydrocarbon stream entering the flare that burns completely to form only carbon dioxide and water. Numerically, this is represented as

$$CE (\%) = \left(\frac{CO_2 (plume)}{CO_2 (plume) + CO (plume) + \Sigma \text{hydrocarbons} (plume)}\right) \times 100 \quad \text{Eq. 1.2}$$

where

CE (%) = combustion efficiency (%)

$CO_2 (plume)$  = volume concentration of carbon dioxide in the plume (ppmv)

$CO (plume)$  = volume concentration of carbon monoxide in the plume (ppmv)

$\Sigma \text{hydrocarbons} (plume)$  = volume concentration of all the unburned hydrocarbons in the plume multiplied by the number of carbons for each hydrocarbon (ppmC)

## Vent Gas Composition and Flow Rates

For this study, the TCEQ specified that the vent gas composition should be a mixture of natural gas, propylene and nitrogen. The ratio of the natural gas to propylene was to be 1:4 by volume. Nitrogen would be used as the diluent to achieve the desired LHV for the vent gas. This study focused on vent gases with low LHV and low flow rates. Flare performance data representative of vent gas streams with LHVs close to 300 Btu/scf was desired by the TCEQ. This range of LHVs was selected because it is at the lowest end of the LHVs allowed by 40 CFR § 60.18 for hydrocarbon streams (300 Btu/scf) in assisted flares.

The desired range of vent gas flow rates to be used was 0.1% to 0.25% of the flare's design capacity. Vent gas flow rates of 0.1% and 0.25% of nominal design capacity were selected as they are in the range of operation for typical flow rates (less than 0.5%) used in industry. These flow rates account for approximately 25% of flare operation time (Environ International Corporation, 2009) and introduce the greatest probability for over-assisted operation of steam flares because of some minimum levels of steam assist recommended to industry by flare manufacturers, 500 lb/hr center, 750 lb/hr upper, for the size and model of steam flare used in this study (email message from R. Nettles, TCEQ, to V. Torres, UT Austin, on September 8, 2010), potentially producing less than a 98% DRE (Marathon June 2010, Marathon November

# DRAFT

2010). It was desired to increase the range to 0.5% of maximum design capacity for both the steam and air flares but the Zink test facility would not have been able to provide the nitrogen gas flow rates needed to achieve the LHVs specified by the TCEQ for the steam flare. Therefore, the vent gas flow rates used for the air flare were increased to 0.25% and 0.65% of the maximum design capacity of the air flare.

## **Quality Assurance**

UT Austin prepared a Category 2 Quality Assurance Project Plan (The University of Texas at Austin, 2010) for this project that complied with the requirements of the Environmental Protection Agency's (EPA) *Requirements for Quality Assurance Project Plans*, EPA QA/R-5, and *Guidance for Quality Assurance Project Plans*, EPA QA/G-5. This QAPP was posted for public comment by the TCEQ and was reviewed by the EPA.

## **Reference Values and Standard Conditions**

The reference values for properties of gases used during the test and for subsequent calculations and analyses are taken from *Perry's Chemical Engineer's Handbook, 8<sup>th</sup> Edition*, 2008, unless otherwise stated. Standard conditions used in this study are atmospheric pressure = 14.696 psia and 68°F.

# DRAFT

## 3.0 Test Plan

UT Austin worked with Zink, ARI and the TCEQ to develop a test plan that would provide data that would form the basis for addressing as many of the study objectives as possible within the project schedule and available budget (\$2,191,332). The test plan developed for the study is included in Appendix A. A summary of the test series actually conducted is shown in Table 1, where steam flare tests begin with the letter “S” in the designation of the test series and air flare tests begin with the letter “A”. The test plan consisted of multiple flare test series conducted on the air-assisted flare tip and multiple test series conducted on the steam-assisted flare tip. The designation used to identify each test point and run was: S[number X].[number Y]R[number Z], where the number X is the test series number, number Y designates the level of assist (air or steam) used in the test series and number Z is the run or repetition number for the test point. So, for example, S3.2R2, is steam flare test series number 3, the second assist condition tested, repetition number 2.

As stated in the previous section, the TCEQ specified that the vent gas be a mixture of natural gas (Tulsa Natural Gas was available at the Zink test facility) and propylene (1:4 ratio by volume) diluted with nitrogen to achieve the desired LHV. To focus on low LHV vent gas streams and still comply with 40 CFR § 60.18, a LHV of 350 Btu/scf  $\pm$  50 Btu/scf was selected as the lowest target LHV for the vent gases used in the Test Plan. To obtain additional data on the effect of LHV on DRE and CE, a second LHV of 600 Btu/scf  $\pm$  80 Btu/scf was also included in the Test Plan.

The steam flare burner used for this study had a design capacity of 937,000 lb/hr for use with propylene. Therefore the 0.1% and 0.25% of design capacity vent gas flow rates for this flare are 937 lb/hr and 2,342 lb/hr, respectively. These two flow rates were the target vent gas flow rates used for the steam flare tests. The air flare burner used for this study had a design capacity of 144,000 lb/hr for use with propylene. The 0.25% and 0.65% of design capacity vent gas flow rates for this flare are 359 lb/hr and 937 lb/hr, respectively. These two flow rates were the target vent gas flow rates used for the air flare tests.

# DRAFT

**Table 3-1. Summary of Flare Test Plan**

**Steam Flare Tests**

Test Series	Vent Gas (Nominal)			Target (Nominal) Steam Assist (lb/hr)	
	Flow Rate lb/hr	LHV Btu/scf	Composition %	Center	Upper
S1	2342	2149	100% Propylene	500	ISP to <Snuff
S2	937	2149	100% Propylene	500	ISP to <Snuff
S3	937	350	20:80 TNG to Propylene Ratio Diluted to Target LHV	500	ISP to <Snuff
S3	937	350	20:80 TNG to Propylene Ratio Diluted to Target LHV	100	230
S3	937	350	20:80 TNG to Propylene Ratio Diluted to Target LHV	0	230
S3	937	350	20:80 TNG to Propylene Ratio Diluted to Target LHV	0	0
S4	2342	350	20:80 TNG to Propylene Ratio Diluted to Target LHV	500	ISP to <Snuff
S4	2342	350	20:80 TNG to Propylene Ratio Diluted to Target LHV	330	110
S4	2342	350	20:80 TNG to Propylene Ratio Diluted to Target LHV	0	330
S5	937	600	20:80 TNG to Propylene Ratio Diluted to Target LHV	500	ISP to <Snuff
S6	2342	600	20:80 TNG to Propylene Ratio Diluted to Target LHV	500	ISP to <Snuff
S7	2342 - 937	350	20:80 TNG to Propylene Ratio Diluted to Target LHV	500	525
S8	2342 - 937	350	20:80 TNG to Propylene Ratio Diluted to Target LHV	0	500
S9	2342 - 937	350	20:80 TNG to Propylene Ratio Diluted to Target LHV	0	1025
S10	2342 - 937	350	20:80 TNG to Propylene Ratio Diluted to Target LHV	0	825
S11	2342 - 937	350	20:80 TNG to Propylene Ratio Diluted to Target LHV	300	525
S12	2342 - 937	350	20:80 TNG to Propane Ratio Diluted to Target LHV	500	525
S13	2342 - 937	350	20:80 TNG to Propane Ratio Diluted to Target LHV	325	525
S14	2342 - 937	350	20:80 TNG to Propane Ratio Diluted to Target LHV	0	525

TNG = Tulsa Natural Gas  
 Snuff = Visible flame extinguished  
 ISP = Incipient Smoke Point  
 LHV = Lower Heating Value

**Air Flare Test Tests**

Test Series	Vent Gas (Targets)			Target (Nominal) Air Assist (lb/hr)
	Flow Rate lb/hr	LHV Btu/scf	Composition %	
A1	937	2149	100 % Propylene	ISP to <Snuff
A2	359	2149	100 % Propylene	ISP to <Snuff
A3	937	350	20:80 TNG to Propylene Ratio Diluted to Target LHV	ISP to <Snuff
A4	937	600	20:80 TNG to Propylene Ratio Diluted to Target LHV	ISP to <Snuff
A5	359	350	20:80 TNG to Propylene Ratio Diluted to Target LHV	ISP to <Snuff
A6	359	600	20:80 TNG to Propylene Ratio Diluted to Target LHV	ISP to <Snuff
A7	359	350	20:80 TNG to Propane Ratio Diluted to Target LHV	ISP to <Snuff

TNG = Tulsa Natural Gas  
 Snuff = Visible flame extinguished  
 ISP = Incipient Smoke Point  
 LHV = Lower Heating Value

# DRAFT

The range of steam or air assist values to be used in this study was bracketed on the lower end by the incipient smoke point and on the upper end by the snuff point. The definition of incipient smoke point (ISP) used for this project is the point of operation of the flare with the minimum amount of air or steam required, as appropriate for the flare type, so that no visible smoke emissions are observed two flame lengths away from the flare tip. For this study, as defined in the QAPP, a panel of three people, R. Schwartz (Zink), R. Nettles (TCEQ), and V. Torres (UT Austin), determined when this criterion was achieved. The snuff point is the point when the visible flame has been extinguished, i.e., no visible combustion is occurring at the flare. Visible smoke emissions are defined in this study as the appearance of a group of black particles produced by the flare combustion process. A requirement of this study was that all data be obtained at flare operating points that comply with 40 CFR § 60.18. A requirement of 40 CFR § 60.18 is that flares be operated with no visible smoke emissions, except for periods not to exceed 5 minutes during any two consecutive hours. If the vent gas in a flare does produce smoke during combustion, then the ISP air or steam assist value represents the flare operating point of minimum assist that achieves compliance with 40 CFR § 60.18. So the incipient smoke point was selected as the lower end of the range of steam or air assist values used for the study.

The snuff point was selected as the upper bound of the range of steam or air assist and the value beyond which there is no further visible flare combustion occurring and therefore no further change in DRE or CE. In practice, the snuff point was never attained during this study before the maximum level of steam or air assist that the Zink test facility was able to provide was reached. So the snuff point was a target not an actually achievable operating point at the maximum level of assist used in any test series.

The target flow rate used for center steam was 500 lb/hr. This value was selected for use as it represented the level reported to the TCEQ by industry (email message from R. Nettles, TCEQ, to V. Torres, UT Austin, on September 8, 2010) as the value recommended most frequently for use by flare burner manufacturers. Zink also agreed (meeting with J. Franklin and Z. Kodesh, Zink with E. Michel and V. Torres, UT Austin, and D. Nesvacil and R. Nettles, TCEQ, on February 11, 2010) that this would be a reasonable level to use with the Zink model steam-assisted flare burner that was to be used on this project.

The Test Plan was designed to systematically vary only one flare operational parameter at a time while holding all other parameters constant. The approach used in implementation of the test plan and reflected in the Test Plan in Appendix A was to start a test series using one of the two study vent gas flow rates (0.1% or 0.25% of flare design capacity) and one of the two study LHVs (350 Btu/scf or 600 Btu/scf) and begin the first test point of the test series with the ISP level of steam or air assist. After data were collected for that test point and while maintaining this vent gas flow rate and LHV, the assist would be increased to the snuff point as the second test point in the series. Then, two more steam or air assist levels between the ISP level and the snuff point would be run to complete the test series for a total of four test points, minimum, per test series. For the core test series, these same test points would be repeated two more times. For the next test series, this process would be repeated with the other LHV. If the 0.1% vent gas flow rate were used first, then the next test series would use the 0.25% vent gas flow rate and this whole process repeated with this vent gas flow rate.

# DRAFT

Test series S1, S2, A1, and A2 do not contain mixtures of natural gas and propylene. These tests were included as preparatory tests to allow all participants to practice with their equipment and optimize their measurement process on the specific flare about to be tested. The data from these tests are not included the data analysis of this study.

Test series S3, S4, S5, S6, A3, A4, A5, and A6 are the core test series that were identified in the Study Plan. Because of very favorable weather conditions and no major equipment problems affecting data quality, the core test series were completed in less time than anticipated and tests in addition to the core test series could be conducted. In compliance with Appendix E, Flare Test Plan Modification Procedure, of the QAPP, a strategy was proposed for conducting additional tests that were not part of the original test plan. The strategy for conducting the additional tests was to run more operating points, which would help to better define the efficiency curve, and fewer, if any, repetitions. Preliminary data indicated that reproducibility of estimated DRE during the repetitions of the core test series was high with a percent standard deviation of less than 5%. (The percent standard deviation being equal to the standard deviation of the DREs for the three repetitions divided by the average DRE for the repetitions.) Another strategy incorporated in the proposal for more tests was to hold steam assist constant and vary vent gas flow rate rather than holding vent gas flow rate constant and varying steam assist. This strategy was proposed because during the core test series it was found that the Zink test facilities had greater difficulty making small incremental increases/decreases in steam flow rates and then returning to reproduce the same steam flow rate. Zink could more easily hold steam rate constant and quickly vary and stabilize the vent gas flow rate. So Test Series S7, S8, S9, S10, S11, S12, S13, S14 and A7 have few, if any repetitions. These test series are conducted at constant nominal steam assist levels (for the S test series) with the vent gas flow rates as the variable during the test series.

One additional test plan modification was the inclusion of propane instead of propylene. Test Series S12, S13, S14, and A7 are test runs substituting propane for propylene. All other parameters remained the same as in the propylene runs for these four test series.

The ARI team collected data in all of the test series, and the IMACC PFTIR and Telops Hyper-Cam collected data during the entire field test campaign. The IMACC AFTIR participated in the core steam tests but did not participate in the air flare tests as the air flare test configuration and height limitations of the scissor lifts supporting the reflectors would have prevented proper alignment of the camera, reflectors, and air flare plume. The data return (percent of test points reporting data relative to the total number of test points conducted) for all quality assured data reported in time to include in this report is reflected in the summary of test data in Appendices D and E.

# DRAFT

## 4.0 Overview of Flare Test Facility and Instrumentation

Once the test plan was developed, UT Austin worked with ARI and Zink to design the test facility and instrumentation needed to make measurements of all the flare operational parameters and flare emissions in the plume. A brief description of the test facility and instrumentation follow. A detailed description the major test facility equipment and instrumentation is included in Appendix B.

The flare test facility was composed of two major systems: the flare test system (Figure 4-1) and the flare plume sampling system (Figure 4-2). The flare test system consisted of the flare burners (air- and steam-assisted), the vent gas supply system, the air- or steam-assist system and the flare control room. The flare plume sampling system consisted of the sample collector, the eductor, global positioning system, crane, meteorology system, and the sampling probes and lines.



Figure 4-1. Overall View of Flare Test Facility

# DRAFT



Figure 4-2. Flare Plume Sampling System During Morning Steam Only Start-up Routine

The operation of the flare burners (Figure 4-3) were controlled by Zink personnel and monitored using their standard process and control instrumentation with additional instrumentation and sampling ports added for this study where necessary. Vent gas supply (Figure 4-4) was controlled, flow rates measured and blended at the vent gas supply station before being sent to the flare. All operating data were recorded in a data acquisition system in the flare control room (Figures 4-5 and 4-6).

To verify and determine the actual composition of the vent gas being used during each test run, a stack testing company, TRC, was employed to provide measurements of the vent gas composition entering the flare from a sample obtained at the beginning of the test run and one five minutes later. From these same samples, TRC made measurements of propylene/propane, methane and ethane in the flare plume as a back-up to ARI's primary determination of DRE and CE. Appendix G describes the method used to calculate the vent gas composition and flow rate from the TRC and Zink measurements.

The exits of the steam- and air-assisted flare burners were 13 and 33 feet above ground level, respectively.

# DRAFT



Figure 4-3. Flare Burners. Air-assisted on left and steam-assisted on right



Figure 4-4. Vent Gas Supply. Piping for flow control, mixing and measurement of the vent gas supply

# DRAFT



Figure 4-5. Control Room for the Flare Test System



Figure 4-6. Control Room Display. Monitor displayed Zink measurement of flare operating parameters (top left), LSI's FLIR and IR video (right half) and ARI's flare emissions measurements (bottom left)

# DRAFT

## *Flare Plume Sampling System*

The primary component of the Flare Plume Sampling System (Figure 4-7) was the sample collector. The goal of this sample collector (Figure 4-8) was to determine the “plume average” DRE and CE for a given set of flare operating conditions. It was not to determine the instantaneous combustion efficiency at a given point in the active combustion zone of the plume. Therefore, the sampler collector was designed to continuously draw as large a sample of the plume as possible, homogenize the sample and then obtain a sample of this well mixed portion of the plume for analysis.



Figure 4-7. Flare Plume Sampling System. Plume sampling system making measurements of flare plume while held in position by crane and ground crew

The sample collector was moved into position so that during a test it was located approximately in the center of the flare plume at a distance far enough downwind from the flare tip to ensure that combustion reactions had ceased and with the face of the inlet oriented perpendicular to the travel of the plume. The method used as the gauge to know that the collector inlet was past the

# DRAFT

combustion zone was to position the inlet to the sample collector so that the plume temperature at the inlet was 250°F or less, as measured by three thermocouples in the inlet to the sample collector. The position of the sample collector at the midpoint of the plume was facilitated using the visual, two FLIR and one IR video camera images (Figure 4-6) filmed by Leak Surveys, Inc. (LSI) and the temperature of the flare plume as it entered the sample collector. The two FLIR cameras were positioned to view the flame approximately perpendicular to the plume and coincident with the wind direction.

The eductor (Figure 4-8) of the sample collector would continuously draw approximately 1950 cfm of flare plume through the collector. The inlet of the sample collector was 20 inches in diameter with an effective draw of more than 24 inches in diameter. A mixing and flow conditioning section at the entrance to the sample collector would mix and then straighten the flow prior to reaching ARI's and TRC's sampling probes. Samples (approximately 1 liter per minute for the vent gas sample line and 8 liters per minute for plume sample line) would be continuously drawn through the sample lines to the analyzers and instruments in each company's mobile laboratory trailers (Figure 4-8).



Figure 4-8. Sample Collector at Near Ground Level. Collector inlet is at foreground and eductor is at far end. In photo, Zink personnel make adjustments to heated transfer line supports. Shackles and cable at center allow crane to lift and position Sample Collector.

# DRAFT

The height of the sample collector inlet was tracked using a graduated chain attached to the sample collector. Zink personnel on the ground would also report the radial distance from the inlet of the sample collector to the center of the flare burner to the control room, where it would be logged. ARI also tracked the position of the inlet to the sample collector using a global positioning system (GPS) attached to the sample collector.

TRC used gas chromatography to analyze both flare stack and plume gases (methane, ethane and propylene). Two grab samples were collected per test run, 5 minutes apart. Flare plume constituents (CO, CO<sub>2</sub>, O<sub>2</sub>, speciated VOCs, HCHO, NO<sub>x</sub>, particulate matter and THC) were measured continuously (1 Hz) by ARI using their mobile laboratory, which has two dual quantum cascade laser instruments and several LiCOR non-dispersive infrared sensor instruments. Destruction removal and combustion efficiencies were calculated based on the measurements of TRC (vent gas) and the ARI (flare plume) measurements using the carbon content of the constituents in the vent gas and flare plume. A detailed description of the method used to calculate the DRE and CE by ARI is included in Appendix I. A discussion of the accuracy and precision of these values is presented in Section 6.0.

Meteorology measurements, i.e., wind speed, direction, temperature, and barometric pressure, were made to characterize the speed and direction of the cross wind at the exit of the flare burners. These measurements were made by ARI (Figure 4-9).

# DRAFT



Figure 4-9. Meteorology System

## Method for Measurement of Flare Emissions and Calculation of DRE and CE

This section describes the methodology used to compute DRE and CE from the time series of measurements on the sample line. A more detailed description of this derivation can be found in Appendix I. The discussion of the sources of error in this approach is outlined in Section 7. The purpose of the description here is to go through an event analysis and describe the computational steps.

The two fundamental characteristics of interest in this test are DRE and CE. The equations that define these quantities have been discussed previously, Equation 1.1 and 1.2. Appendix I derives an alternative form of Equation 1.1, labeled here as Equation 4.1

$$DRE/100 = 1 - \frac{\left[ \frac{\text{propylene}_{out} \text{ (molesC)}}{C_{out} \text{ (molesC)}} \right]}{\left[ \frac{\text{propylene}_{in} \text{ (molesC)}}{C_{in} \text{ (molesC)}} \right]} = 1 - \frac{CF^{propylene} \text{ (out)}}{CF^{propylene} \text{ (in)}} \quad \text{Eq. 4.1}$$

# DRAFT

where  $CF^{propylene} (in)$  is based on the fraction of carbon found as propylene in the vent gas mixture. Nominally, in the 80% propylene, 20% TNG mixture this can be approximated as

$$CF^{propylene} (in) = \frac{propylene (ppmC)}{propylene (ppmC) + methane (ppmC) + \sum other carbon (ppmC)}$$

Eq. 4.2

or

$$CF^{propylene} (in) = \frac{3 * 0.8}{3 * 0.8 + 1 * 0.2 + \sum other carbon (ppmC)} \approx 0.923$$

Eq. 4.3

where the contribution of other carbon constituents in the Tulsa Natural Gas are considered to be negligible. Note that for the actual computation of DRE, the measurement of the vent gas composition has been used, the example above is used for illustration.

The other term required for DRE evaluation using Equation 4.1 is the  $CF^{propylene} (out)$  term. In this case, the combustion has occurred and species such as  $CO_2$  and  $CO$  are significant in the carbon fraction.

$$CF^{propylene} = \frac{propylene (ppmC)}{propylene (ppmC) + CO_2 + CO + \sum other carbon (ppmC)}$$

Eq. 4.4

It will be illustrative to demonstrate how  $CF^{propylene} (out)$  is calculated for one of the test conditions. As a prelude to the calculation, however, it is important to examine the event from some simple metrics to be sure that the sample collector is sampling the flare plume.

The first detail to be examined is the relationship between the temperature of the incoming sample and the relationship with the 1 Hz  $CO_2$  measurement, presuming this is the dominant product of the flare's combustion. During every test series, ARI would continuously extract a sample from the portion of the flare plume drawn through the sample collector using a probe that would dilute the sample with pure dry nitrogen immediately as it entered the probe tip. Sample collection would begin well before a test series was conducted. Figure 4-10, shows a time series of the sample collector inlet temperature and  $CO_2$  concentration of the sample obtained by the dilution probe.

# DRAFT

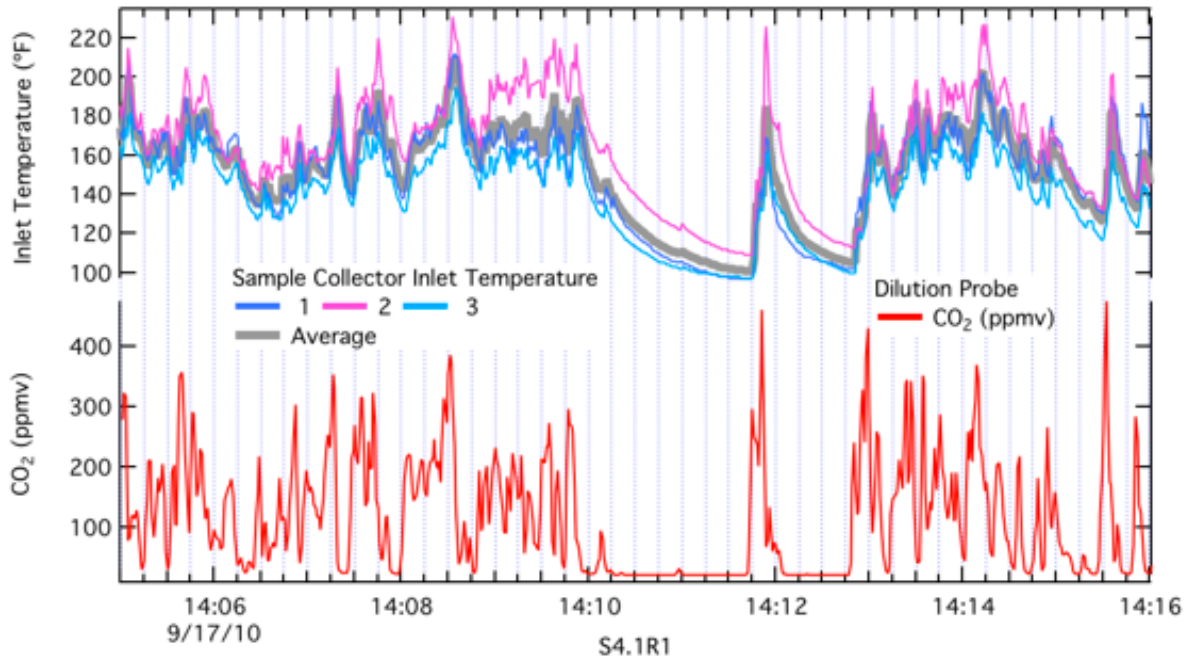


Figure 4-10. Time Series of Sample Collector Inlet Thermocouples and CO<sub>2</sub> Concentration for Test Point S4.1R1. In the upper panel, the temperatures of the three thermocouples at the sample collector inlet (shown in Figure 4-8) are shown in the noted pastel colors. An average of these three is also shown in the grey trace. The CO<sub>2</sub> time series of the sample obtained by the dilution probe is depicted in the lower panel in red.

The test point, S4.1R1, sample collector data is characterized by three periods. In the first section, from ~ 14:05 to 14:10, the sample collector is capturing significant plume intensity, i.e., plume “hits”. In the second period, from ~14:10 to 14:12:30, the sampler collector inlet is out of the flare plume as evidenced by the rapid decrease in CO<sub>2</sub> concentration and the slower decrease in sample collector inlet temperature. This is likely due to the fact that the flange around the sample collector inlet has a large thermal mass while the volumetric flow rate through the sample collector is very high, ~ 2,000 scfm, and is rapidly ventilated with ambient air. Note that the ambient concentration of CO<sub>2</sub> is ~ 380 ppmv, but the probe tip diluent (N<sub>2</sub>) is causing a 17 fold dilution at the inlet to the probe. In the final section, from ~14:12:30 to 14:16, the sample is characterized by plume hits with increasing frequency. Dilution of the sample with dry nitrogen was required to prevent condensation of moisture in the sample transfer line.

The second analysis that will be considered prior to looking at the steps used to compute DRE for this event is the physical location of the sample collector inlet. The differential GPS system digitized the physical location of the sample collector. A top-down view of the event with the measured CO<sub>2</sub> concentration and flare location has been combined with wind data to look at the sample collector inlet location and wind during test point S4.1R1.

# DRAFT

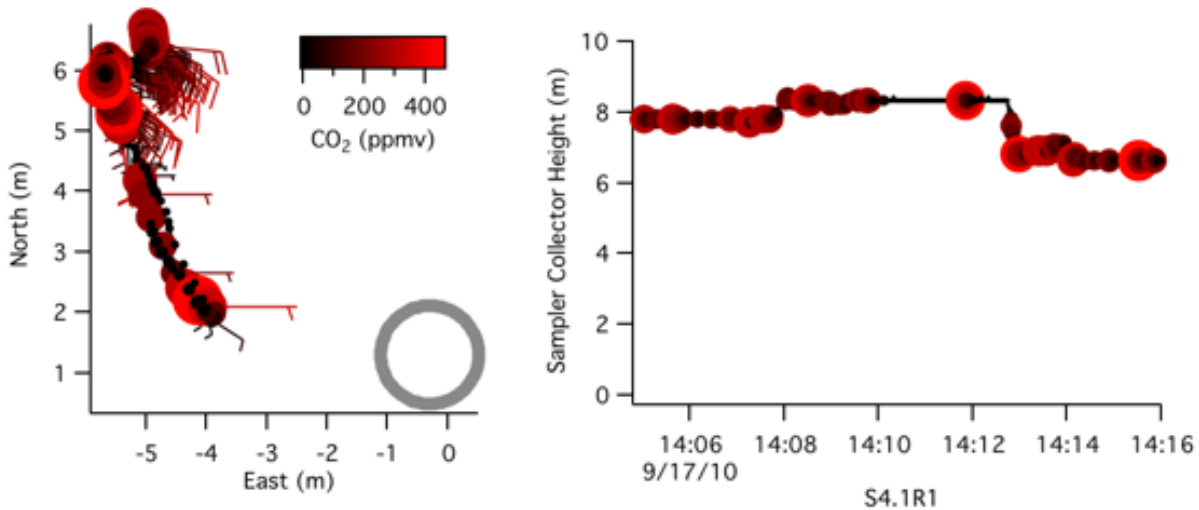


Figure 4-11. Sampler Collector Location and Wind Data. The left hand frame depicts the location of the center of the sample collector physically as meters (m) north and east of the flare (shown conceptually as a gray circle in the lower right hand corner); wind directions are shown as wind barbs ending at the point indicating the sample collector position; and the right hand frame shows the vertical position of the sample collector inlet. The shading of the data points in both panels are based on CO<sub>2</sub> concentration according to the color scale. The size of the point has been adjusted based on the large CO<sub>2</sub> ‘plume hits’.

The wind barbs that have been added to the top-down depiction of the sampler location (left hand frame of Figure 4-11) all roughly point back to the flare, shown as the grey circle in the bottom right of the frame. The wind for this event was from the southeast and varied during the test point from ~ 100 to 170 degrees. The ground crew maneuvered the sample collector inlet to intercept the plume to adjust for the intra-test wind changes. This is seen in the photograph depicted in Figure 4-7.

The time series for several species measured by the dilution probe (along with the CO<sub>2</sub> concentration discussed above) are plotted in Figure 4-12.

# DRAFT

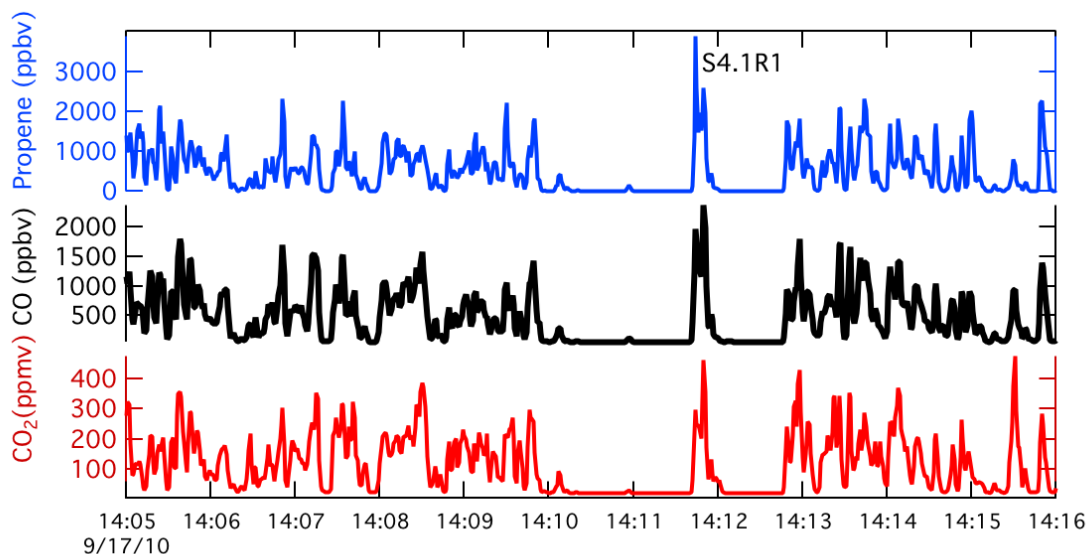


Figure 4-12. Time Series of S4.1R1 of CO<sub>2</sub>, CO and Propylene Concentrations of the Dilution Probe. Each panel is the 1 Hz data for the dilution probe in mixing ratio by volume.

The characteristic pattern of the time series for the event, discussed in light of CO<sub>2</sub> concentration and sample collector inlet temperature is qualitatively mirrored in CO as well as unburned propylene. A simplistic approach to the evaluation of Equation 4.4 would be to insert the absolute mixing ratios depicted in the time series. This approach however would require that additional knowledge about the ambient dilution and ambient mixing ratios be accounted for. What is really of interest is the combustion-associated fraction. If the numerator and denominator of Equation 4.4 are divided by the CO concentration the following formula results.

$$CF^{propylene}(out) = \frac{propylene (ppmC)/CO}{propylene (ppmC)/CO + CO_2/CO + 1 + \sum other carbon (ppmC)/CO}$$

Eq. 4.5

The terms in Equation 4.5 are all intended to be *flare combustion associated* ratios. As a result, if the time-series data is plotted against CO rather than time, the following representations of the event result.

# DRAFT

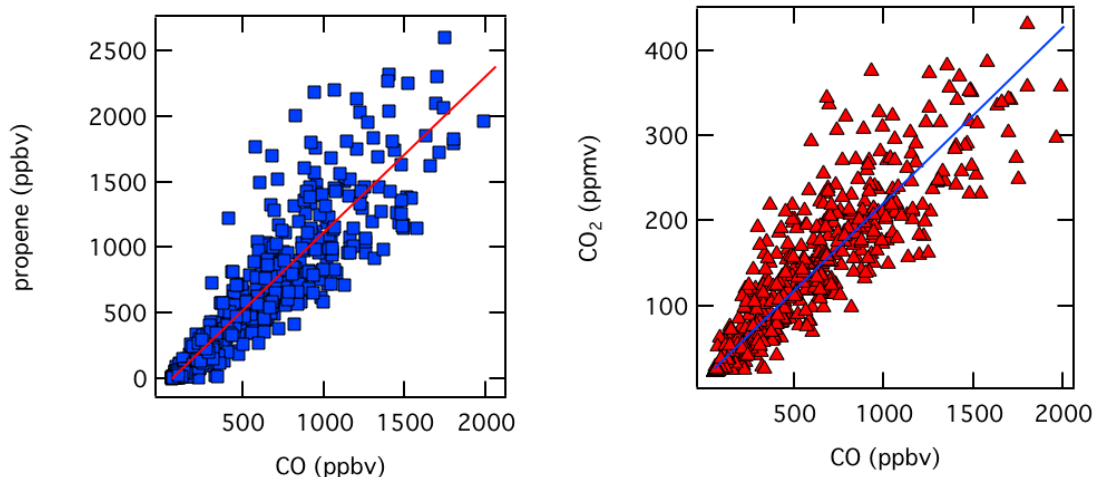


Figure 4-13. Propylene and CO<sub>2</sub> Concentrations Relative to CO Concentration in the Combustion-Associated Plume Intercept.

The relationship between the propylene and CO concentrations (left hand side of Figure 4-13) for the totality of event S4.1R1 is characterized by a linear slope of  $1.19 \pm 0.04$  moles per mole, where the uncertainty is the  $2 \sigma$  precision determined from the fit assuming a normal distribution of error in the propylene measurement. The Pearson's  $R^2$  statistic for this fit is 0.84. When the value is used in Equation 4.5, it must be converted to a ratio of ppmC, which in the case of propylene means multiplying by 3 to account for the three carbon atoms in propylene (e.g.,  $3.57 \pm 0.12$ ). The relationship between the CO<sub>2</sub> and CO concentrations (right hand side of Figure 4-13) is evaluated using a linear fit with slope  $206 \pm 4$  ppmC per ppmC. The Pearson's  $R^2$  for this fit is 0.89.

As a first step in the pursuit of evaluating Equation 4.5 and eventually DRE for this test point, these combustion-associated slopes will be used to evaluate Equation 4.5 using only three chemical forms for carbon (propylene, CO, CO<sub>2</sub>).

$$CF^{propylene} (out) = \frac{(3.57 \pm 0.12)}{(3.57 \pm 0.12) + (206 \pm 4) + 1} = (1.69 \pm 0.06)\% \quad \text{Eq. 4.5a}$$

Assuming there is no other form of carbon, the evaluation of Equation 4.5a, suggests that propylene in the *flare plume* is 1.69% of the total carbon considered in this example.

# DRAFT

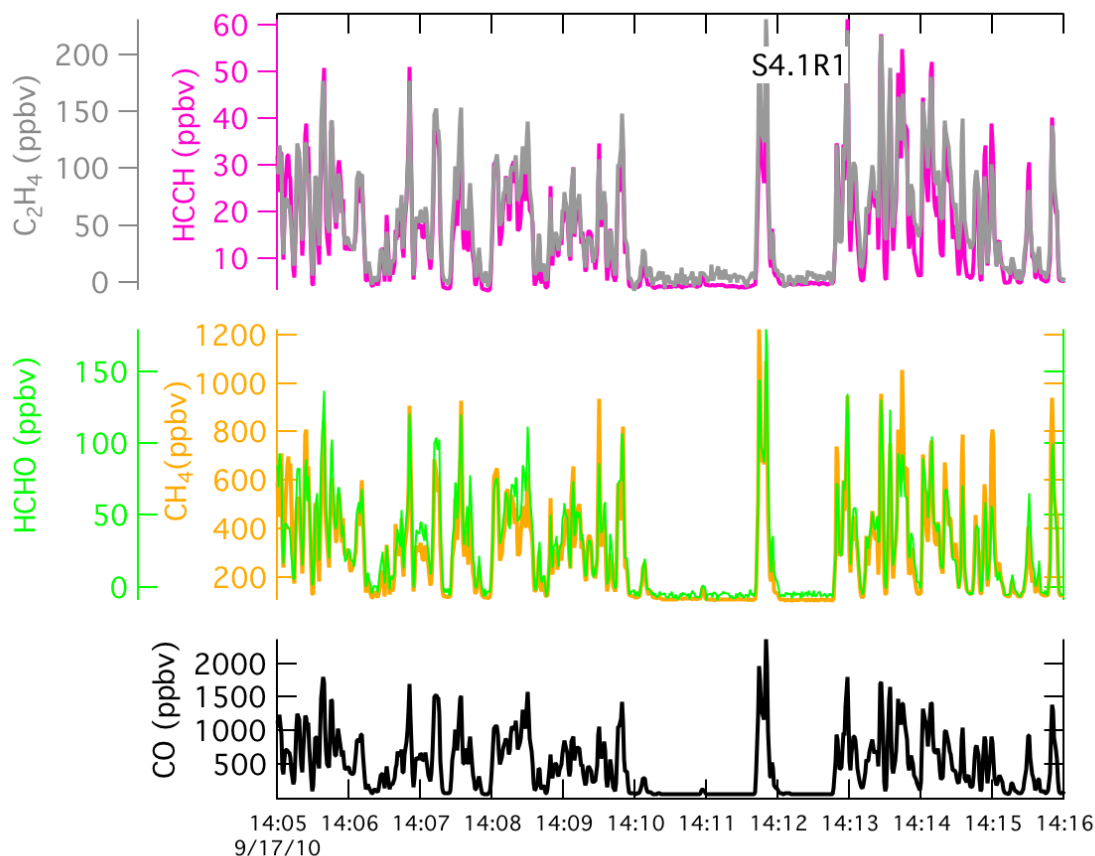


Figure 4-14. Time Series for CO Concentration and Other Trace Selected Hydrocarbons Species. The measurements of the dilution probe for test point S4.1R1 for ethene ( $C_2H_4$ ), ethyne ( $C_2H_2$ ), formaldehyde ( $HCHO$ ) and methane ( $CH_4$ ).

Time series data for this event for other trace forms of carbon in the matrix are depicted in Figure 4-14. Note that CO concentration has been repeated for reference from the previous figures. The relationship of the trace hydrocarbon concentration relative to CO concentration is summarized in Figure 4-15.

# DRAFT

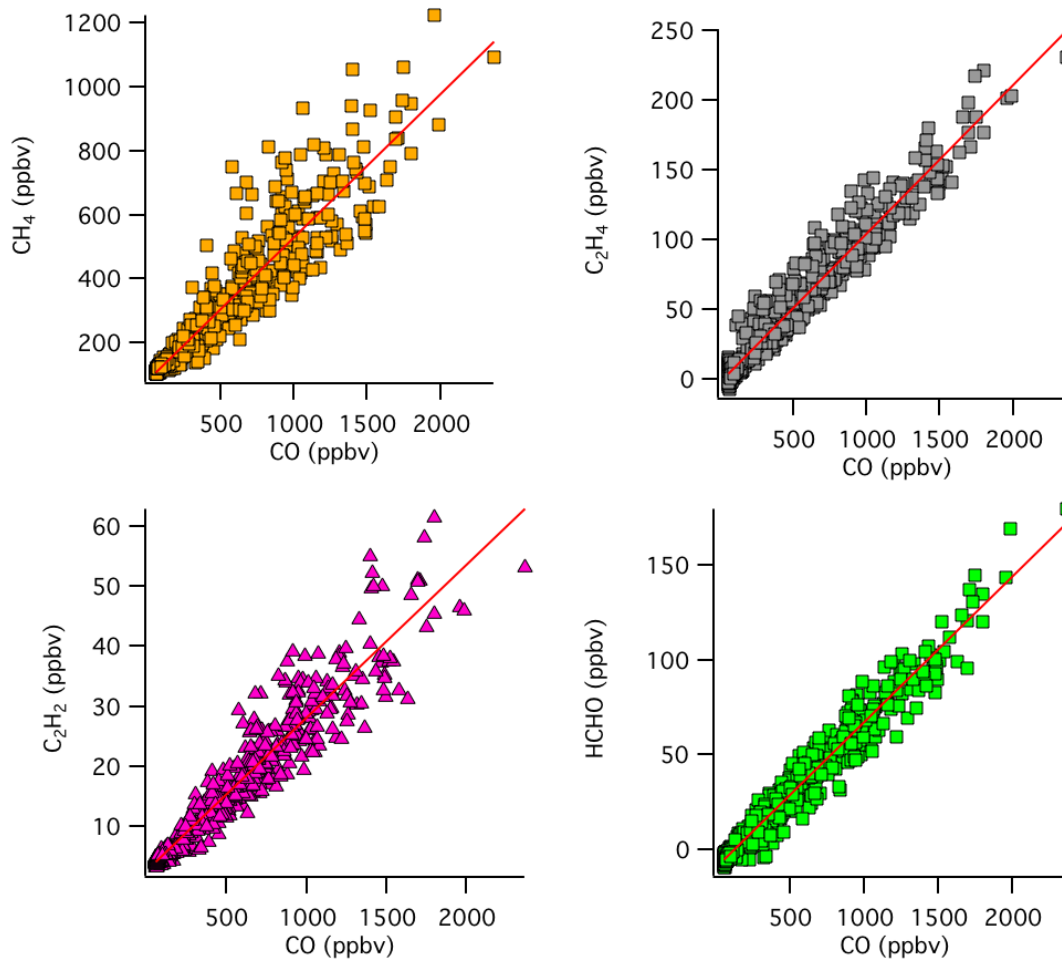


Figure 4-15. Correlation of Trace Hydrocarbon Concentration with CO Concentration for S4.1R1. The results of the fit parameters depicted by the red lines in each panel are tabulated in ppmC below.

Table 4-1. Fit Parameters for Selected Trace Hydrocarbons for S4.1R1

<i>Species</i>	ppmC/ppmC CO	2 <sigma>	R <sup>2</sup>	Influence on CF for S4.1R1
CH <sub>4</sub>	0.45	0.01	0.87	0.2%
C <sub>2</sub> H <sub>4</sub>	0.212	0.004	0.95	0.1%
HCHO	0.0767	0.0001	0.96	0.03%
C <sub>2</sub> H <sub>2</sub>	0.050	0.002	0.92	0.02%

The carbon fraction that results from including these trace species in the denominator of Equation 4.5 (the sum of ‘other’ carbon) is unchanged within the precision based error band, CF<sup>propylene</sup> (out) = 1.69%. Using the nominal 80/20 propylene/TNG mixture, it is estimated that

# DRAFT

$CF^{\text{propylene}}(in) = 92.3\%$ . This implies the DRE for this test point, based on the definition in Equation 4.1 is  $1 - 1.69/92.3$  or 98.17% (98.10 - 98.23%). An analogous form of the combustion efficiency equation can be derived.

Additional discussion of the sources of systematic error in this approach will be discussed in Section 7. The reader is also referred to Appendix I for additional information.

## **Remote Sensing Technologies**

Remote sensing technologies were also included in this study to measure CE (IMACC and Telops) and/or flare emissions (Telops). The measurements made by the remote sensing technologies will be compared to the measurements made by ARI to assess and evaluate the performance of the remote sensing technologies (see Section 8.0).

# DRAFT

## 5.0 Results of Flare Tests

The field tests were performed during the month of September 2010 at the Zink flare test facility in Tulsa, Oklahoma. The test plan (Appendix A) identified 56 test points, including replicates, to be performed on each of the air- and steam-assisted flares. Because of favorable weather conditions and more rapid than anticipated completion of test conditions, a larger number of test points than originally planned were completed. The actual number of test points and replicates that were performed were almost twice the number of steam test points and 27% more air test points than originally planned. These additional test points included tests using propane in place of propylene. Propane was not included in the original test plan. Summaries of the test results follow. Summaries of all test data for the steam and air flare tests are included in Appendices D and E, respectively. The values for DRE and CE are presented in this report using three significant figures based on the probable uncertainty in these measurements as explained in Section 7 of this report.

### Steam-Assisted Flare: DRE (propylene) and CE

*Please refer to Figures 5-10a and 5-10b.*

At a total steam assist flow rate of 970 lb/hr (center = 540 lb/hr) for a vent gas LHV of 350 Btu/scf and constant flow rate of 930 lb/hr, the DRE (propylene) was 46.6% (Test Point S3.1 Run 1). No higher steam assist levels were performed at this combination of flare operating parameters since the DRE was already below 50%. The CE for this test point was 42.9%. The average wind speed during this test was 2.6 mph.

At a total steam assist flow rate of 666 lb/hr (center = 555 lb/hr) for a vent gas LHV of 349 Btu/scf and constant flow rate of 2,335 lb/hr, the DRE (propylene) was 99.2% (S4.2 Run 3). Total steam assist levels greater than 666 lb/hr produced DREs below 99.2%. The CE for this test point is 98.8%. The average wind speed during this test was 4.8 mph.

*Please refer to Figures 5-11a and 5-11b.*

At a total steam assist flow rate of 228 lb/hr (center = 0 lb/hr) for a vent gas LHV of 346 Btu/scf and constant flow rate of 926 lb/hr, the DRE (propylene) was 99.5% (S3.7 Run 1). Total steam assist levels greater than 228 lb/hr produced DREs below 99.5%. The CE for this test point was 99.2%. The average wind speed during this test was 7.1 mph. When the total steam assist rate was reduced to zero (S3.6 Run 1), the DRE (propylene) was 99.9% and the CE was 99.7% for this test point. The average wind speed during this test was 7.3 mph.

At a total steam assist flow rate of 327 lb/hr (center = 0 lb/hr) for a vent gas LHV of 363 Btu/scf and constant flow rate of 2,372 lb/hr, the DRE (propylene) was 98.3% (S4.4 Run 1). The CE for this test point was 97.6%. The average wind speed during this test was 5.9 mph.

# DRAFT

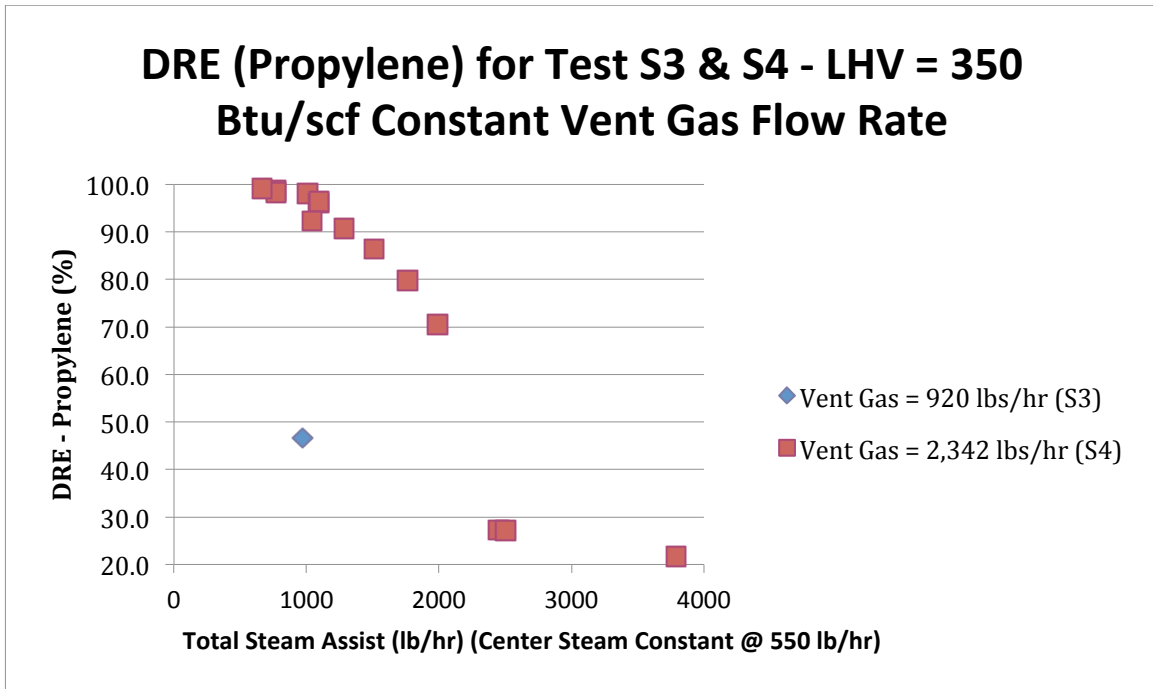


Figure 5-10a. DRE vs Steam Assist for Test Series S3 and S4

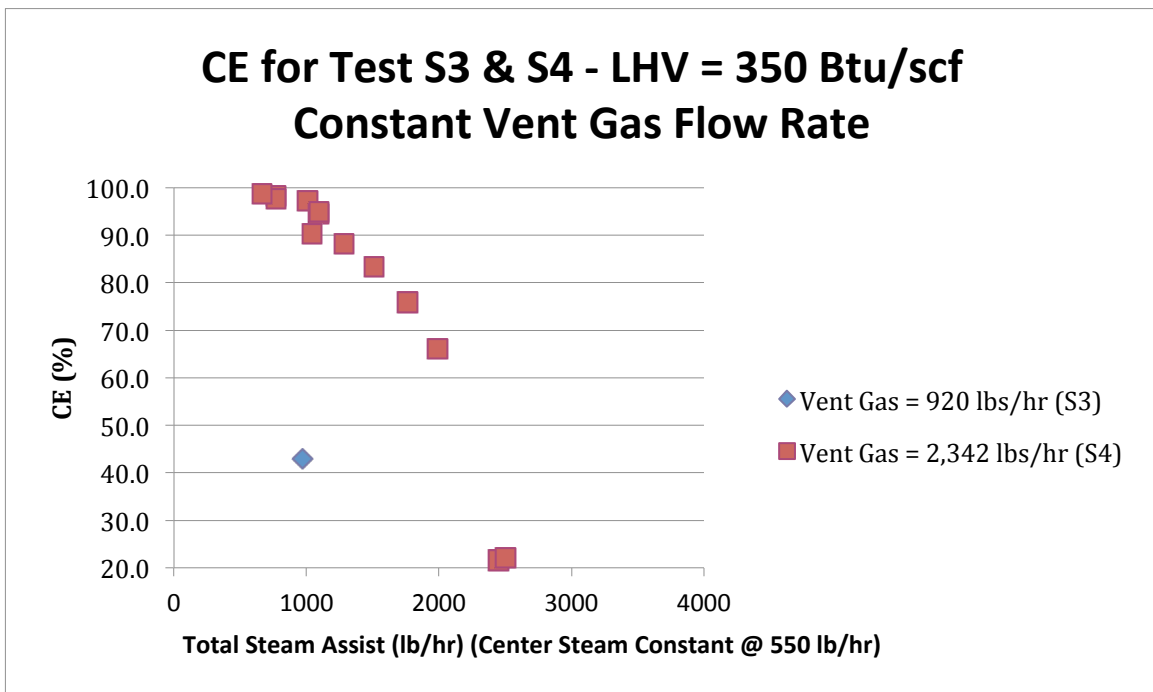


Figure 5-10b. CE vs Steam Assist for Test Series S3 and S4

# DRAFT

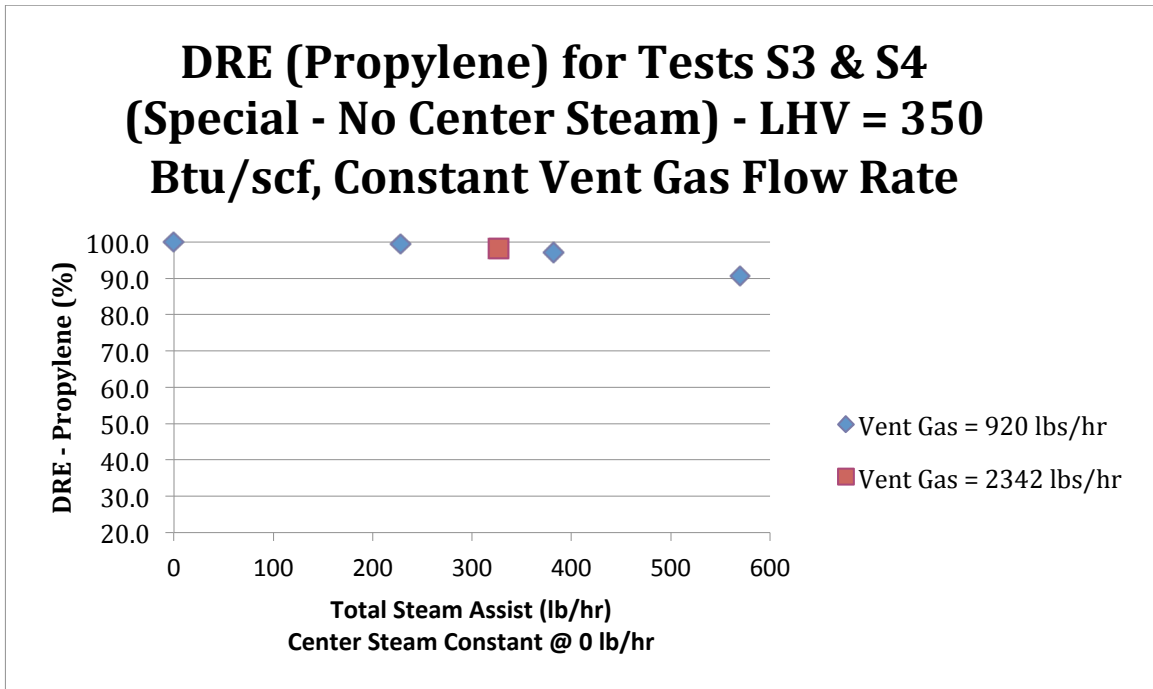


Figure 5-11a. DRE vs Steam Assist for Test Series S3 and S4 (Special - No Center Steam)

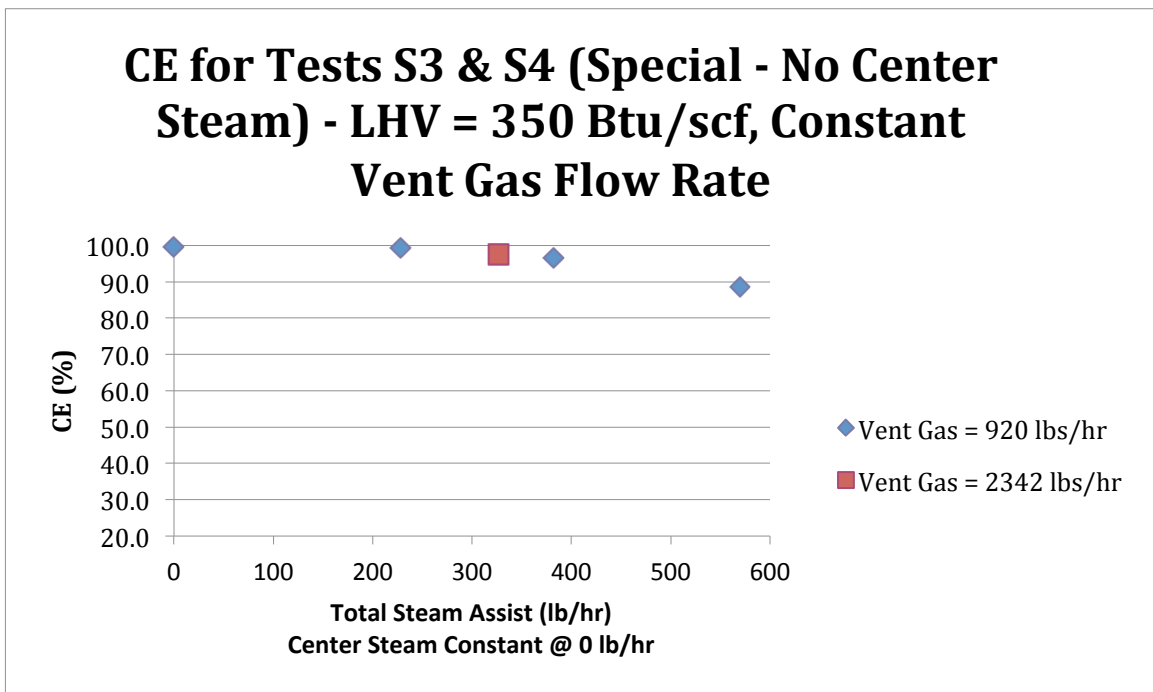


Figure 5-11b. CE vs Steam Assist for Test Series S3 and S4 (Special - No Center Steam)

# DRAFT

*Please refer to Figures 5-12a and 5-12b.*

These two figures are composites of the data for all test points from Test Series S3 and S4 shown in the previous four figures. These graphs illustrate and compare the effect increasing steam rate has on DRE and CE at a LHV of approximately 350 Btu/scf for these two vent gas flow rates.

# D R A F T

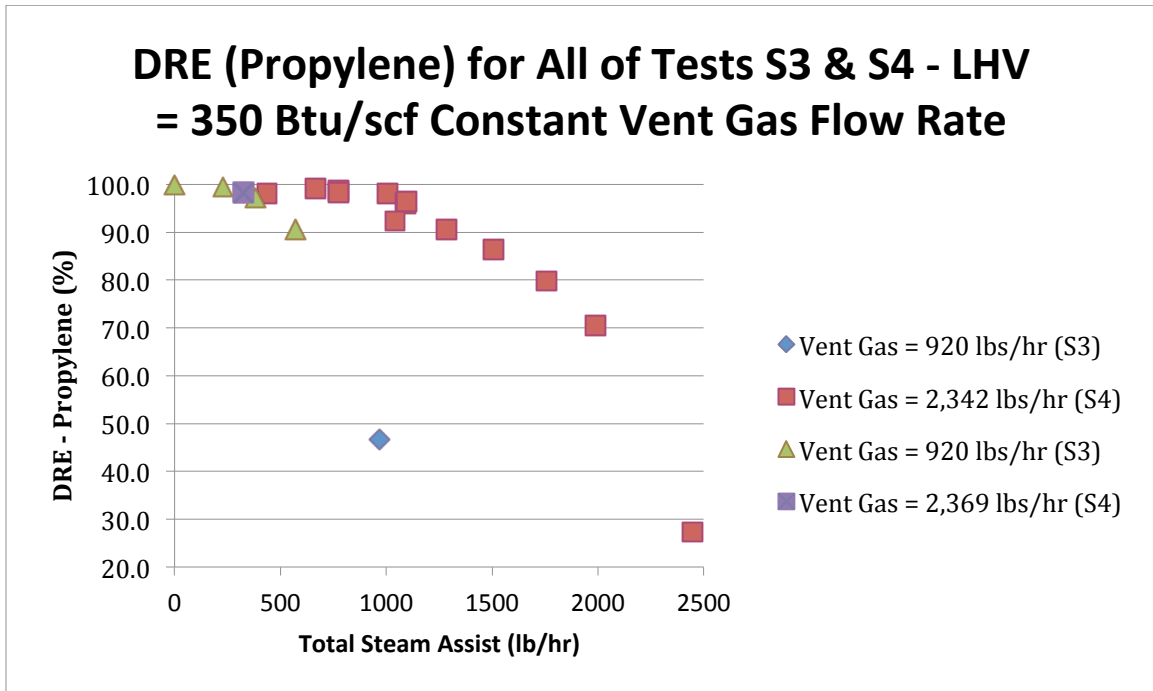


Figure 5-12a. DRE vs Steam Assist for All Test Series S3 and S4

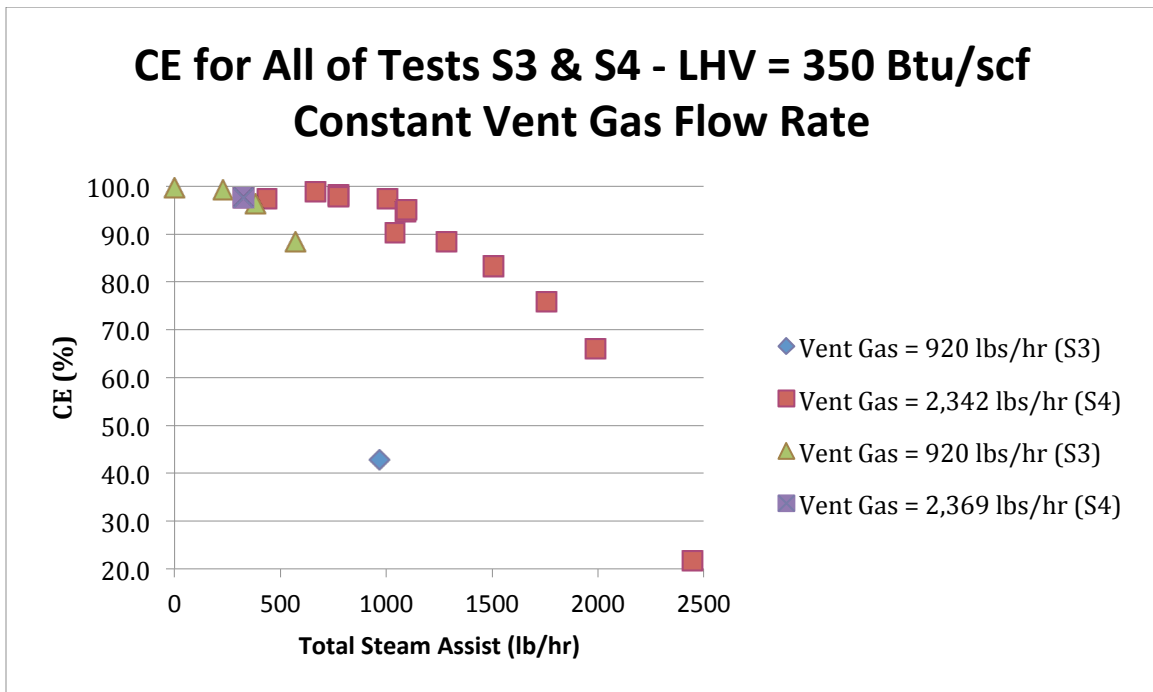


Figure 5-12b. CE vs Steam Assist for All Test Series S3 and S4

# DRAFT

*Please refer to Figure 5-13a and 5-13b.*

At a total steam assist flow rate of 768 lb/hr (center = 488 lb/hr) for a vent gas LHV of 594 Btu/scf and constant flow rate of 940 lb/hr, the DRE (propylene) was 98.3% (S5.1 Run 1) or less. Total steam assist levels greater than about 768 lb/hr produced DREs below 98.3%. The CE for this test point was 97.9%. The average wind speed during this test was 8.0 mph.

At a total steam assist flow rate of 1,529 lb/hr (center = 510 lb/hr) for a vent gas LHV of 625 Btu/scf and constant flow rate of 2,423 lb/hr, the DRE (propylene) was 99.3% (S6.1 Run 3). Total steam assist levels greater than about 1,529 lb/hr produced DREs below 99.3%. The CE for this test point is 98.8%. The average wind speed during this test was 7.5 mph.

## ***DRE (Propylene) and CE vs Steam-to-Vent Gas Ratio (S/VG)***

*Please refer to Figure 5-14a, 5-14b, 5-15a and 5-15b.*

DRE (Propylene) vs S/VG for all test points in Test Series S3 and S4 is shown in Figure 5-14a and 5-15a. Figure 5-14b and 5-15b show CE vs S/VG for the same test points. Figures 5-15a and 5-15b are provided to focus on a smaller DRE range to provide greater resolution between data points for easier analysis.

*Please refer to Figure 5-16a, 5-16b, 5-17a and 5-17b.*

DRE (Propylene) vs S/VG for all test points in Test Series S5 and S6 is shown in Figure 5-16a and 5-17a. Figure 5-16b and 5-17b show CE vs S/VG for the same test points. Figures 5-17a and 5-17b are provided to focus on a smaller DRE range to provide greater resolution between data points for easier analysis.

# DRAFT

## DRE (Propylene) for Tests S5 & S6 - LHV = 600 Btu/scf, Constant Vent Gas Flow Rate

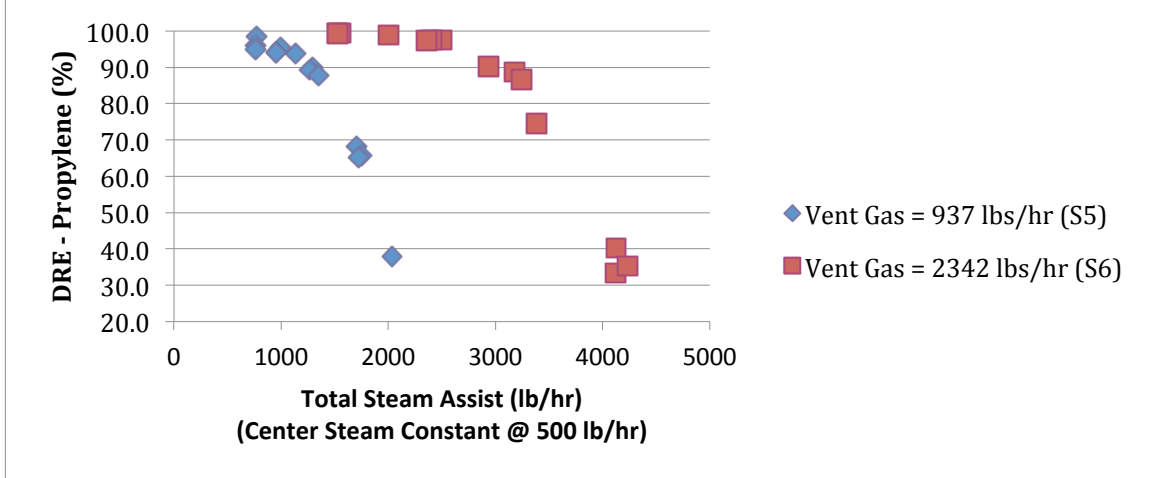


Figure 5-13a. DRE vs Steam Assist for Test Series S5 and S6

## CE for Tests S5 & S6 - LHV = 600 Btu/scf, Constant Vent Gas Flow Rate

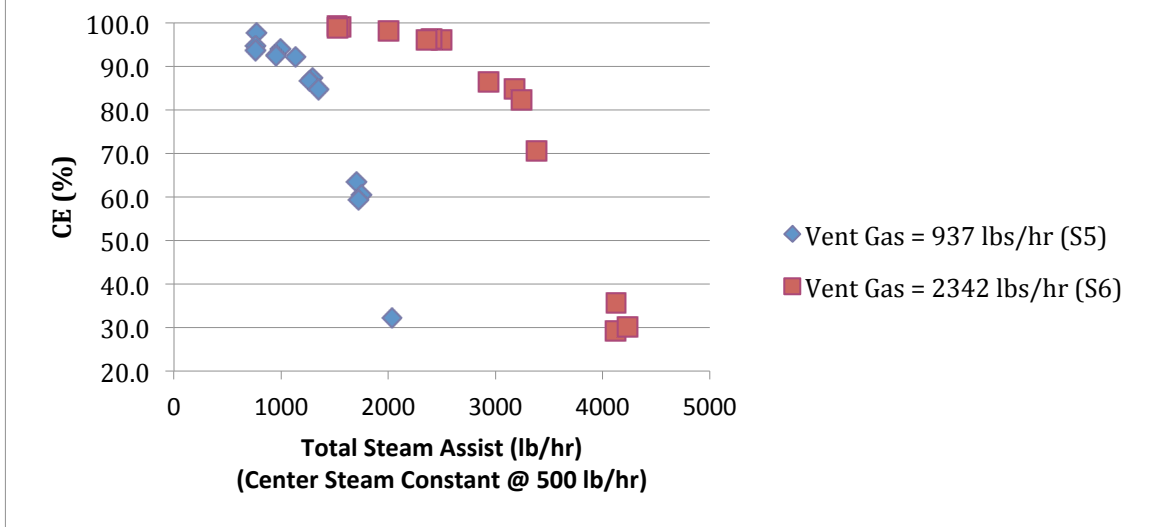


Figure 5-13b. DRE vs Steam Assist for Test Series S5 and S6

# DRAFT

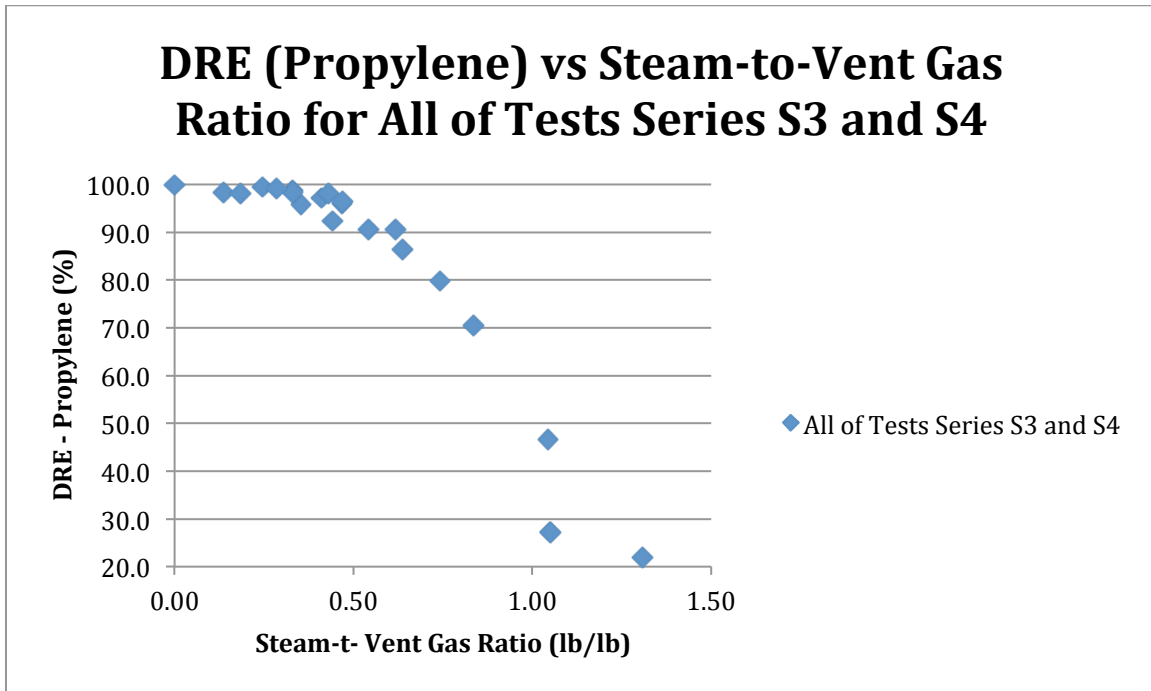


Figure 5-14a. DRE vs Steam-to-Vent Gas Ratio for All Test Series S3 and S4

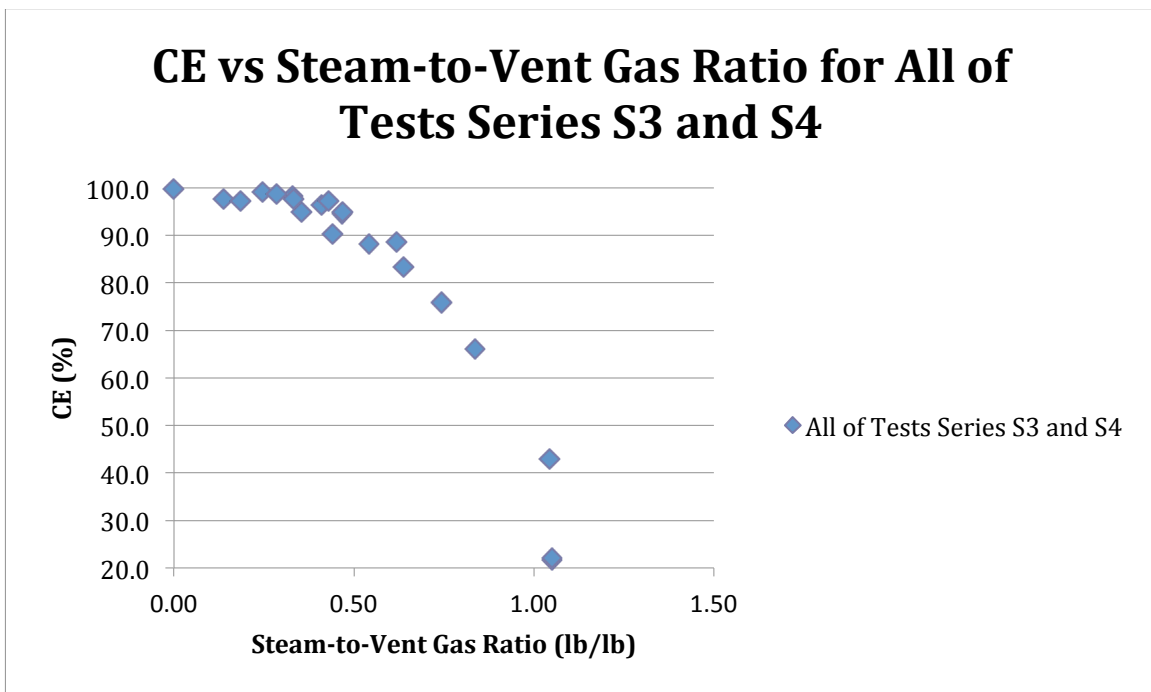


Figure 5-14b. CE vs Steam-to-Vent Gas Ratio for All Test Series S3 and S4

# DRAFT

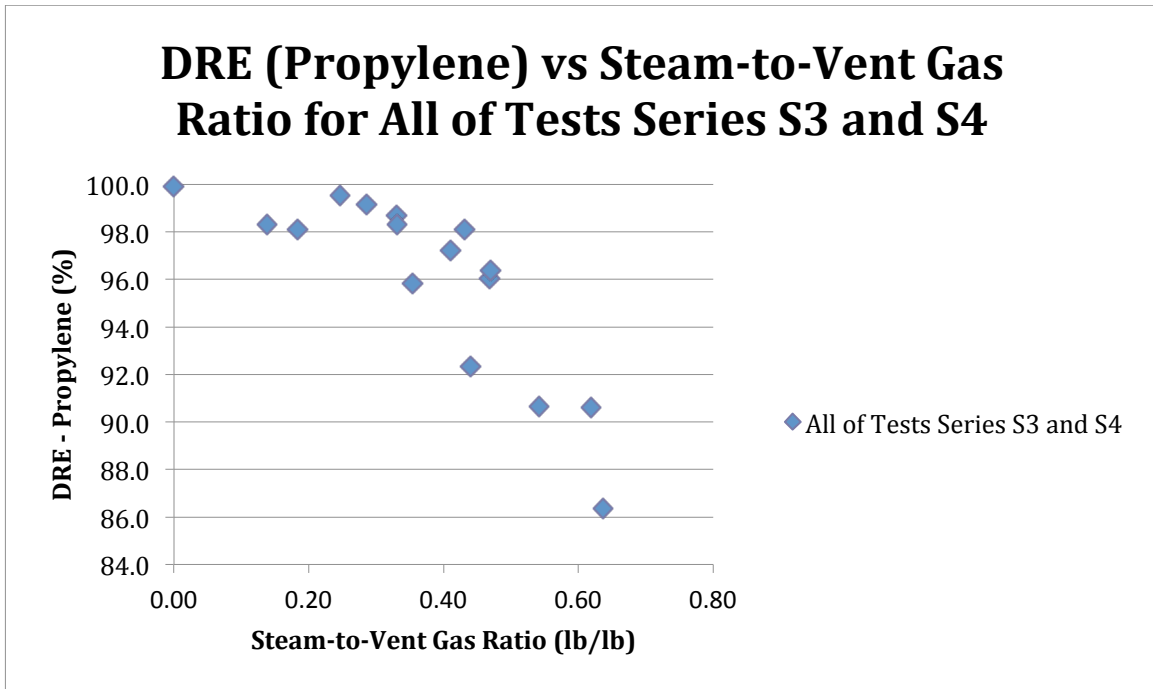


Figure 5-15a. DRE vs Steam-to-Vent Gas Ratio for All Test Series S3 and S4

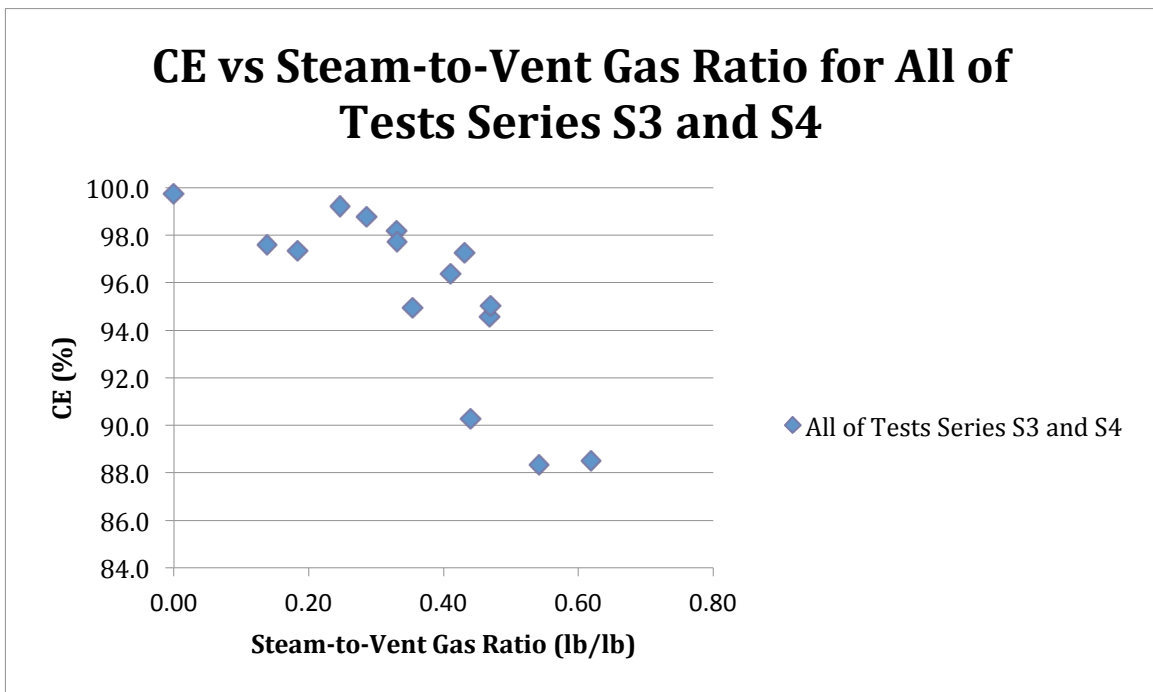


Figure 5-15b. CE vs Steam-to-Vent Gas Ratio for All Test Series S3 and S4

# DRAFT

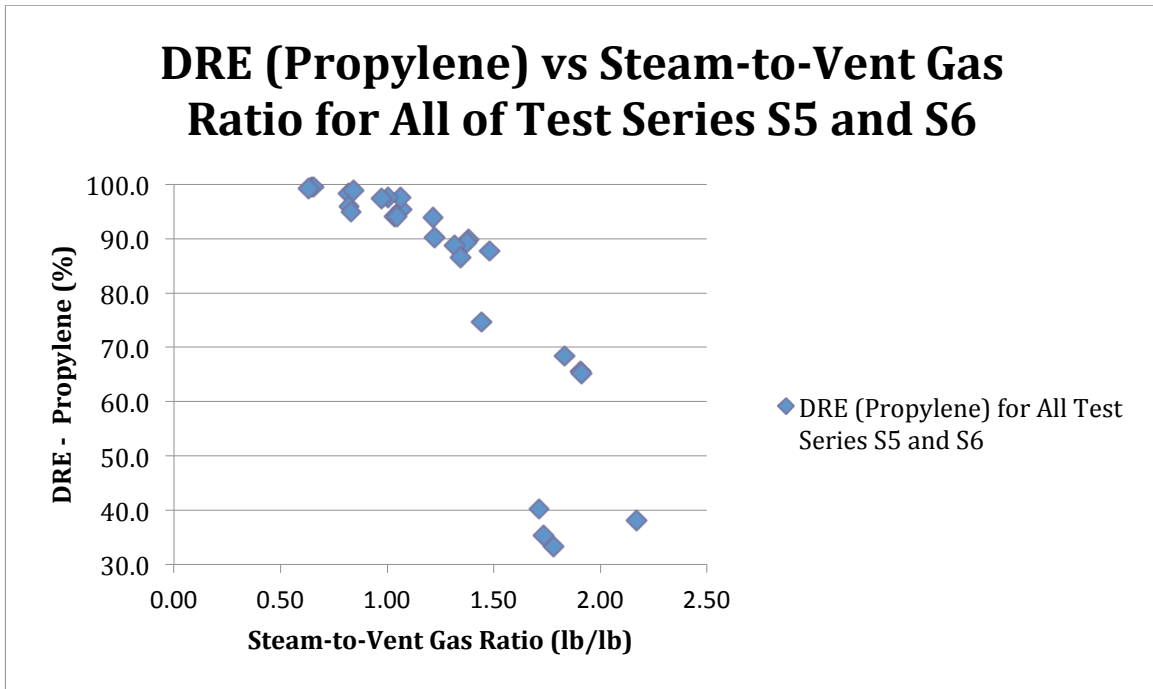


Figure 5-16a. DRE vs Steam-to-Vent Gas Ratio for All Test Series S5 and S6

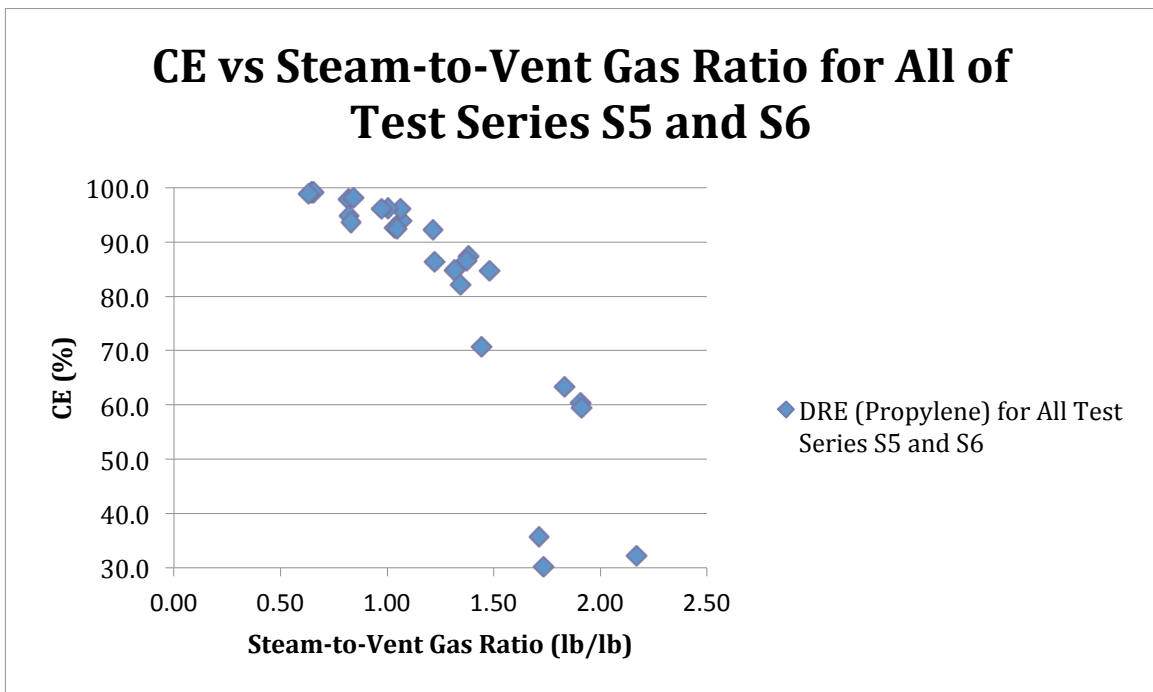


Figure 5-16b. CE vs Steam-to-Vent Gas Ratio for All Test Series S5 and S6

# DRAFT

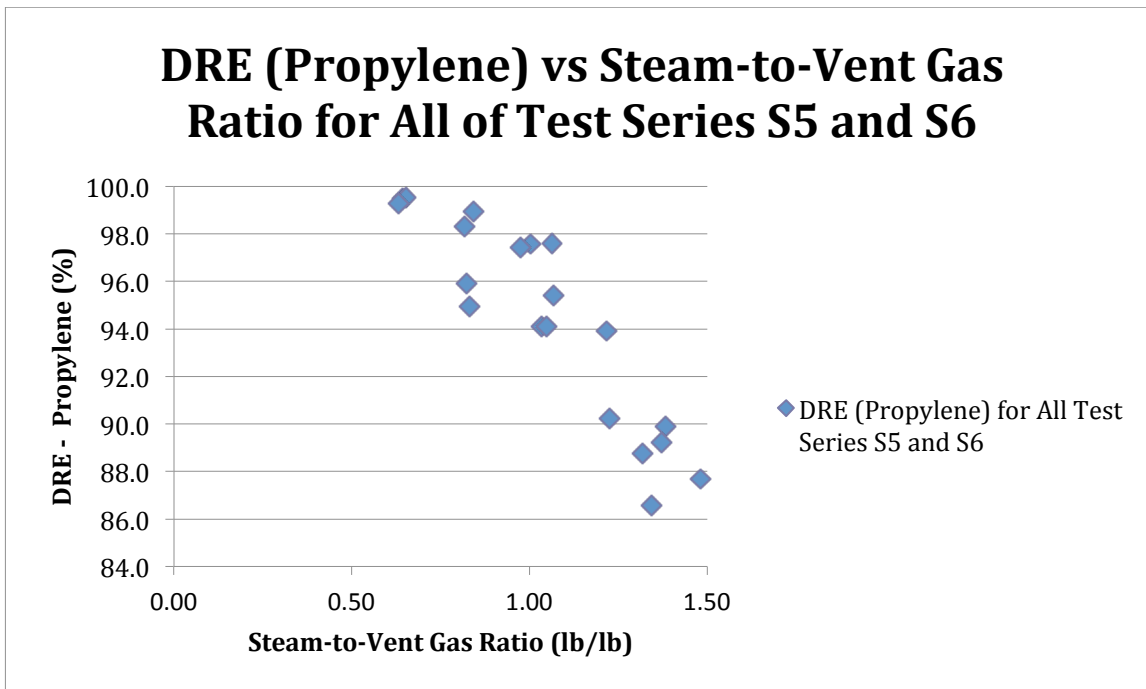


Figure 5-17a. DRE vs Steam-to-Vent Gas Ratio for All Test Series S5 and S6

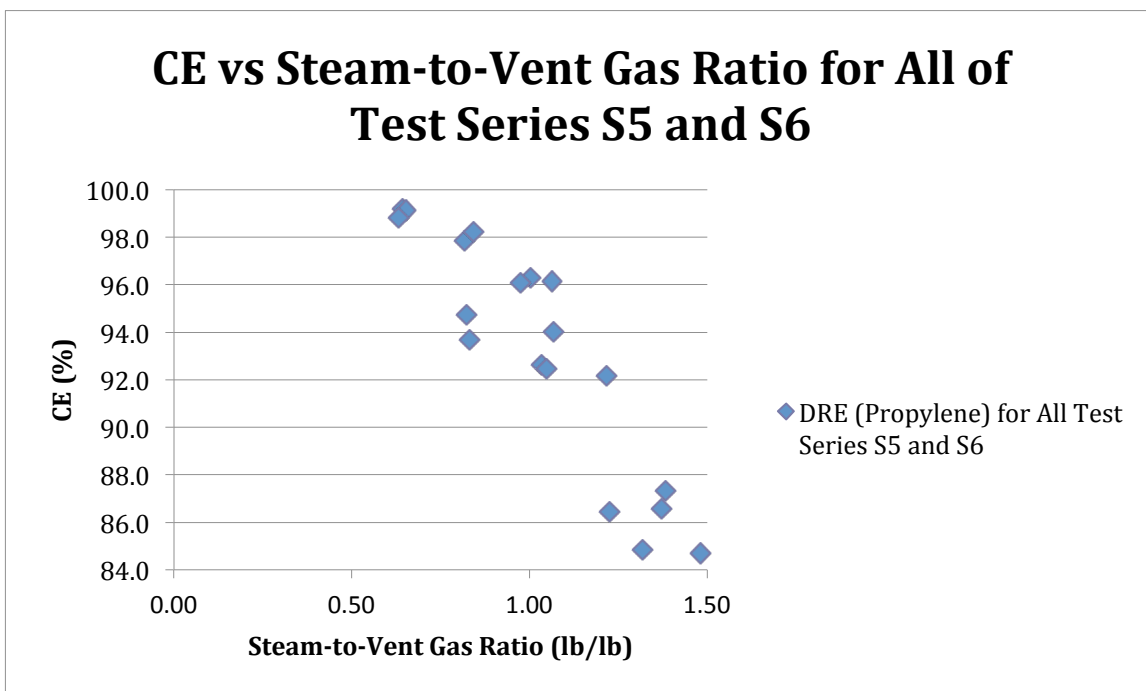


Figure 5-17b. CE vs Steam-to-Vent Gas Ratio for All Test Series S5 and S6

# DRAFT

The next five test series illustrate the impact of center steam on DRE. Please refer to Figures 5-18a, 5-18b, 5-19a and 5-19b for these cases.

Using a recommended center steam flow rate of 501 lb/hr and 536 lb/hr upper steam, at a vent gas LHV of 354 Btu/scf and a flow rate 3,028 lb/hr, the highest DRE achieved was 95.2% (S7.6 Run 1). The CE for this test point was 94.6%. The average wind speed during this test was 10.8 mph.

Using no center steam and 534 lb/hr upper steam and a vent gas LHV of 356 Btu/scf and a flow rate of 2,399 lb/hr, the highest DRE achieved was 98.1% (S8.1 Run 1). The CE for this test point was 97.4%. The average wind speed during this test was 12.6 mph.

Using no center steam but twice as much upper steam (1,007 lb/hr) and a vent gas LHV of 347 Btu/scf and a flow rate of 2,364 lb/hr, the highest DRE achieved 94.4% (S9.1 Run 1). The CE for this test point was 92.9%. The average wind speed during this test was 12.2 mph.

Using no center steam, an upper steam rate of 542 lb/hr and a vent gas LHV of 353 Btu/scf and a flow rate of 2,348 lb/hr, the highest DRE achieved was 95.8% (S10.1 Run 1). The CE for this test point was 94.7%. The average wind speed during this test was 10.9 mph.

Lastly, with 286 lb/hr of center steam and 830 lb/hr upper steam, a vent gas LHV of 355 Btu/scf and a flow rate of 2,354 lb/hr, the highest DRE achieved was 96.1% (S11.1 Run 1). The CE for this test point was 95.1%. The average wind speed during this test was 10.5 mph.

Figures 5-19a and 5-19b are the same data as Figures 5-18a and 5-18b except the horizontal axis has been reversed to show a decline in DRE and CE as the values on the horizontal axis increase proceeding to the right. These figures also focus only on values of DRE and CE above 84%.

# DRAFT

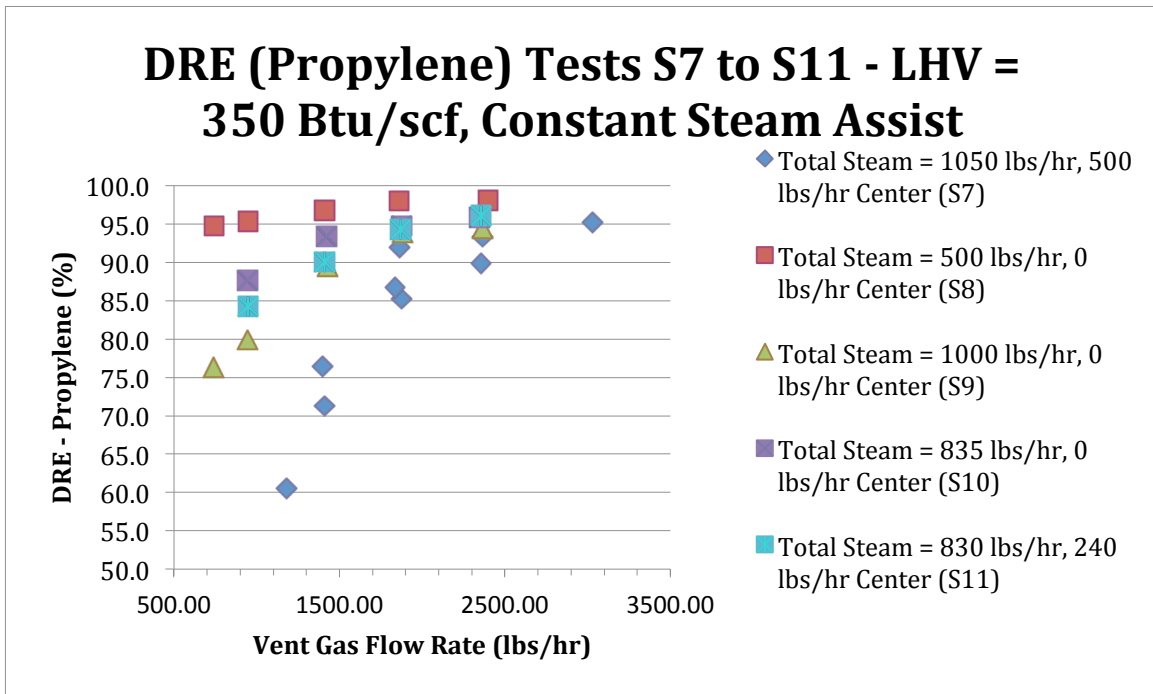


Figure 5-18a. DRE vs Vent Gas Flow Rate for Test Series S7, S8, S9, S10 and S11

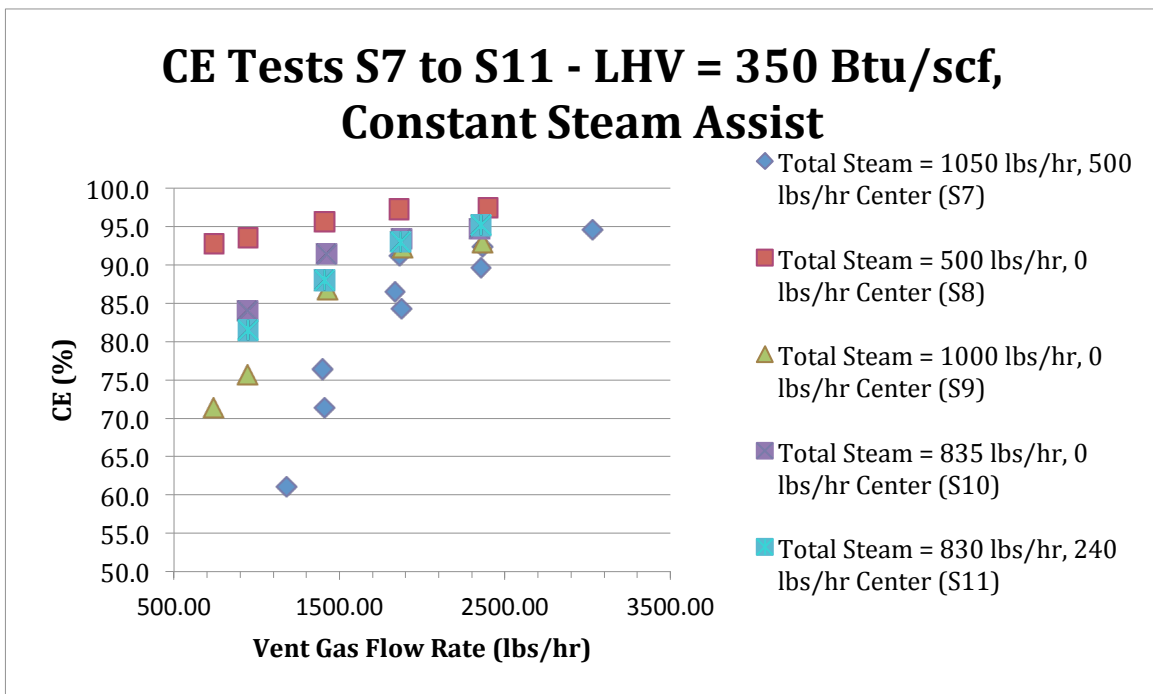


Figure 5-18b. CE vs Vent Gas Flow Rate for Test Series S7, S8, S9, S10 and S11

# DRAFT

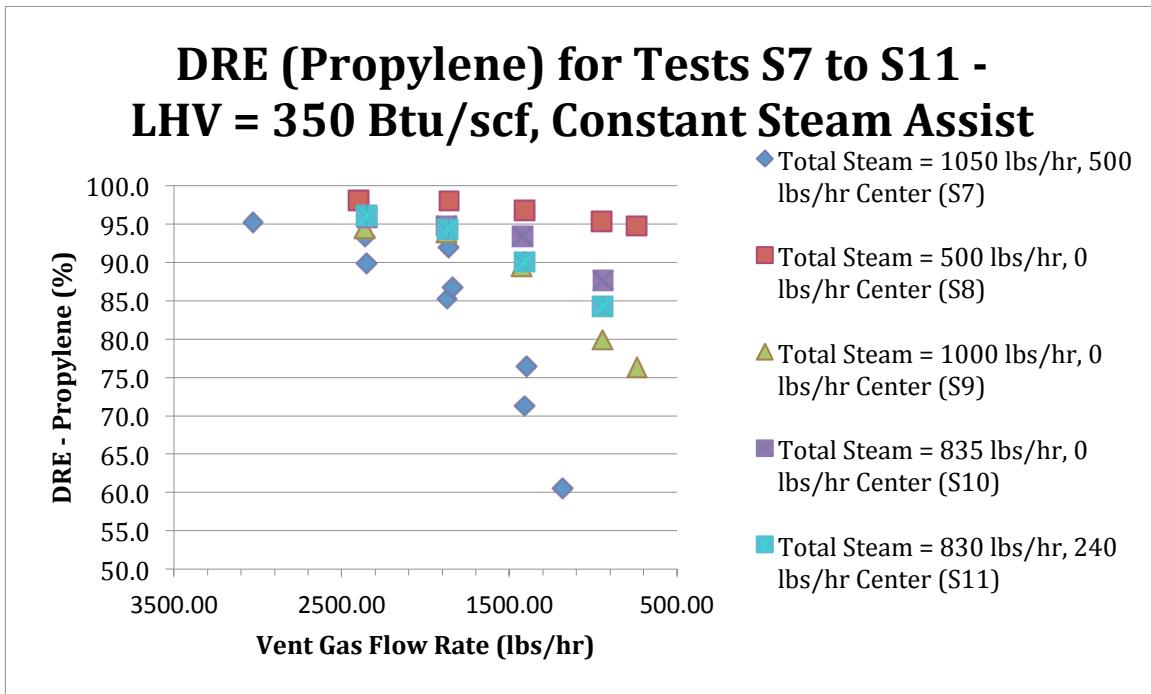


Figure 5-19a. DRE vs Vent Gas Flow Rate for Test Series S7, S8, S9, S10 and S11

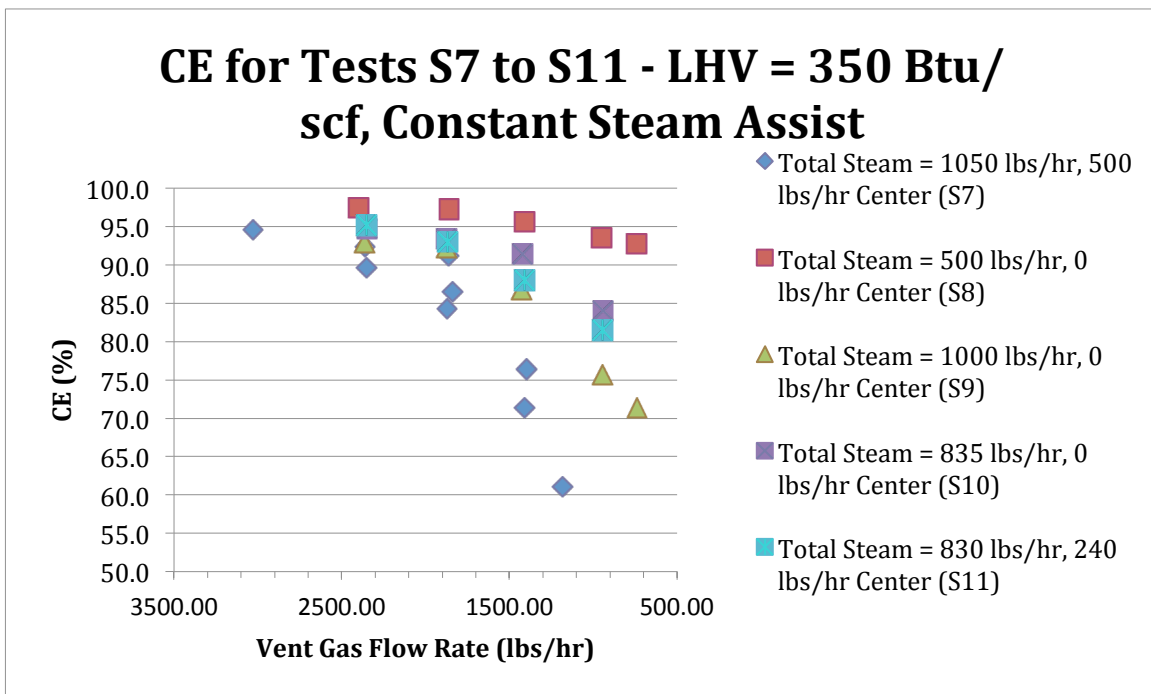


Figure 5-19b. CE vs Vent Gas Flow Rate for Test Series S7, S8, S9, S10 and S11

# DRAFT

The Combustion Zone Gas Net Heat Value (CZG NHV), Btu/scf, is defined in this study as the ratio of the sum of the combustion heating value (LHV) of the vent gas going through the flare plus the combustion heating value of the flare pilots to the total volume of gases going to the flare, including steam, i.e., vent gas plus pilot gas plus total steam assist. It is expressed numerically as

$$CZG\ NHV = \frac{[(VG)(LHV_{VG})(386.3/MW_{VG})] + [(PG)(LHV_{PG})(386.3/MW_{PG})]}{[(VG)(386.3/MW_{VG}) + (PG)(386.3/MW_{PG}) + (S)(386.3/18.02)]} \quad \text{Eq. 5.1}$$

where

CZG NHV = combustion zone gas net heating value, Btu/scf

VG = Vent gas mass flow rate, lb/hr

LHV<sub>VG</sub> = Vent gas lower heating value, Btu/scf

MW<sub>VG</sub> = Vent gas molecular weight, lb/lb-mol

PG = Pilot gas mass flow rate, lb/hr

LHV<sub>PG</sub> = Pilot gas lower heating value, Btu/scf

MW<sub>PG</sub> = Pilot gas molecular weight, lb/lb-mol

S = Total steam mass flow rate, lb/hr

386.3 = Ideal gas volume (scf) per lb-mol at 68°F and 1 atmosphere

18.02 = Steam molecular weight, lb/lb-mol

*Please refer to Figures 5-20a, 5-20b, 5-21a, and 5-21b*

Figure 5-20a plot the DRE (Propylene) vs CZG NHV for all test points in Test Series S3 through S6. Figure 21a plot the DRE (Propylene) vs CZG NHV for Test Series S7 through S11. Figures 5-20b and 5-21b have the horizontal axis reversed and focus only on DRE and CE values above 84%, which is the more important section of these graphs for the study. It appears that until the CZG NHV gets above 300 Btu/scf for Test Series S3 through S6, does the DRE (Propylene) appear to have a single value of DRE above 98%. There is insufficient data to estimate a similar value for Test Series S7 through S11.

# DRAFT

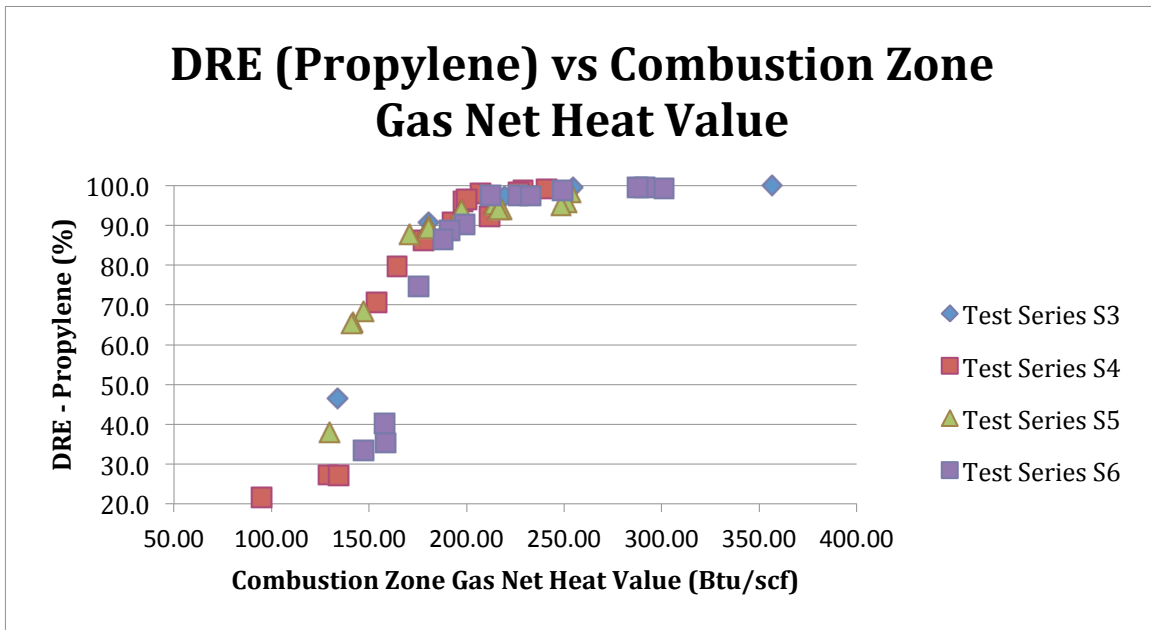


Figure 5-20a. DRE vs CZG NHV for Test Series S3, S4, S5 and S6

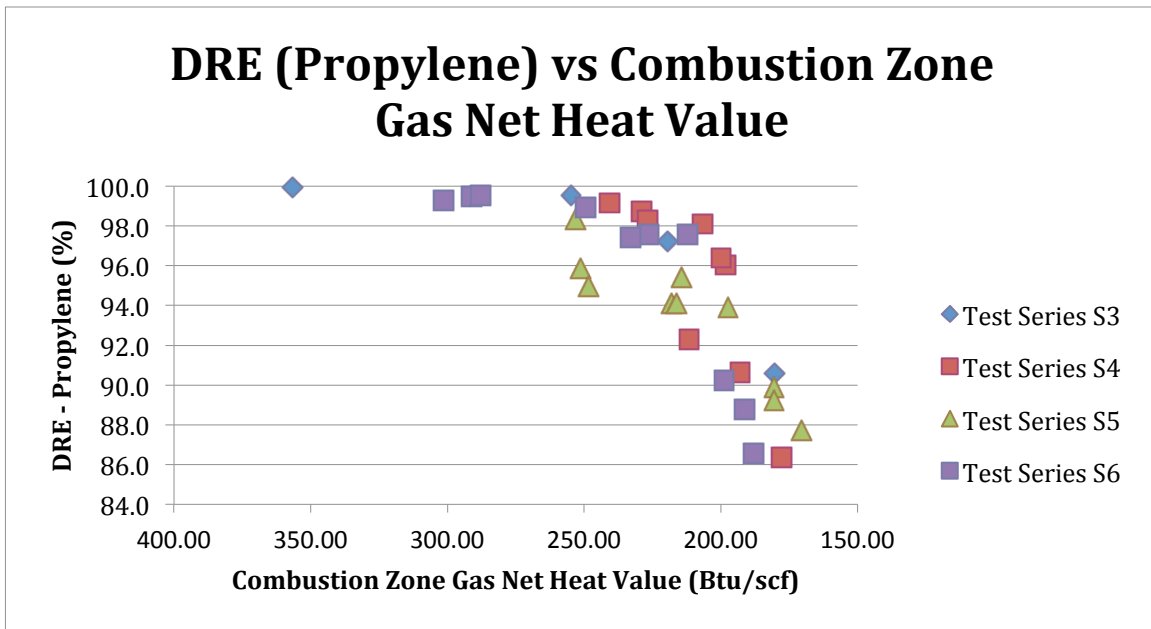


Figure 5-20b. DRE vs CZG NHV for Test Series S3, S4, S5 and S6

# D R A F T

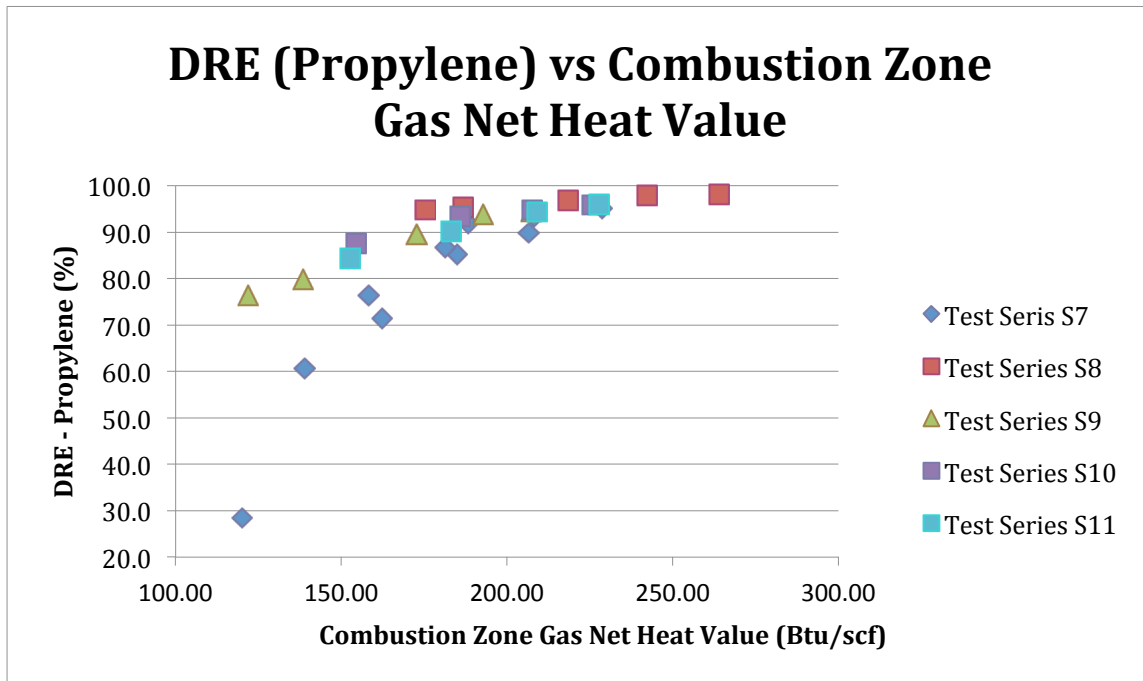


Figure 5-21a. DRE vs CZG NHV for Test Series S7, S8, S10 and S11

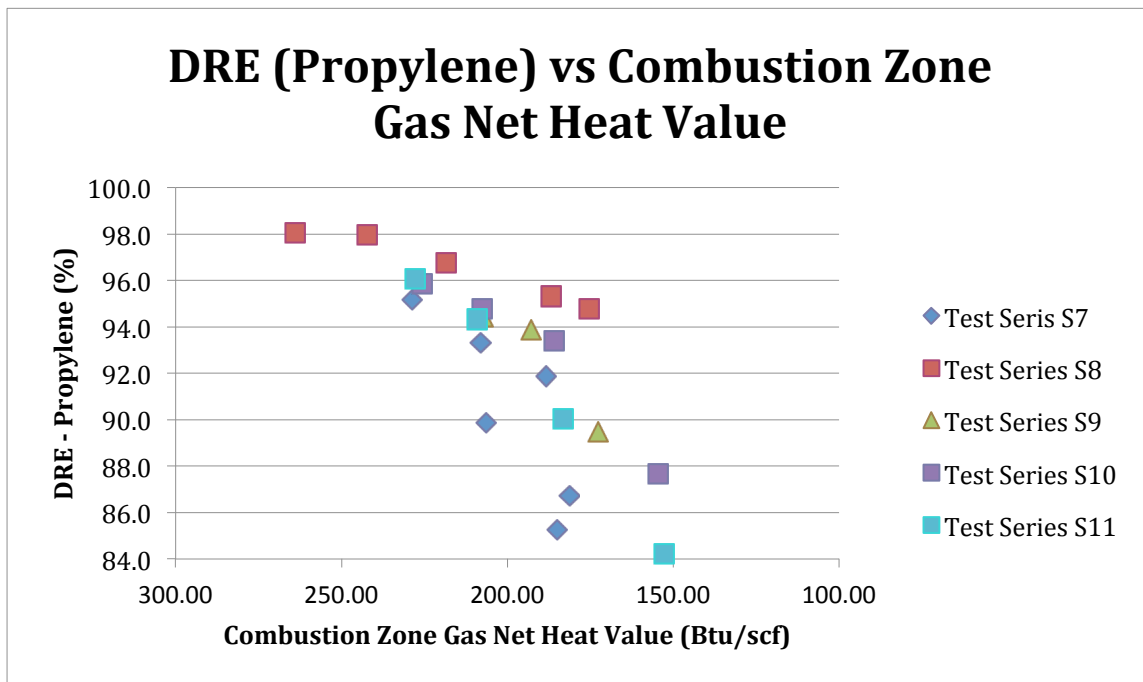


Figure 5-21b. DRE vs CZG NHV for Test Series S7, S8, S10 and S11

# DRAFT

## Air-Assisted Flare: DRE (Propylene) and CE

The theoretical air mass is the amount of air required to provide the exact stoichiometric quantity of oxygen required for combustion. In the following summaries the term “X A/F” will be used where X represents the ratio of actual air assist (lb/hr) used during the test to the amount of theoretical stoichiometric air (lb/hr) required for complete combustion of the fuel, i.e., actual air to theoretical stoichiometric air (SA) to fuel ratio on a mass basis. The following theoretical SA to fuel ratios were used: propylene -14.807 lb/lb, propane – 15.246 lb/lb, and TNG – 15.737 lb/lb. All values for theoretical SA/fuel ratios are from *The John Zink Combustion Handbook* (Baukal, 2001). The value for TNG is based on the average composition shown in Table H-1.

*Please refer to Figures 5-22a and 5-22b.*

At an air assist flow rate of 21,300 lb/hr (7.2 A/F), for a vent gas LHV of 339 Btu/scf and a constant flow rate of 902 lb/hr, the DRE (propylene) was 99.0% (A3.1 Run 3). Higher air assist levels produced lower DREs. The CE for this test point was 98.3%. The average wind speed during this test was 10.4 mph.

At an air assist flow rate of 7,930 lb/hr (6.5 A/F), for a vent gas LHV of 350 Btu/scf and a constant flow rate of 355 lb/hr, the maximum DRE (propylene) was 97.1% (A5.1 Run 2). Higher air assist levels produced lower DREs. The CE for this test point was 96.5%. The average wind speed during this test was 9.0 mph. The average wind speed during this test was 3.8 mph.

*Please refer to Figures 5-23a and 5-23b.*

At an air assist flow rate of 12,600 lb/hr (6.5 A/F), for a vent gas LHV of 584 Btu/scf and a constant flow rate of 352 lb/hr, the DRE (propylene) was 99.4% (A6.1 Run 3). Higher air assist levels produced lower DREs. The CE for this test point was 99.0%. The average wind speed during this test was 13.8 mph.

At an air assist flow rate of 30,200 lb/hr (6.2 A/F), for a vent gas LHV of 570 Btu/scf and a constant flow rate 594 lb/hr, the DRE (propylene) was 99.4% (A4.6 Run 1). Higher air assist levels produced lower DREs. The CE for this test point was 98.7%. The average wind speed during this test was 16.3 mph.

# DRAFT

## DRE (Propylene) for Tests A3 & A5 - LHV = 350 Btu/scf, Constant Vent Gas Flow Rate

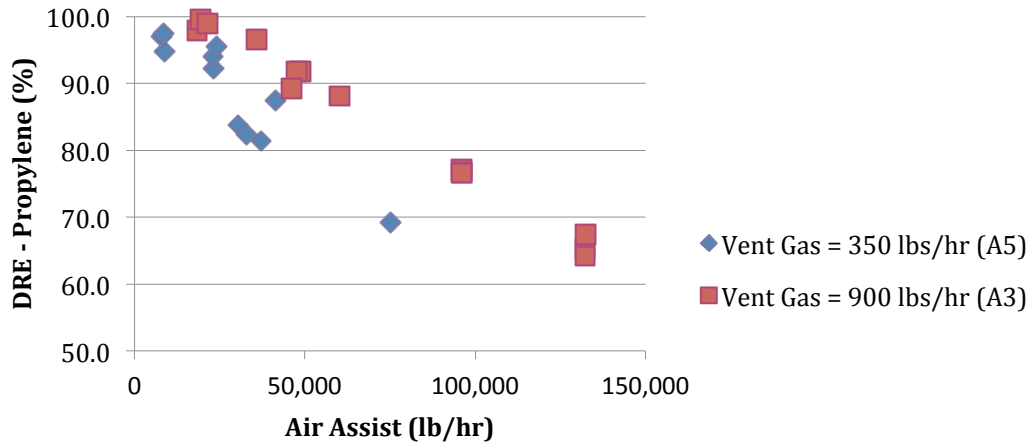


Figure 5-22a. DRE vs Air Assist for Test Series A3 and A5

## CE for Tests A3 & A5 - LHV = 350 Btu/scf, Constant Vent Gas Flow Rate

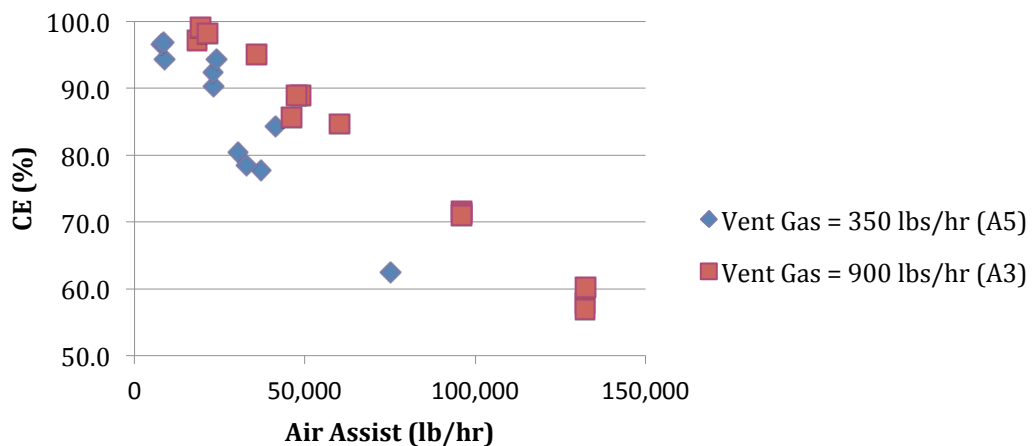


Figure 5-22b. CE vs Air Assist for Test Series A3 and A5

# DRAFT

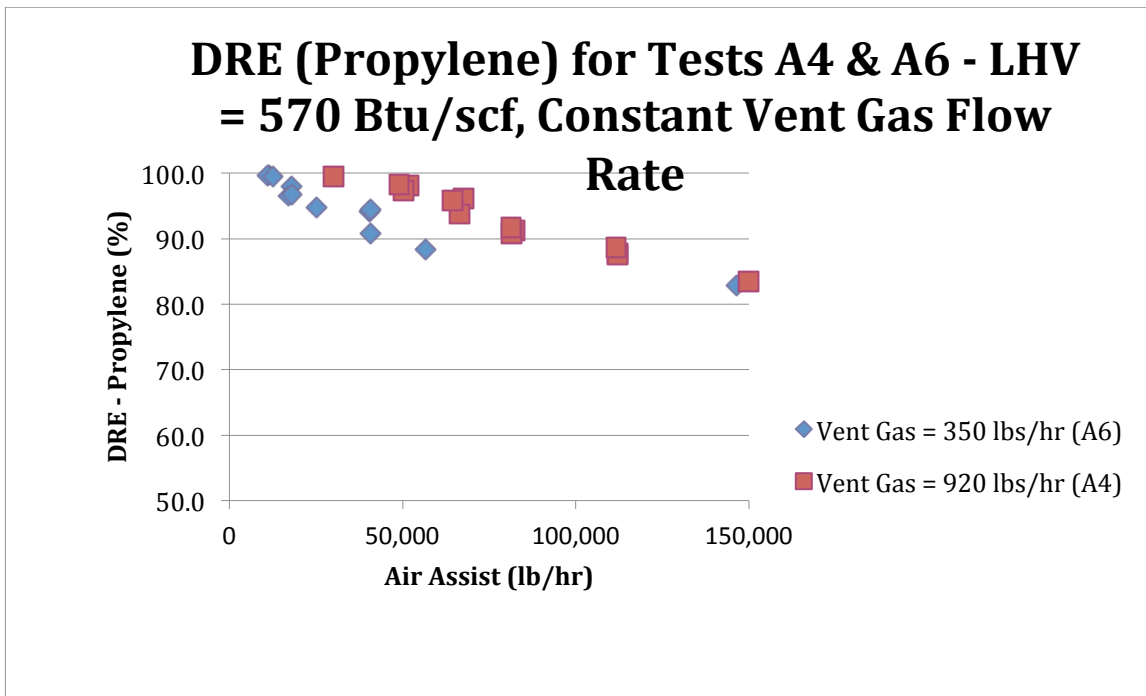


Figure 5-23a. DRE vs Air Assist for Test Series A4 and A6

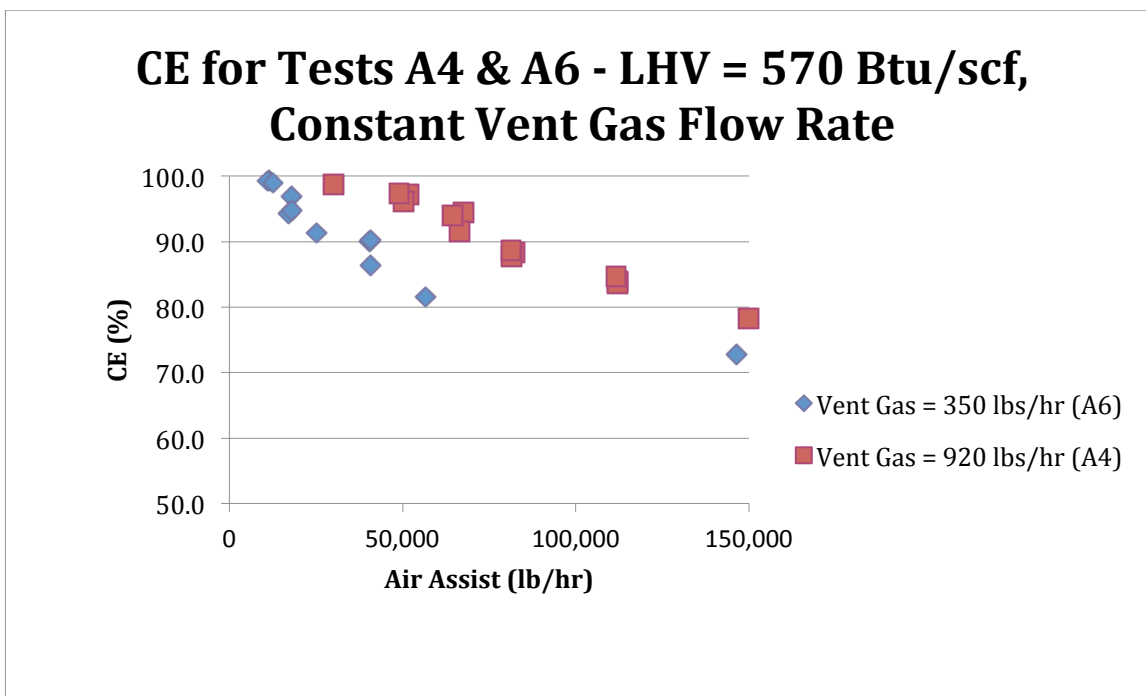


Figure 5-23b. CE vs Air Assist for Test Series A4 and A6

# DRAFT

## ***Steam-Assisted Flare: DRE (Propane) and CE***

*Please refer to Figures 5-24a and 5-24b.*

For the combination of operating parameters shown in Figures 5-24a and 5-24b, with a vent gas flow rate of 2,363 lb/hr, the maximum DRE was 97.5% (S12.1 Run 1). The CE for this test point was 99.3%. The average wind speed during this test was 2.9 mph.

For the combination of operating parameters shown in Figures 5-24a and 5-24b, with a vent gas flow rate 2,394 lb/hr, the maximum DRE was 98.3% (S13.1 Run 1). The CE for this test point was 99.3%. The average wind speed during this test was 5.2 mph.

For the combination of operating parameters shown in Figures 5-24a and 5-24b, with a vent gas flow rate 2,370 lb/hr, the DRE was 99.1% (S14.1 Run 1). The CE for this test point was 99.6%. The average wind speed during this test was 4.7 mph.

## ***Air-Assisted Flare: DRE (Propane) and CE***

*Please refer to Figures 5-25a and 5-25b.*

At an air assist flow rate of 7,120 lb/hr (5.5 A/F), for a vent gas LHV of 356 Btu/scf and a constant flow rate of 365 lb/hr, the DRE (propane) was 99.8% (A7.1 Run 2). Higher air assist levels produced lower DREs. The CE for this test point was 99.8%. The average wind speed during this test was 3.8 mph.

# DRAFT

## DRE (Propane) for Tests S12 to S14 (Propane) - LHV = 340 Btu/scf, Constant Steam Assist

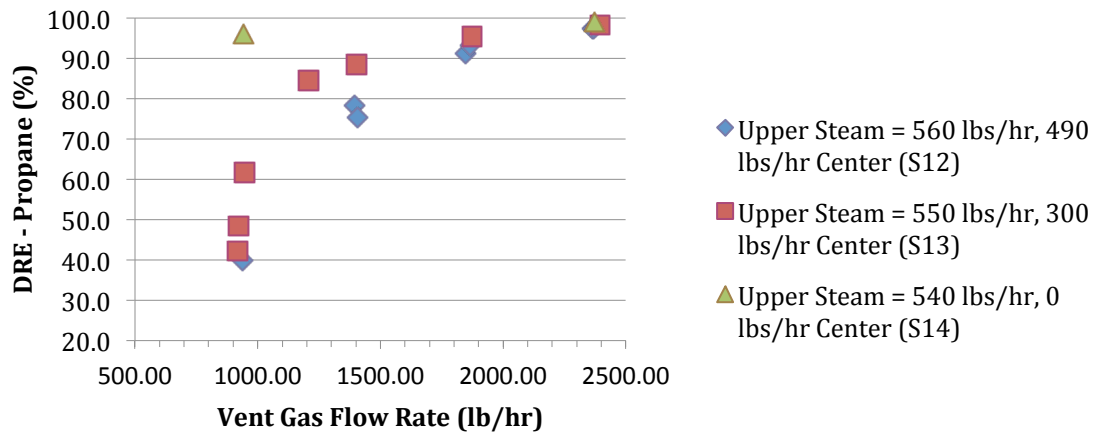


Figure 5-24a. DRE vs Vent Gas Flow Rate for Test Series S12, S13 and S14

## CE for Tests S12 to S14 (Propane) - LHV = 340 Btu/scf, Constant Steam Assist

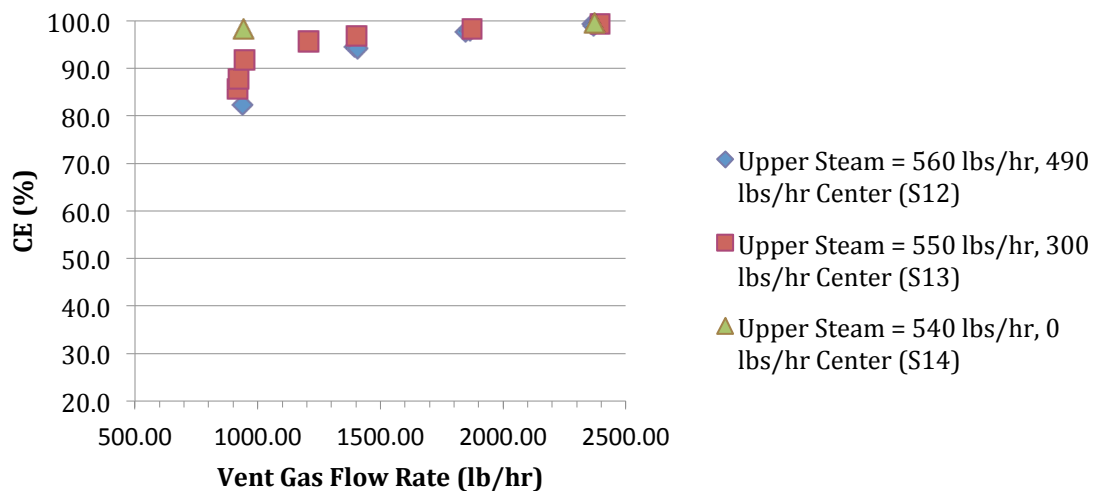


Figure 5-24b. CE vs Vent Gas Flow Rate for Test Series S12, S13 and S14

# DRAFT

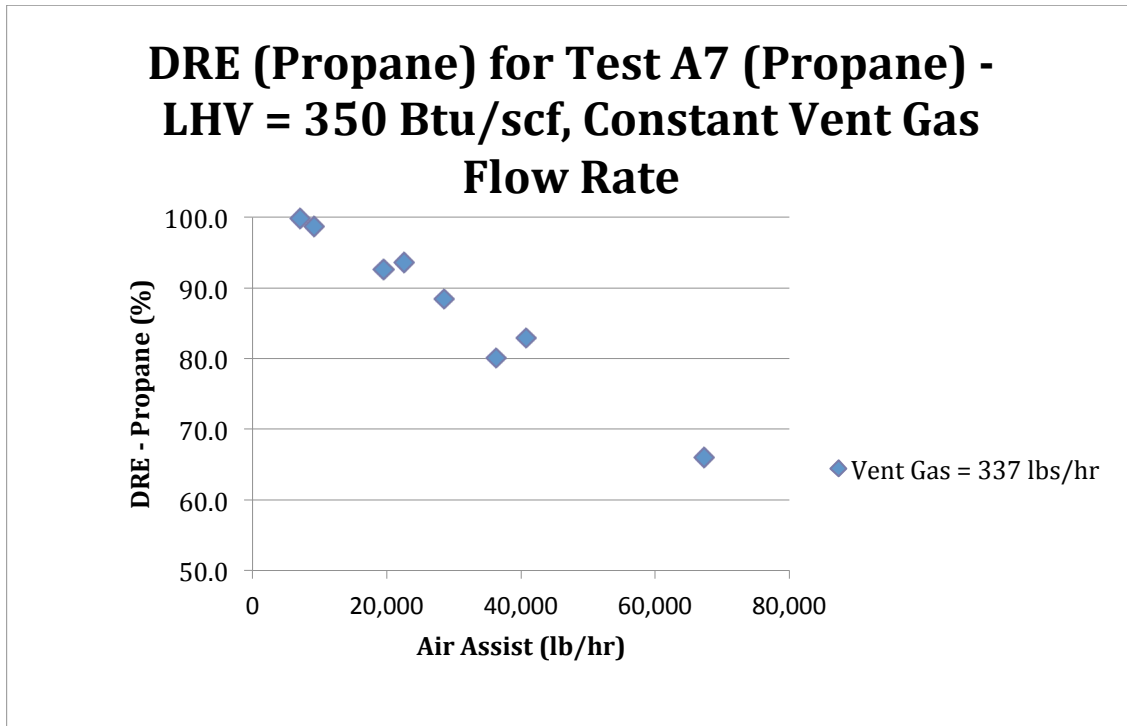


Figure 5-25a. DRE vs Air Assist for Test Series A7

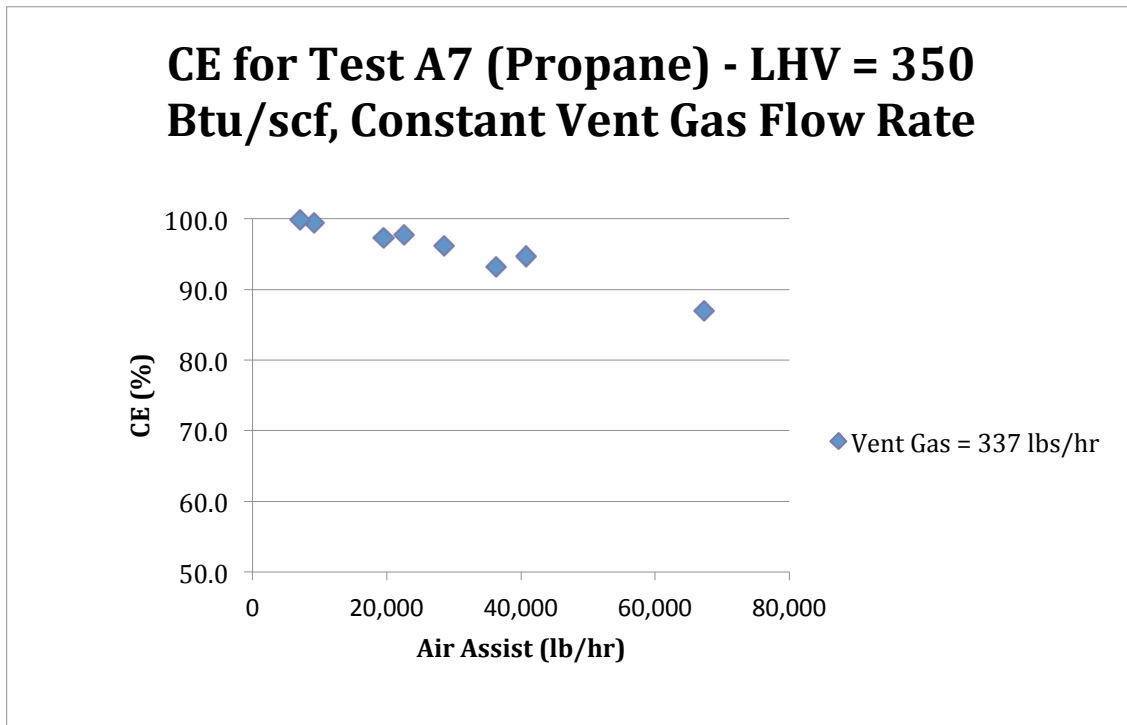


Figure 25b. CE vs Air Assist for Test Series A7

# DRAFT

## 6.0 Discussion of Test Results

The study objectives for this project included assessing the performance of industrial flares operating with low vent gas flow rates (high turn down ratios) and low LHV vent gas properties and assessing the impact of air and steam assist on DRE and CE for these low flow, low LHV vent gas streams. The analyses of the test results will focus on answering the TCEQ Study Objectives even though many more questions could be addressed with these data. In this discussion, the flare performance will always be evaluated in terms of DRE and CE. When the term DRE is used in the propylene tests, it will always refer to DRE (propylene). When the term DRE is used in the propane tests, it will always refer to DRE (propane). The DRE was not computed for any other hydrocarbons during this test series.

### **Steam Flare Tests with Propylene** (please refer to Table D-1)

For the lowest nominal LHV (350 Btu/scf) and lowest nominal vent gas flow rate (920 lb/hr) used in the study for the steam flare tests, Figures 5-12a and 5-12b illustrate the sensitivity of the flare's performance to steam assist with this vent gas stream (S3), particularly the addition of center steam. The average wind speed for the S3 test series ranged between 2.6 mph and 7.5 mph. When the center steam was zero (S3.6 and S3.7) and total steam did not exceed about 230 lb/hr, the DRE and CE were the highest, in excess of 99%, even with the highest wind speed of the test series (7.5 mph) during S3.5R2. However, as soon as the steam assist was progressively increased (S3.5 and S3.2) with average wind speeds ranging from 7.2 mph to 7.5 mph, comparable to or less than the S3.6 and S3.7 tests, which had the highest DRE and CE, the DRE and CE progressively decreased. The DRE and CE were lowest, 46.6% and 42.9%, respectively, for S3.1, which had the lowest wind speed and nominal steam assist (center = 540 lb/hr, upper = 430 lb/hr) equating to a steam-to-vent gas ratio (S/VG) of 1.04. Industry reported to the TCEQ (email message from R. Nettles, TCEQ, to V. Torres, UT Austin, on September 8, 2010) prior to the study that this level of steam assist, is slightly lower than that recommended (center = 500 lb/hr, upper = 750 lb/hr) by flare manufacturers to industry for this size and model of steam flare.

This one test series showed three characteristics of this flare at these operating conditions:

1. Average wind speeds up to 7.5 mph do not prevent this flare from achieving 99% DRE and 99% CE.
2. This flare's performance curve as measured by DRE and CE versus steam assist, has a very short, almost nonexistent, DRE "cliff" that is adversely affected by the addition of center steam.
3. Steam assist levels currently used by industry would be too high to achieve the desired DRE of 99%.

Using the same LHV (350 Btu/scf) and a vent gas flow rate of nominally 2,342 lb/hr (S4.2R3), the DRE is sustained at 99% for a slightly greater amount of steam assist (S/VG = 0.29), approximately 666 lb/hr total (center = 555 lb/hr) before the DRE and CE start to fall below 99%. Once again, steam assist levels currently used by industry would be too high to achieve the desired DRE of 99%.

# DRAFT

Test series S4.1 to S4.4 were conducted on September 17, when the average wind speeds during these tests were 4.1 mph to 5.9 mph. Test series S4.5 to S4.11 were conducted on September 21, when average wind speeds during these tests ranged from 12.7 mph to 18.0 mph. In comparing similar test series S4.1 to S4.5, with average wind speeds of 5.8 mph and 16.0 mph, respectively, it does appear that the higher wind speed may have adversely affected the DRE. The average DRE for test series S4.1 was 96.8% versus 92.3% for test point S4.5. In comparing a second set of similar test points, S4.3R1 and S4.11, with average wind speeds of 5.7 mph and 12.7 mph, respectively, it does not appear that the wind speed adversely affected the DRE. The DRE for test series S4.3R1 was 27.3% versus 27.2% for test point S4.11R1. There are no other data at this set of operating conditions to make additional comparisons and draw a definitive conclusion on what level of wind speed begins to adversely affect the flare's performance for this operating condition.

For the highest nominal LHV (600 Btu/scf) used in this study for the steam flare tests and a nominal vent gas flow rate of 937 lb/hr (Test Series S5), as shown in Figures 5-13a and 5-13b, the flare's best performance in response to steam assist is similar to the S3 test series but more robust in its response to center steam. In Test Point S5.1R1, with center steam = 480 lb/hr and upper steam = 283 lb/hr (S/VG = 0.82), the average DRE was 96.4% and CE was 95.4%. The average wind speed was 8.0 mph during this test. Whereas, Test Point S3.2R2, with only 570 lb/hr total steam (52 lb/hr center, 518 lb/hr upper), resulted in a DRE of 90.6% and a CE of 88.5% with a very comparable average wind speed of 7.5 mph. No operating condition in the Test Series S5 would have achieved a DRE  $\geq$  99% with levels of steam assist of 500 lb/hr center steam and 750 lb/hr upper steam.

In Test Point S5.1 with all flare operating parameters held approximately the same during the three repetitions, the average wind speed varied from 8.0 mph to 10.7 mph. The repetition (S5.1R1) conducted with the average wind speed of 8.0 mph resulted in a DRE = 98.3%. The other two repetitions, S5.1R2 and S5.1R3, were conducted with an average wind speeds of 10.3 mph and 10.7 mph and resulted in DREs of 95.9% and 95.0%, respectively. It appears that in the higher wind speed test, the wind may have contributed to the slight adverse effect on the flare's performance.

In Test Series S6 with the same nominal LHV (600 Btu/scf) and the higher vent gas flow rate of nominally 2,342 lb/hr, the DRE and CE exceed 99% (S6.1) and the DRE is sustained at almost 99% (S6.5) with additions of steam of up to approximately 2,000 lb/hr total (S/VG = 0.84). Average wind speeds in these two test series ranged from 7.5 mph to 8.0 mph. This combination of LHV and vent gas flow rate would achieve DRE  $\geq$  99% with levels of steam assist of 500 lb/hr center steam and 750 lb/hr upper steam.

In Test Point S6.1, the average wind speed varied from 7.5 mph (S6.1R3) to 8.8 mph (S6.1R1) and the DRE varied from 99.3% to 99.5%, respectively. There does not appear to be a discernable effect on the flare's performance from this variation in average wind speed.

In Test Point S6.2, the average wind speed varied from 6.2 mph (S6.2R1) to 12.2 mph (S6.2R3) and the DRE varied from 33.3% to 35.3%, respectively. The average wind speed for the

# DRAFT

intermediate repetition (S6.2R2) was 8.1 mph and the DRE was 40.2%. At this DRE, the wind speed does not appear to be reason for the variation in DRE between repetitions.

While it appears from Figure 5-14a that a S/VG value of approximately 0.4 or less ensures that the DRE is above 98%, expanding the graph for the region greater than 84% (Figure 5-15a and Figure 5-15b) reveals something different. Examining Figure 5-15a and the data summary in Appendix D, there are multiple values for DRE for a given S/VG until the S/VG gets much closer to 0.15 or less for this LHV (= 350 Btu/scf) and vent gas flow rates. A similar trend is noted for the CE (Figure 5-15b) with the critical S/VG value to obtain CE = 98% being much less than 0.1, perhaps even close to zero, since in general, the CE values are less than the DRE values for a given S/VG.

As was seen at a LHV = 350 Btu/scf, it appears in Figure 16a that a S/VG = 0.9 or less would ensure a DRE of 98% or more. However, upon closer inspection of Figure 5-17a, in which the region DRE > 84% is expanded, and the summary data in Appendix D, once again due to multiple DRE values for a given S/VG, the S/VG must be less than about 0.70 to ensure a DRE above 98% for a LHV of 600 Btu/scf and these vent gas flow rates. As above, the S/VG must be less than 0.65 for the CE to be above 98% but there is insufficient test data to estimate what it might be as shown in Figure 5-17b.

One general observation in the steam flare's performance, the DRE was always greater than the CE using these propylene, TNG and nitrogen mixtures, indicating the propylene is easier to destroy than it is to convert all of the components to CO<sub>2</sub>.

## **Air Flare Tests with Propylene** (please refer to Table E-1)

For the lowest nominal LHV (350 Btu/scf) and lowest nominal vent gas flow rate (350 lb/hr) used in this study for the air flare tests, Figures 5-22a and 5-22b illustrate the sensitivity of the flare's performance to air assist with this vent gas stream (A5). When the air assist was 8,330 lb/hr (7 A/F), the DRE for this test point (A5.1R3) was 97.5% and the CE was 96.8%. This was the lowest air assist rate that satisfied the study's definition of incipient smoke point so no lower air assist conditions were tested. As the air assist increased, the DRE and CE decreased almost linearly. The average wind speed for the A5 test series ranged from 2.1 mph to 5.6 mph.

For the same nominal LHV (350 Btu/scf) and a nominal vent gas flow rate of 900 lb/hr, when the air assist rate was at or very near the incipient smoke point, the air assist rate was 19,400 lb/hr (6.5 A/F), the DRE for this test point (A3.1R2) was 99.6% and the CE was 99.1%. As the air assist increased, the DRE and CE decreased almost linearly. The average wind speed for the A3 test series varied from 10.3 mph to 13.4 mph.

# DRAFT

Equation 6.1 defines the air assist tip exit velocity.

$$\text{air assist tip exit velocity (mph)} = \frac{\text{air assist (scfm)}}{7.5 \text{ ft}^2} \times \frac{P_{STP}}{P} \times \frac{T}{T_{STP}} \times \frac{60 \text{ min/hr}}{5,280 \text{ ft/mile}}$$

Eq. 6.1

where

air assist tip exit velocity (mph) = speed of the air assist in mph as it exits the flare tip

air assist (scfm) = volumetric flow rate of the air assist, scfm, from Table E-1

7.5 ft<sup>2</sup> = free flow area of the air assist only

P<sub>STP</sub> = standard pressure, 14.696 psia

P = ambient air pressure, psia, from Table E-1

T (°R) = ambient air temperature, °F, from Table E-1, plus 459.7 °R

T<sub>STP</sub> (°R) = standard temperature, °R, 527.7 °R (= 459.7 + 68)

For the flare tests conducted, the range of molecular weights of the vent gas were 29.6 lb/lb-mol to 30.8 lb/lb-mol, similar to or slightly greater than that of air, 28.96 lb/lb-mol. Exit velocities for the vent gas from Table 1 for Test Series A3 and A4 were 1.9 fps, for A5 and A7 were 0.8 fps and for A6 were 0.7 fps. Converting these vent gas exit velocities to mph we get Test Series A3 and 4 were 1.3 mph, A5 and A7 were 0.6 mph and A6 were 0.5 mph.

The volumetric flow rate for the air assist during this test series ranged from about 4,000 scfm to 29,400 scfm. Calculating the air assist tip exit velocity using Equation 6.1, these two volumetric flow rates equate to 6.4 mph and 47.1 mph, respectively. Comparing the air assist exit velocities with the vent gas exit velocities and their very comparable molecular weights, the velocity of the air assist will be the dominant driver in characterizing the momentum of the vent gas/air assist mixture exiting the tip of the flare, which is proportional to the square of the velocity.

At every test point in this A3 test series, the velocity of the air assist exiting the flare was equal to or greater than the wind speed except for A3.1. So the momentum of the vent gas/air assist mixture exiting the flare tip was greater than the momentum of the crosswind. Therefore, particularly at the higher air assist rates (> 9,000 scfm), any adverse effect from the wind speed during these test series was difficult to distinguish from the adverse air assist impact.

For the highest nominal LHV (600 Btu/scf) used in this test series in the study for the air flare tests and a nominal vent gas flow rate of 350 lb/hr (Test Series A6), as shown in Figures 5-23a and 5-23b, for this test point (A6.1R1), the DRE was 99.7% and the CE was 99.3% using an air assist rate of 11,400 lb/hr (5.9 A/F). The average wind speed during this test point ranged from 13.8 mph to 16.0 mph. At these slightly higher wind speeds, any impact from the cross wind appears to be minimal, if any. As the air assist increased, the DRE and CE decreased almost linearly.

# DRAFT

In examining test point A6.4R3, which had a DRE of 94.4% with an average wind speed of 12.3 mph and test point A6.4R2, which had a DRE of 94.2% with an average wind speed of 15.4 mph, it does not appear that the average wind speed adversely affected the flare performance.

When the nominal LHV of 600 Btu/scf and the highest vent gas flow rate were used for the air flare tests (A4), for the test point A4.6, the DRE was 99.4% and the CE was 98.7% using an air assist rate of 30,200 lb/hr (6.2 A/F). The average wind speed for this test point was 16.3 mph. Using Equation 6.1, an air assist volumetric flow rate of 6,700 scfm equates to an air assist exit velocity of 10.5 mph. Even when the average wind speed was 55% greater than the air assist exit velocity, the DRE was > 99%.

As with all of the other air flare tests, as the air assist increases, there appears to be a linear decrease in the DRE. In this test series, the decrease in DRE and CE has a slope that is less than in the previous tests.

## **Steam Flare Tests with Propane** (please refer to Table D-1)

This test series (please see Figures 5-24a and 5-24b), conducted with the substitution of propane for propylene, was conducted at only one LHV, 350 Btu/scf.

With the knowledge of the propylene test series, and the greater challenges the test system had with variation of steam assist at low steam levels, the propane test series were conducted at three nominal steam assist conditions, each held constant when employed: center = 0 lb/hr, upper = 550 lb/hr; center = 300 lb/hr, upper = 550 lb/hr; and center = 500 lb/hr, upper = 550 lb/hr.

At a nominal LHV of 350 Btu/scf and a nominal vent gas flow rate of 2,342 lb/hr, with no center steam and 540 lb/hr upper steam ( $S/VG = 0.23$ ) in Test Series S14.1, the DRE was 99.1% and the CE was 99.6%. The average wind speed for this test series was 4.7 mph. When steam was added to the center, center = 300 lb/hr ( $S/VG = 0.35$ ), the DRE decreased (S13.1) to 98.3% and the CE to 99.3%. The average wind speed for this test series was 5.2 mph. As center steam was increased to 500 lb/hr (S12.1),  $S/VG = 0.44$ , the DRE decreased to 97.4% and the CE to 99.1%. The average wind speed for this test series was 2.3 mph.

The remainder of the propane test series were conducted at combinations of lower vent gas flow rates and lower steam assist than Test Series 12.1 that did not achieve higher levels of DRE or CE than Test Series S14.1. No operating condition in the propane tests conducted would have achieved a  $DRE \geq 99\%$  with levels of steam assist of 500 lb/hr center steam and 750 lb/hr upper steam.

The average wind speed during the propane test series varied from 0.5 mph to 7.2 mph. These levels of average wind speed did not affect the steam flare's performance during the propane test series.

## **Air Flare Tests with Propane** (please refer to Table E-1)

This test series (please see Figures 5-25a and 5-25b), conducted with the substitution of propane for propylene, was conducted at only one LHV, 350 Btu/scf.

# DRAFT

At a nominal LHV of 350 Btu/scf and a nominal vent gas flow rate of 350 lb/hr, with an air assist rate of 9,100 lb/hr (5.5 A/F) in Test Series A7.2R2, the DRE was 99.8% and the CE was 99.8%. The average wind speed for this test series was 3.8 mph.

The remainder of the air flare propane test series was conducted at higher air assist rates, which produced progressively lower DREs and CEs.

The average wind speed, during the air flare propane test series, varied from 3.6 mph to 5.8 mph. These levels of average wind speed do not appear to have adversely affected the air flare's performance during the propane test series.

# DRAFT

## 7.0 Accuracy and Precision of Plume Sampling System Measurements

The sources of ‘error’ in the extractive plume sampling methodology employed during the flare tests are addressed in this section. The known sources of bias, variability and noise present in this methodology are defined and addressed in this discussion. Before outlining the section, however, as an introduction we first consider a qualitative discussion looking at two chronological test points with different assist rates. The sampling measurement dataset has been described in Section 5. This introduction is a review of the method for determining the carbon fraction carried by propylene in the flare plume. It also depicts the time series data for two consecutive tests with different DRE on the same scale to illustrate the qualitative differences in the measurements.

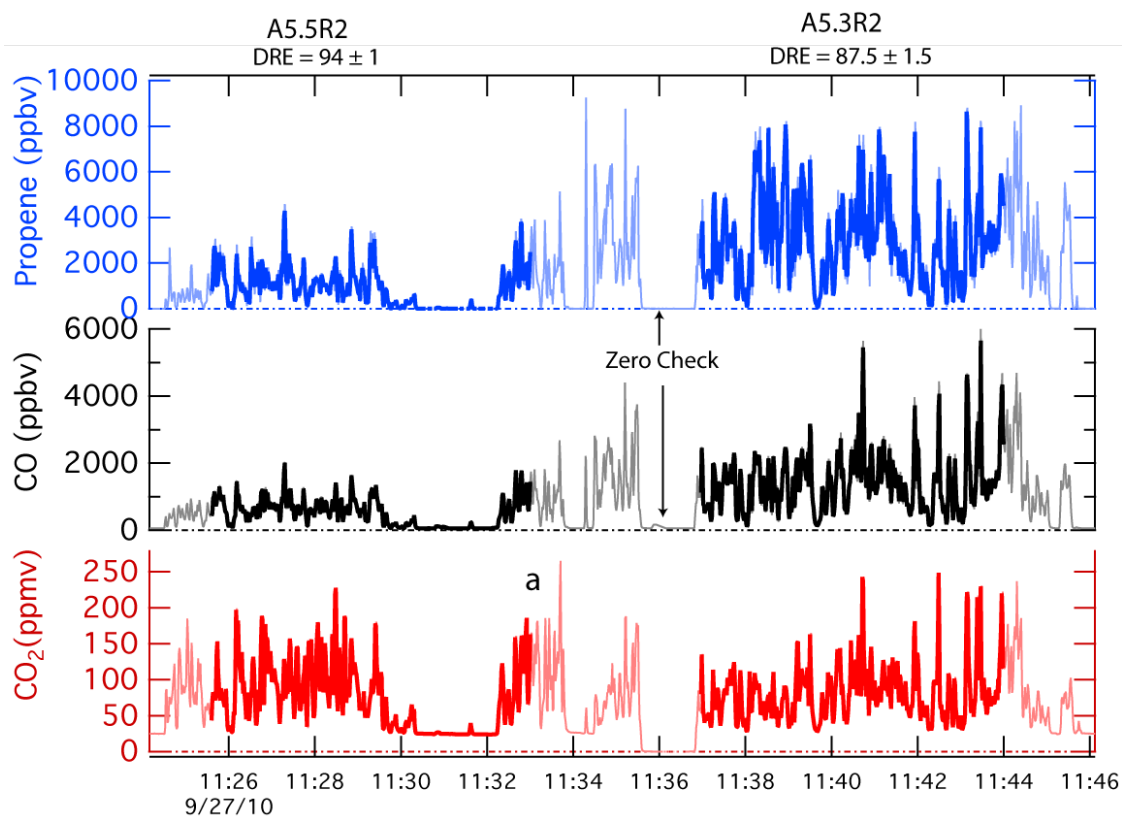


Figure 7-1. Time Series During Air Flare Tests A5.5R2 and A5.3R2. The time series for the sample collector data is plotted for CO<sub>2</sub>, CO and propylene. The official stable test periods are denoted by the heavier line style. The point marked “a” is where the flare operational parameters were changed as described in the text. The “zero check” refers to overblowing the sample probe tip with dilution air to verify instrument zero drift performance.

Figure 7-1 depicts a time series for propylene, carbon monoxide and carbon dioxide. The light coloring is the complete data time series and the two heavier line sections are the test conditions A5.5R2 and A5.3R2. The tests depicted here were run on the air flare using 80% propylene/20% TNG for the vent gas composition. The wind direction during the pair of events was consistently

# DRAFT

from the north (bearing 339° and 340° respectively). The median wind speed for the events depicted here were 3.1 and 5.0 mph respectively. The most significant change was the increase in air assist rate (made in the control room at or near the point marked “a”) which increased the air assist from 23,100 lb/hr to 41,300 lb/hr. The change in air assist was the only planned difference between A5.5R2 and A5.3R2.

Inspection of Figure 7-1 reveals that the relative magnitude of high frequency plume intercepts by the sample collector for CO<sub>2</sub> is qualitatively similar for the two test conditions. The CO and propylene however are significantly increased (A5.3R2 relative to A5.5R2). Although it is not depicted in the figure, the identical increases appear for methane, acetylene, ethylene, formaldehyde, and acetaldehyde. The carbon balance methodology, described briefly in Section 4 and more thoroughly in Appendix I, uses the following expression for determining DRE.

$$DRE/100 = 1 - \frac{\left[ \frac{\text{propylene}_{out} \text{ (molesC)}}{C_{out} \text{ (molesC)}} \right]}{\left[ \frac{\text{propylene}_{in} \text{ (molesC)}}{C_{in} \text{ (molesC)}} \right]} = 1 - \frac{CF^{propylene} \text{ (out)}}{CF^{propylene} \text{ (in)}} \quad \text{Eq. 7.1}$$

In Equation 7.1, CF refers to the carbon fraction for the superscripted species and the DRE would be for propylene. The (*in*) term refers to the vent gas mixture, where the carbon fraction carried by propylene has been set according to the relative flow rates of propylene and TNG, but verified with gas chromatographic measurements (typically twice per test point). The (*out*) term refers to the flare plume emission to the atmosphere. Due to complete and partial combustion, there are several potential forms the vent gas carbon can take. “Complete combustion” will produce CO<sub>2</sub> and a minor amount of CO and some trace hydrocarbons. The computation of CF must account for all forms of carbon in the flare plume. The expression for CF in the flare plume, derived in Appendix I, is repeated here as Equation 7.2.

$$CF^{propylene} \text{ (out)} = \frac{\text{propylene (ppmC)}/CO}{\text{propylene (ppmC)}/CO + CO_2/CO + 1 + \sum \text{other carbon (ppmC)}/CO} \quad \text{Eq. 7.2}$$

In Equation 7.2, each of the terms divided by CO are intended to be the ‘flare plume associated’ ratios. Figure (7-1) suggests that a time series analysis can extract the flare-associated ratios without any need to artificially subtract ambient levels or even know the extent of dilution if the time response for each of the instruments has been matched and any time offsets between the vectors accounted for.

# DRAFT

Although Figure 7-1 depicts two different test conditions, where the difference in the air assist rate is driving an obvious difference in DRE, the purpose of this section is to discuss the accuracy and precision in the DRE and CE reported by the sampling method. This section focuses on the topics below and will conclude with some overall assessment of the uncertainty in this approach.

- 7.1 Instrumentation Error
  - a. Measurement accuracy (e.g., “span errors”)
  - b. Measurement precision (e.g., Instrument noise)
- 7.2 Intra-test variability
  - a. Vent gas composition variability
  - b. Flare assist and operational control variability
  - c. Sample intercept variability
    - i. Height of sample probe
    - ii. Wind/transverse location of sample probe
- 7.3 Test Condition Reproducibility

# DRAFT

## 7.1.a Measurement Accuracy

The majority of the analytical instruments used for the *in-situ* sampling were chosen for their speed, sensitivity, accuracy and whenever possible their selectivity. Appendix I contains a description of the calibration procedures and results for each instrument. As was discussed in Section 4, the major constituents that determine DRE in the 80% propylene/20% TNG vent gas composition tests are CO<sub>2</sub>, CO, propylene and methane. The other trace hydrocarbon species constitute a smaller portion of the carbon in the exhaust. The accuracy of the specific trace hydrocarbon measurements does not affect the overall uncertainty in carbon fraction to the same extent as CO<sub>2</sub>, CO, propylene and methane. The accuracy of these species is more germane to the efforts to close the carbon balance which is discussed elsewhere. The CO<sub>2</sub> was measured using three different Licor brand non-dispersive infrared gas analyzers. The CO and methane were measured using different ARI quantum cascade laser (QCL) instruments based on tunable infrared laser differential absorption spectroscopy (TILDAS). The propylene was measured using proton transfer reaction mass spectrometry (PTRMS) and was verified using gas chromatography using a flame ionization detector (GC-FID).

Table 7-1. Measurement Accuracy and Calibration Checks for Selected Species

Compound	Analytical Accuracy <sup>1</sup>	Calibration Check <sup>2</sup>
CO <sub>2</sub>	1%	1%
CO	3%	1%
Methane	6%	2%
Propylene via PTRMS	15%	4%

### Table Notes

<sup>1</sup>The tabulated analytical accuracy is the overall systematic uncertainty present in the specific method as deployed in general. It is either a manufacturer's specification or is based on a propagation of systematic error present in the technique.

<sup>2</sup>The tabulated calibration check is an assessment of how well the specific instrument used for the test and data post-processing returned the input value when checked via some independent standard. The PTRMS calibration check tabulated here is explained in the text.

The overall theoretical analytical accuracy for selected measurements is tabulated in Table 7-1 along with the *in-field* calibration evaluation. The instrument calibrations are described in Appendix-I. In the case of propylene quantification via PTRMS, the calibration check is the raw level of agreement between the returned mixing ratios (concentrations) measured during the test at 1 Hz averaged and compared to the periods where the GC-FID was also sampling from the diluted flare plume sample.

The combined implication of instrument span error on the measured DRE should not be random. Based on the calibration checks that were performed over the course of the measurement period, for these species no obvious abrupt change in calibration or instrument sensitivity occurred. As a

# DRAFT

result, the instrument span source of error should be regarded as a uniform potential bias, thus consistent throughout the entire dataset. An estimate of the magnitude of this source of error is depicted in Figure 7-2. The variability in the uncertainty versus DRE expressed in Figure 7-2 reflects the associated accuracy of the different instruments. At high DRE where most of the carbon is CO<sub>2</sub> the uncertainty approaches the accuracy limit ( $\pm 1\%$ ) that measurement. At low DRE the uncertainty increases towards the accuracy limit imposed by the measurement of propylene by the PTRMS technique.

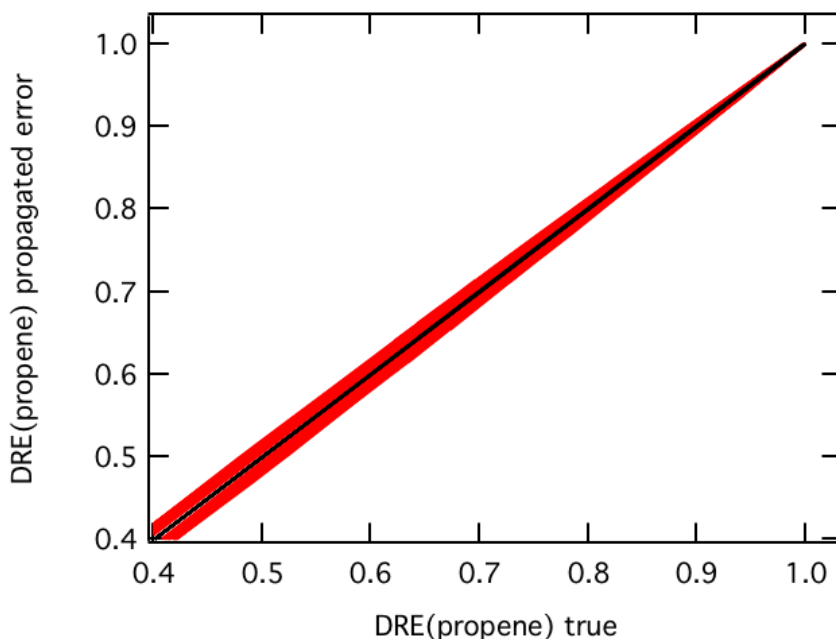


Figure 7-2. DRE Instrument Span Error for the 80/20 Propylene/TNG Vent Gas Conditions. The red band reflects the propagated error sources in Table 7-1 expressed as DRE.

# DRAFT

## 7.1b Measurement Precision

The majority of the results discussed in this report were derived from test conditions that exceeded 8 minutes in duration. As a result, the random noise associated with each specific instrument does not appreciably influence the computed carbon fraction when the whole test period is used as an ensemble.

Table 7-2. Instrument Precision Specifications

	Low Scale Noise (1 $\sigma$ )	High Scale Noise (1 $\sigma$ /average)
Propylene	1.6 ppbv	6%
CO <sub>2</sub>	38 ppbv	< 1%
CO	800 pptv	< 1%
Methane	3 ppbv	< 1%

In Table 7-2 some precision related benchmarks are tabulated for the instrument as operated during the study. The low scale noise refers to the baseline instrument noise when the sample was at the lower ranges of signal detected in this study. The high-scale noise is more related to the proportional noise and has been quantified by expressing the ratio of 1 standard deviation of the sample to the mean value for the mid point of the calibration range for the instrument. The random noise performance of the instrument is not expected to appreciably influence the carbon fraction or DRE for the test point.

## 7.2. Intra-test variability

Several parameters might vary during the test period where the flare has been called *stable*. The vent gas composition could be drifting during the event or not what was specified for the nominal composition for the test point. Operational characteristics (e.g., assist rate, total vent gas flow) might be drifting or variable. The sample collector flare plume intercept events (see Figure 7-1 for the nature of plume intercept events) will be influenced during the test by factors such as the height of the sample collector and the gusting nature of a variable wind.

### 7.2.a Vent gas composition variability

The method for measuring the vent gas composition is described in detail in Appendix G. The TRC mobile laboratory collected a sample of the vent gas and analyzed the hydrocarbon concentration using GC every 5 minutes. The calibrated response for each of the peaks in the chromatogram was used to quantify the mixing ratio of the species in the vent gas exhaust. The carbon fraction of propylene in the vent gas, for the test conditions which nominally used 80%/20% propylene/TNG is computed from the measurement data using the following formula.

$$CF^{propylene} (in) = \frac{3 \times [propylene]}{3 \times [propylene] + 1 \times [methane] + 2 \times [ethane] + \sum n[other VOC]}$$

Eq. 7.3

# DRAFT

In Equation 7.3, the bracketed species are the molar mixing ratios by volume and  $n$  is the carbon number for the specific compound.

The vent gas composition was nominally set by separately controlling the flow of propylene and TNG. An estimate of the carbon fraction of propylene in the vent gas can be computed using only the measured flow rates of the constituents.

$$CF^{propylene}(in)^{flow} = \frac{3/42 \times F^{propylene} (lb\ hr^{-1})}{3/42 \times F^{propylene} (lb\ hr^{-1}) + 1/16 \times F^{methane} (lb\ hr^{-1})} \quad \text{Eq. 7.4}$$

In Equation 7.4, the contribution of ethane (present in TNG) has been ignored.

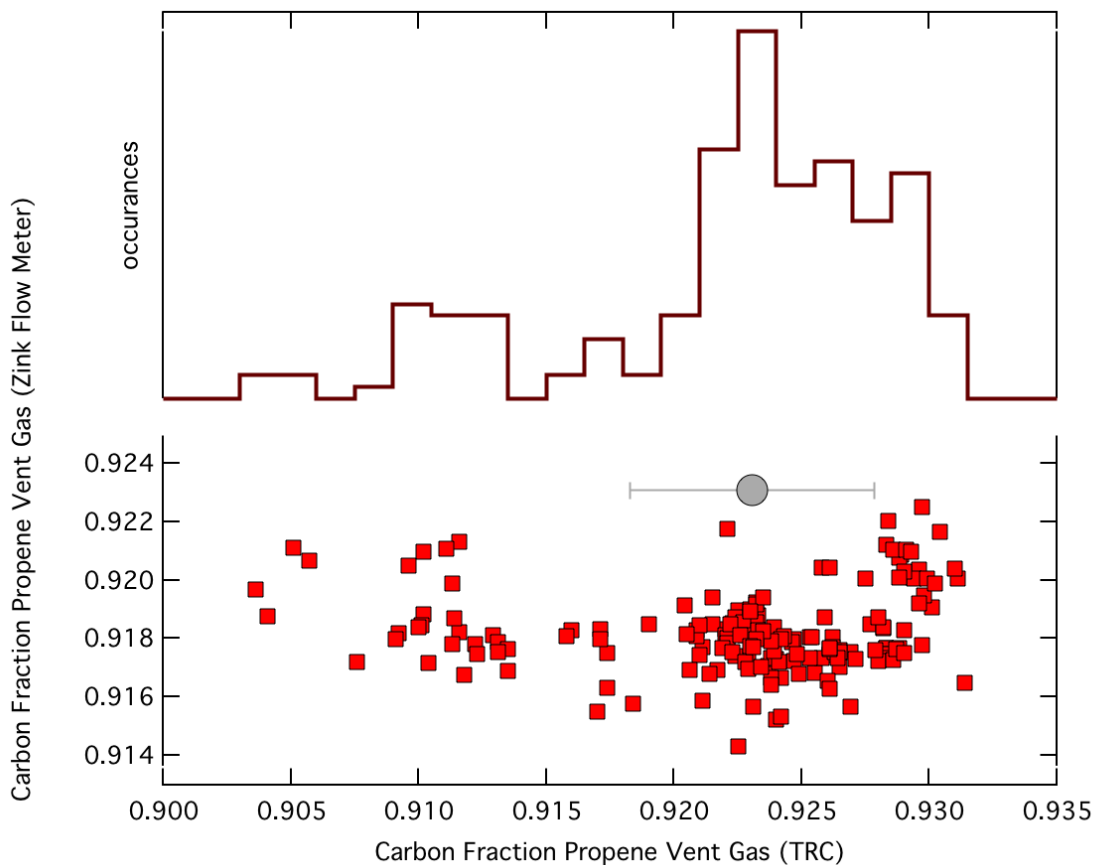


Figure 7-3. Carbon Fraction of Propylene in the Vent Gas for the 80/20 Propylene/TNG Composition. In the lower panel, for each test point (red squares) the estimate based on relative flow rates is compared to the composition measurements. In the lower panel the grey circle is the nominal propylene carbon fraction. In the upper panel, a histogram of the TRC measurement results is depicted.

# DRAFT

Figure 7-3 compares the carbon fraction of propylene in the vent gas computed using the flow rate data to the actual measurement using GC. Equation 7.1 uses the carbon fraction of propylene in the vent gas to compute DRE. The apparent variability based on the TRC measurements is 0.5%,  $1\sigma$  of a Gaussian fit of the histogram of measurements. Based on the level of agreement observed between the flow rate and direct measurement methods, and the magnitude of variability in the resulting vent gas propylene carbon fraction, this source of error is not considered to be significant.

## 7.2.b Flare assist and operational control variability

Zink personnel controlled the operation of the flare burners (air- and steam-assisted) and the vent gas supply control system. The process control instrumentation monitors were digitized and recorded. Prior to the establishment of a particular test point, the flare controls were set. Typically, three minutes elapsed while the flare control system was adjusted and monitored for stability. During the stable test periods, no modifications were made to the flare control parameters. Examination of the time series of the digitized parameters for flow assist rate (total steam and center steam for the steam flare and air flow for the air flare) does not suggest the control system had significant drift during the test point. At two points during the test, the near-real time diagnostics of flare control parameters alerted the control room when something was not following the test design and the data for the test point was set aside. The digital data record does not reveal any significant changes or variability in the operational flare control parameters.

## 7.2.c Sample collection variability

The purpose of the TCEQ Comprehensive Flare Study was to determine the representative DRE as a function of flare operational parameters. It was not part of the project to quantify inhomogeneity in the combustion at varying flare radii. The study design deliberately attempted to sample a large volume of air and force mixing before characterizing the sampled constituents. Furthermore, during the project design phase, the sample collector was assumed to be at least 2 flame lengths away in the horizontal plane in order to sample plume that was done with the combustion, or no longer actively burning at high temperature.

Using estimates of stoichiometric combustion and the measured volumetric draw of the sample collector it physically, drew up to ~15 - 20% of the total flare plume volume. At the distances the sample collector was deployed (away from the flare center), the flare combustion products were unavoidably diluted by an unknown, uncontrolled amount of non-combustion ambient air prior to entering the sample collector. It is clear though that the sampler did rapidly pull in air that was highly influenced by the flare plume. By the metric of inlet probe temperature the flare plume that entered the sampler was between 50 and 140° Fahrenheit above ambient. The air mass sampled during plume encounters saw increases in CO<sub>2</sub> above ambient by a factor of 2 to 50 (e.g., *diluted* flare plume CO<sub>2</sub> mixing ratios of 800 ppmv to 2%).

The time series analysis approach used to generate the terms in Equation 7.2 that have the form carbon-containing-compound per CO is not sensitive to the dilution by ambient. In effect, the method is almost counting on variability in the dilution extent so that the concomitant increases in carbon-containing-compound and CO reveal the flare plume associated ratio clearly against the ambient mixing ratios.

# DRAFT

The most important data quality indicator for DRE determined in the sampling methodology is an insensitivity of the extracted ratio with chosen test time periods. To the extent that the ‘plume hits’ converge, this methodology asserts that the deduced DRE is the *representative* DRE needed to assess the emissions to the atmosphere.

To test the intra test point variability that this analysis produces, test condition S4.6R1 has been parsed into different intervals. The entire test point (~ 10.5 min) has been parsed into ten second, twenty second, forty second and one minute bins and processed using the same methodology as the total ensemble analysis. The results of this analysis are depicted in Figure 7-4. The red diamond is the result from the whole event taken as an ensemble and reduced to a single DRE using Equation 7.2. The dark blue histogram in Figure 7-4 reflects the frequency that the shorter duration analysis resulted in a DRE within that bin width. The central value of this histogram (fit to a Gaussian function) agrees well with the tabulated value 98.1 vs 98.3%.

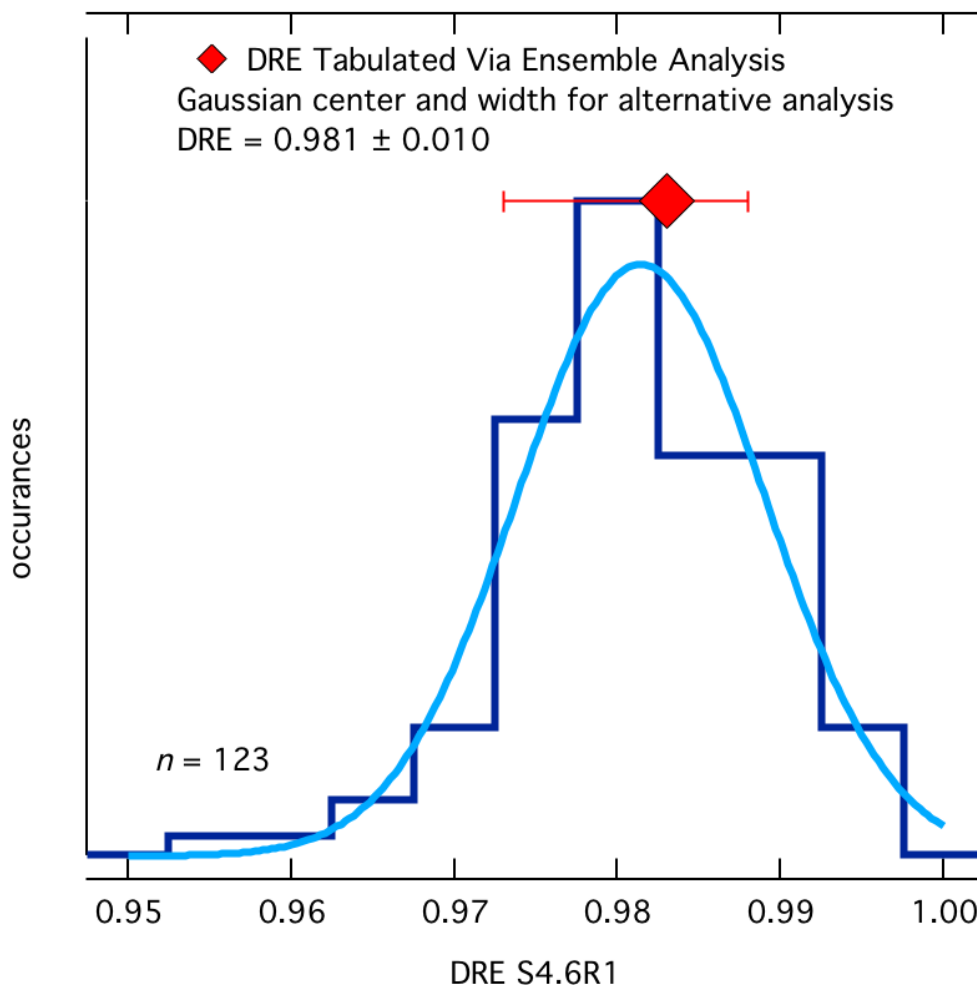


Figure 7-4. DRE Variability Analysis for S4.6R1. The graph depicts the tabulated “ensemble” DRE and error bars (red diamond) along with the results of finer scale analysis described in text (histogram results and fit).

# DRAFT

## 7.2.c.i Height of sample probe

The height of the sample probe was varied during many of the test conditions. Some additional tests for vertical profiling were conducted. The condition described earlier in Section 4, S4.1R1 was one of the conditions where the sample collector was moved in the vertical direction deliberately to test whether or not a difference in the sampled DRE would be observed. There were other observations at much reduced DRE (less than 70%) that exhibited some vertical variability that is part of the ongoing analysis. For the DRE cases that were greater than 85% no detectable dependence on DRE with sample collector height was observed. Here, an alternative analysis of S4.1R1 has been performed to evaluate the effect of sample collector height as well as to verify the extractive sampling method using alternative analysis techniques.

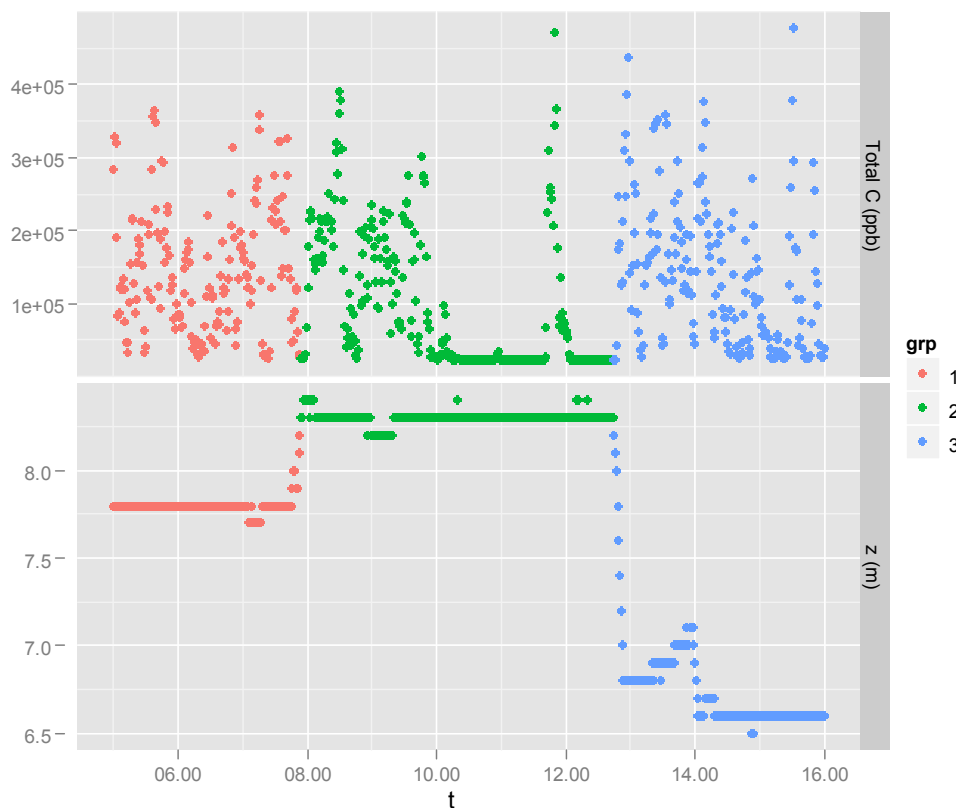


Figure 7-5. Grouping by Sample Collector Height (z). See text for description of the color banding

Figure 7-5 plots the sample collector height time series along with observed total carbon (C) concentration. The analysis described here was conducted completely independently from ARI. The time series analysis here does not use either of the ‘ensemble’ slope or the time segment analysis. Figure 7-5 is color coded into three segments, where DRE is calculated for each using the 1-second data and an independently derived formula for DRE.

# DRAFT

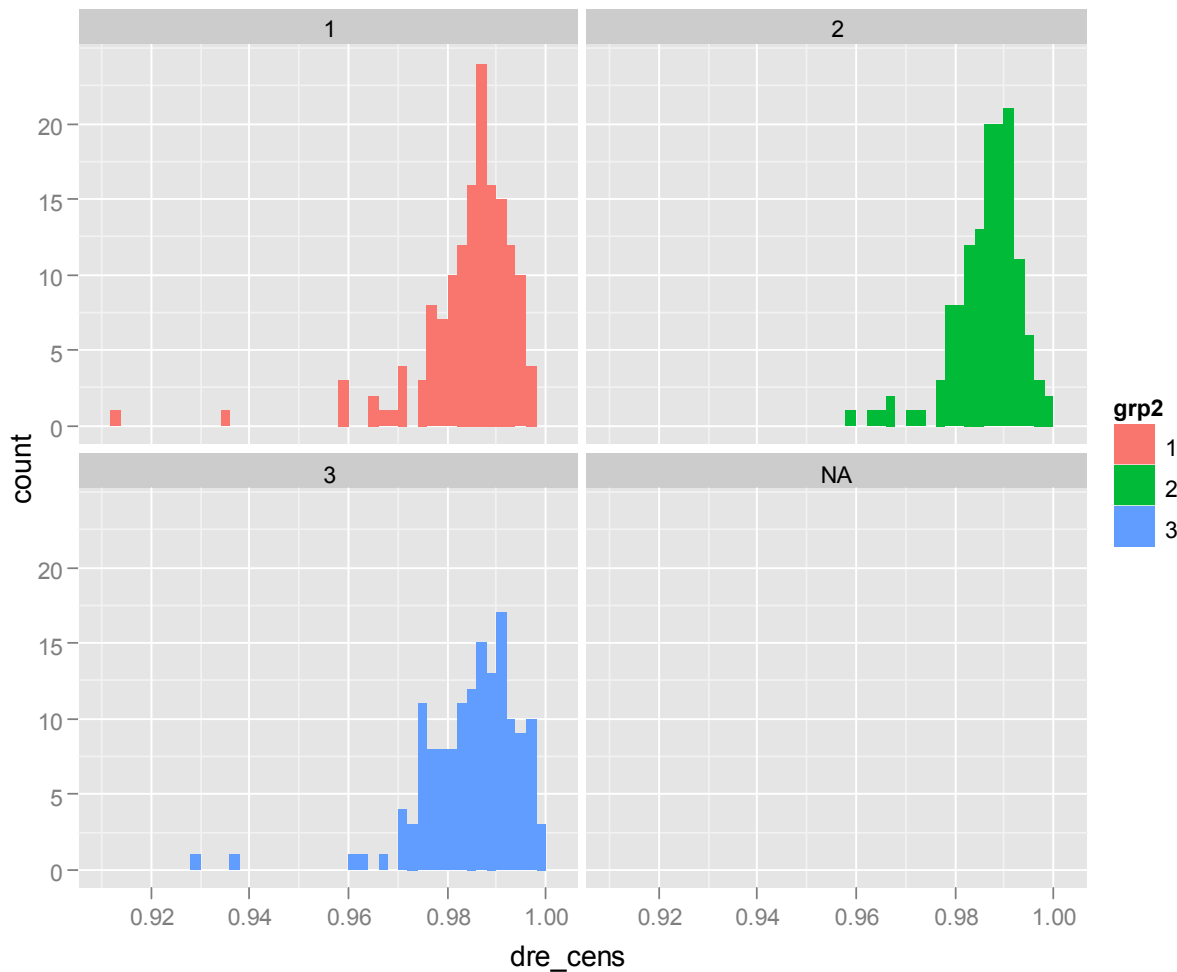


Figure 7-6. Histogram of Second-by-Second DRE Grouped by Sample Collector Height

Figure 7-6 depicts the results for the alternative DRE methodology, which is based on the least amount of data (second-by-second calculations, from instrumentation that had time responses between 0.9 and 1.2 seconds). The results of a statistical analysis are tabulated in Table 7-3. For this test, at a relatively high DRE, the sample collector height does not vary DRE, in this test there is no distinguishable difference observed.

# D R A F T

Table 7-3. Summary of Second-by-Second DRE by Sample Collector Height Groups

Group No.	Accepted Records	Dropped Records	Mean (%)	Std. Dev. (%)	Min (%)	1Q (%)	Median (%)	3Q (%)	Max (%)
1	150	24	98.45	1.05	91.33	98.17	<b>98.64</b>	99.03	99.69
2	134	157	98.66	0.68	95.94	98.34	<b>98.77</b>	99.08	99.96
3	147	49	98.49	1.00	92.97	97.97	<b>98.65</b>	99.14	99.91
All Data	431	230	98.53	0.93	91.33	98.17	<b>98.69</b>	99.08	99.96

For the same grouping, DRE was verified using the slope methodology. These values are collected in Table 7-4. The net ensemble DRE calculated here agrees with the value reported in the ARI analysis. Table 7-4 shows relevant statistics from the analysis and subsequent calculations to derive DRE. The slope approach also did not indicate the sample collector height as a significant variable in explaining the variation in DRE. In fact, the estimated range in DRE using the slope approach is far smaller than that of the second-by-second approach. This is anticipated, as the nature of the range estimate of each is different. In the 1-second analysis method, the standard deviation captures the spread of the observation. In the slope approach, the standard error is of the slope and it incorporates all of the observations to derive the slope. It is not a measure of spread of each data point. It should also be less sensitive to the estimate of ambient total carbon.

Table 7-4. Estimated DRE Based on Slope Approach for Each of the Sample Collector Height Groups. Mid values are calculating using best estimates of slopes. Low/high value of CF and DRE are estimated using best estimate  $\pm 2\sigma$ , assuming that CO<sub>2</sub> and C<sub>3</sub>H<sub>6</sub> do not correlate.

Group No.	CO <sub>2</sub> /CO slope		C <sub>3</sub> H <sub>6</sub> /CO slope		CF (C <sub>3</sub> H <sub>6</sub> )			DRE		
	best estimate	std. err.	best estimate	std. err.	Low (%)	mid (%)	High (%)	Low (%)	mid (%)	High (%)
1	182.69	6.99	3.28	0.13	1.503	1.754	2.045	97.78	<b>98.10</b>	98.37
2	205.66	4.05	3.60	0.08	1.577	1.714	1.861	97.98	<b>98.14</b>	98.29
3	205.97	8.81	3.86	0.13	1.576	1.829	2.128	97.69	<b>98.02</b>	98.29
All Data	199.38	3.52	3.57	0.06	1.637	1.752	1.875	97.97	<b>98.10</b>	98.23

### 7.2.c.ii Wind influence probe

Between the diagnostics of temperature, CO<sub>2</sub> and the video record, it was somewhat straightforward to reposition the sample collector whenever there was a significant wind shift. During the test, the near real time analysis of the data stream suggested that the extracted DRE was not strongly influenced by wind changes during the test. The measurements of DRE using the bulk sample collector, rapidly drawing a large volume of mixed flare plume with ambient *did not* exhibit a strong sensitivity to gusting and changes in the wind. This is not an assertion that the degree of flare plume was not dependent on wind speed and direction. When the wind

# DRAFT

changed, the sample collector had to be repositioned to the new ‘downwind’. The data do suggest, however that at the typical distance away from the sample collector the extracted DRE depends most significantly on the flare operational parameters.

In Section 6, the apparent influence of average wind speed during the test on DRE has been discussed. It is apparent from the flare performance data, i.e., DRE and CE, that regardless of the level of steam or air assist, at wind speeds less than 7.5 mph, for the air and steam flare models used in this study, the adverse effect of wind speed is either negligible or so small that it is dominated by the adverse effect of the assist on the flare’s performance. It also appears that at or above about 16 mph, for low levels < 1,100 lb/hr of steam assist, that there is evidence that the DRE is reduced, probably due to the effect of the wind. At higher levels of steam assist, the adverse effect of the steam assist more than offset any adverse effect of the crosswind speed. For the air flare, in general, any adverse effect of the wind speed was dominated by adverse effect of the levels of air assist used for many of the test points in the study. In general, the test conditions were favorable for obtaining data to address the study objectives. As the study objectives were not to develop a correlation between DRE and wind speed, additional analysis would be required to attempt determine a relationship between DRE and crosswind speed for the two flare models used in this study.

### 7.3 Test Condition Reproducibility

The test conditions were typically repeated three times for the core test series. The measurements were not done chronologically; they were mixed throughout the test interval or in some cases on completely different days. The repeatability between test runs is analyzed in Section 10. When the DRE was large (greater than 80%) the apparent variation in DRE determined at separate times was low (generally less than 4%). When the DRE was small (less than 70%) the apparent variability between DRE determinations was not as good, sometimes as large a 30% of the average DRE. There is little reason to believe this is an instrumental or systematic artifact and determining the reasons for the breakdown in reproducibility is part of the ongoing analysis. It should be noted that the degree of reproducibility at DRE greater than 80% is a strong indicator of test data quality particularly as it relates to determining the effect of flare operating parameters on the DRE versus assist performance curve as it approaches the rapid fall-off in DRE.

# DRAFT

## 8.0 Measurements Made by Remote Sensing Technology Instruments

There were three remote sensing technologies participating in the study: IMACC PFTIR and AFTIR spectrometers, Telops Hyper-Cam passive imaging radiometric spectrometer, and LSI FLIR GasFindIR and thermal IR cameras. The LSI cameras provide visual images of hydrocarbons in the gas phase and are useful in detection of these gases but cannot be used for quantitative assessment of flare combustion. The discussion in this section will focus on the IMACC and Telops instruments, which can measure the combustion efficiency of the flare. Telops can also make mass flow rate measurements of hydrocarbons in the plume. However, the final quality assured Telops data were provided in February 2011 so comparison of the Telops mass flow rate results will be provided as an addendum to this report at a later date.

As summarized in Section 3, the measurement of emissions in samples extracted from the plume and analyzed by ARI provided the baseline or reference DRE and CE values against which the remote sensing technologies would be compared. The results of the analyses of the extractive samples and determination of DRE and CE by ARI were not provided to IMACC or Telops. Subsequent to the field tests, IMACC and Telops submitted their CE measurements for each test run, including their standard deviation ( $\sigma$ ) for their measurements.

Three statistical criteria were selected to compare the measurements of IMACC and Telops with the ARI values. The first two are the mean difference and the standard deviation of the difference. These terms are defined numerically as follows.

$$\text{mean difference} = \frac{\sum_{i=1}^N \text{ABS}(CE_{RS} - CE_{ARI})_i}{N} \quad \text{Eq. 8.1}$$

$$\text{standard deviation} = \sqrt{\frac{\sum_{i=1}^N [(CE_{RS} - CE_{ARI})_i]^2}{N - 1}} \quad \text{Eq. 8.2}$$

where

mean difference = average of the absolute values of the difference between the CE determined by the remote sensing contractor and the CE determined by ARI for test point  $i$

standard deviation = standard deviation of the differences between the CE determined by the remote sensing contractor and the CE determined by ARI for the test point  $i$

$CE_{RS}$  = combustion efficiency determined by the remote sensing contractor for the test point  $i$

$CE_{ARI}$  = combustion efficiency determined by ARI for the test point  $i$

$N$  = total number of test points in the subset

# DRAFT

The third criterion is data return. Data return is the percentage of the total number of possible test points for which data were reported. It is defined numerically as follows.

$$\text{data return} = \frac{\text{Number of test points for which data were reported}}{\text{Total number of test points}} \times 100 \quad \text{Eq. 8.3}$$

Tables D-1 and E-1 summarize data for all flare test results, including the IMACC and Telops CE and  $\sigma$ , by test series and run number. The CE values of ARI, IMACC and Telops for all steam flare tests have been graphed in Figure 8-1. These same data for all air flare tests are shown in Figure 8-2. As can be seen from these graphs, the scatter between values tends to increase significantly after about CE = 80%. Since the focus of this study is about DRE and CE above 90%, there is less importance in examining the performance of these remote sensing technologies much below CE = 90%. Therefore, the remainder of the comparison of these remote sensing technologies will focus on their performance in the range  $100\% \geq \text{CE} \leq 80\%$ .

To more easily compare IMACC's and Telops' data with ARI's, the CE data have been extracted from Tables D-1 and E-1 and sorted by ARI CE ( $\text{CE}_{\text{ARI}}$ ) value in descending order for the range  $100\% \geq \text{CE} \leq 80\%$  in Tables D-2 and E-2. On the assumption that the accuracy of the CE values may not be constant across this entire range, the data have been further divided as follows:  $\text{CE}_{\text{ARI}} \geq 95\%$ ;  $90 \geq \text{CE}_{\text{ARI}} < 95\%$ ;  $85\% \geq \text{CE}_{\text{ARI}} < 90\%$ ; and  $80\% \geq \text{CE}_{\text{ARI}} < 85\%$ . The difference between the IMACC's and Telops's CE values and the  $\text{CE}_{\text{ARI}}$  values are shown in each table. At the bottom of the column of the CE differences are the mean difference and the standard deviation of the CE differences are calculated as described in Equations 8-1 and 8-2. These two criteria are summarized in Table 8-1, where data return has also been calculated from the data in Tables D-2 and E-2.

## *Steam Flare Tests*

The CE data for the four ranges are graphed in Figures 8-3 to 8-6 in descending CE order. As shown in Table 8-1, the mean difference and the standard deviation of the CE differences for the IMACC AFTIR and PFTIR increase as the  $\text{CE}_{\text{ARI}}$  decreases. The mean difference and the standard deviation of the CE differences for the Telops CE values do not have a clear trend. In examining the differences in CE values in Table D-2, the IMACC AFTIR and PFTIR do not appear to have a bias relative to  $\text{CE}_{\text{ARI}}$ , while the Telops values tend to be biased lower than the  $\text{CE}_{\text{ARI}}$  values.

# DRAFT

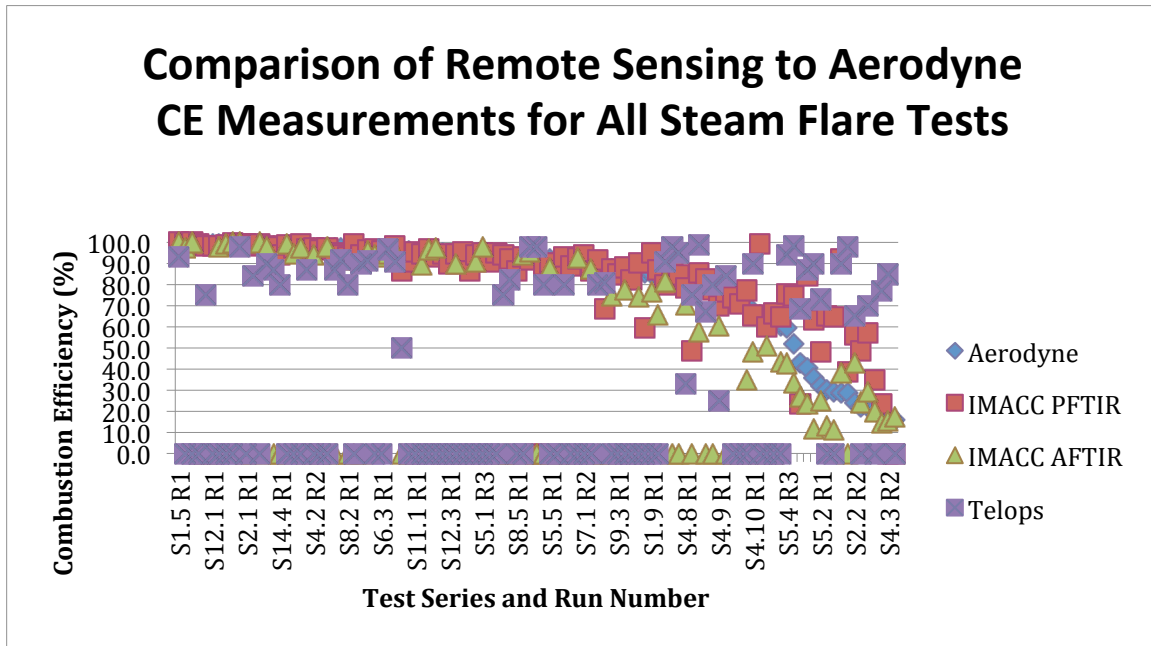


Figure 8-1. Comparison of All Remote Sensing Measurements Made to ARI Steam Flare CE Measurements

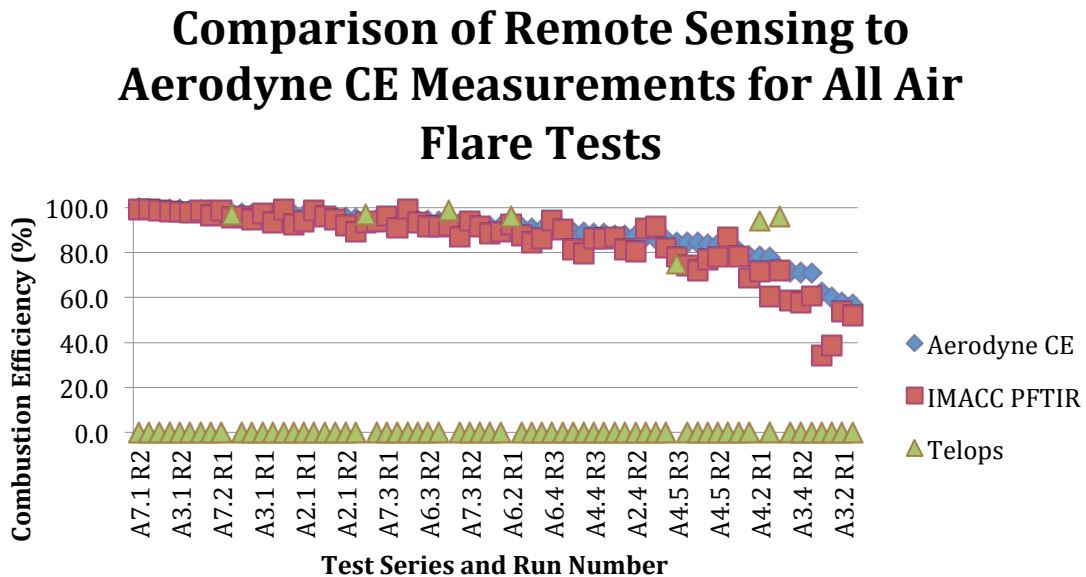


Figure 8-2. Comparison of All Remote Sensing Measurements Made to ARI Air Flare CE Measurements

# D R A F T

**Table 8-1. Summary of Comparison Criteria for Remote Sensing CE Values  
for CE<sub>ARI</sub> > 80%**

Steam					
Range	Criterion	Telops	AFTIR	PFTIR	ARI
CE <sub>ARI</sub> ≥ 95%	Mean Difference (% pts)	17.2	1.7	1.4	40
	Standard Deviation (% pts)	29.6	2.4	2.2	
	Data Return (%)	45	100	100	
	Number of Test points	17	23*	40	
90% ≤ CE <sub>ARI</sub> < 95%	Mean Difference (% pts)	22.5	3.3	2.2	22
	Standard Deviation (% pts)	86.0	4.0	3.1	
	Data Return (%)	32	100*	95	
	Number of Test points	7	8	21	
85% ≤ CE <sub>ARI</sub> < 90%	Mean Difference (% pts)	5.1	10.2	6.4	12
	Standard Deviation (% pts)	7.4	12.4	10.6	
	Data Return (%)	17	100*	100	
	Number of Test points	3	6	12	
80% ≤ CE <sub>ARI</sub> < 85%	Mean Difference (% pts)	17.1	14.8	6.9	8
	Standard Deviation (% pts)	23.8	19.4	13.3	
	Data Return (%)	88	100*	100	
	Number of Test points	7	4	8	
Air					
Range	Criterion	Telops	AFTIR	PFTIR	ARI
CE <sub>ARI</sub> ≥ 95%	Mean Difference (% pts)	0.4	-	1.8	22
	Standard Deviation (% pts)	0.4		2.5	
	Data Return (%)	5		100	
	Number of Test points	1		22	
90% ≤ CE <sub>ARI</sub> < 95%	Mean Difference (% pts)	4.0	-	2.7	20
	Standard Deviation (% pts)	5.1		3.3	
	Data Return (%)	15		100	
	Number of Test points	3		20	
85% ≤ CE <sub>ARI</sub> < 90%	Mean Difference (% pts)	NMR	-	4.8	10
	Standard Deviation (% pts)	NMR		5.7	
	Data Return (%)	0		100	
	Number of Test points	0		10	
80% ≤ CE <sub>ARI</sub> < 85%	Mean Difference (% pts)	9.7	-	7.1	7
	Standard Deviation (% pts)	9.7		8.3	
	Data Return (%)	14		100	
	Number of Test points	1		7	

NMR = No CE values were reported for these tests.

\*Instrument not on site to obtain measurements during some of these test points.

# D R A F T

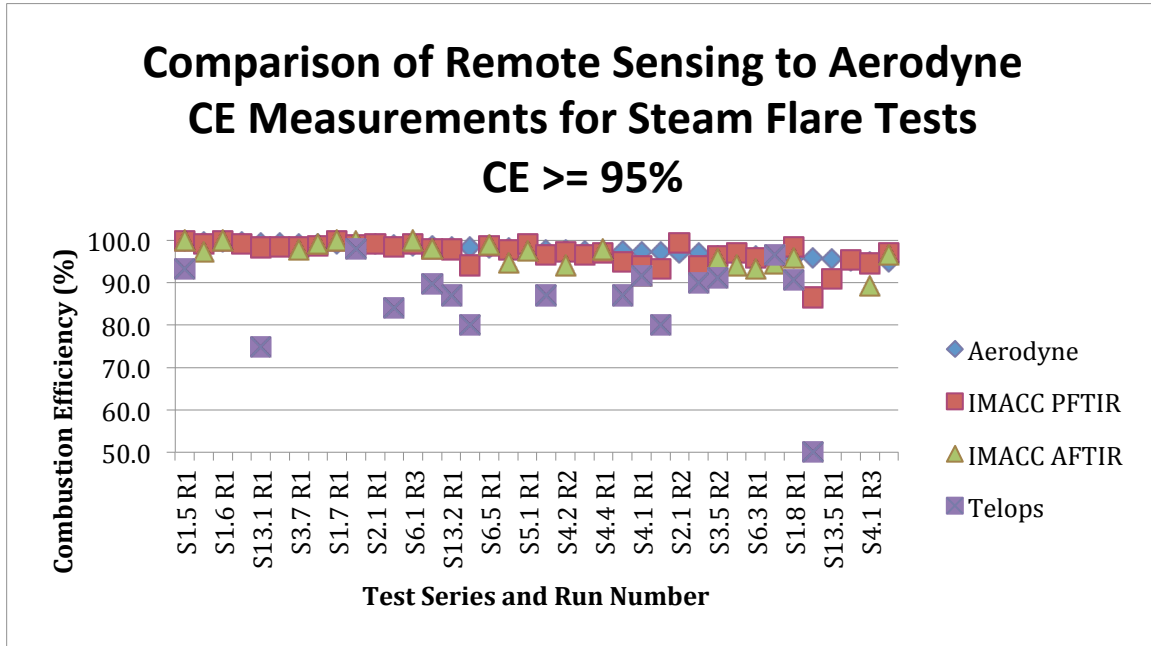


Figure 8-3. Comparison of All Remote Sensing Measurements Made to ARI Steam Flare CE Measurements  $\geq$  95%

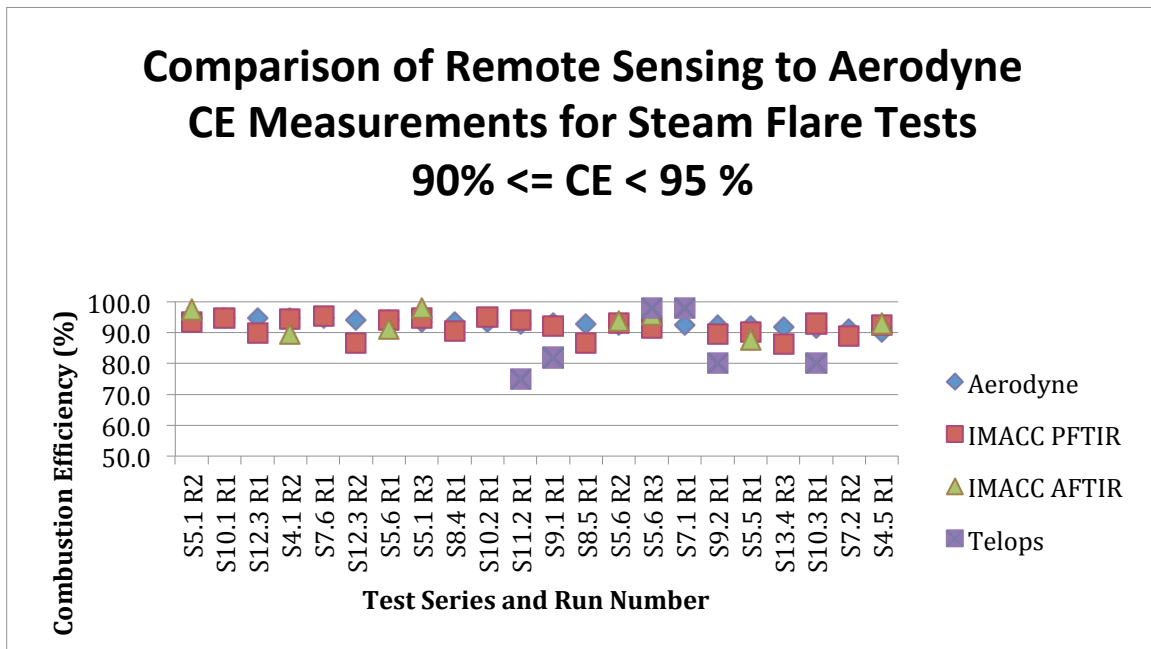


Figure 8-4. Comparison of All Remote Sensing Measurements Made to ARI Steam Flare CE Measurements  $90\% \leq CE_{ARI} < 95\%$

# DRAFT

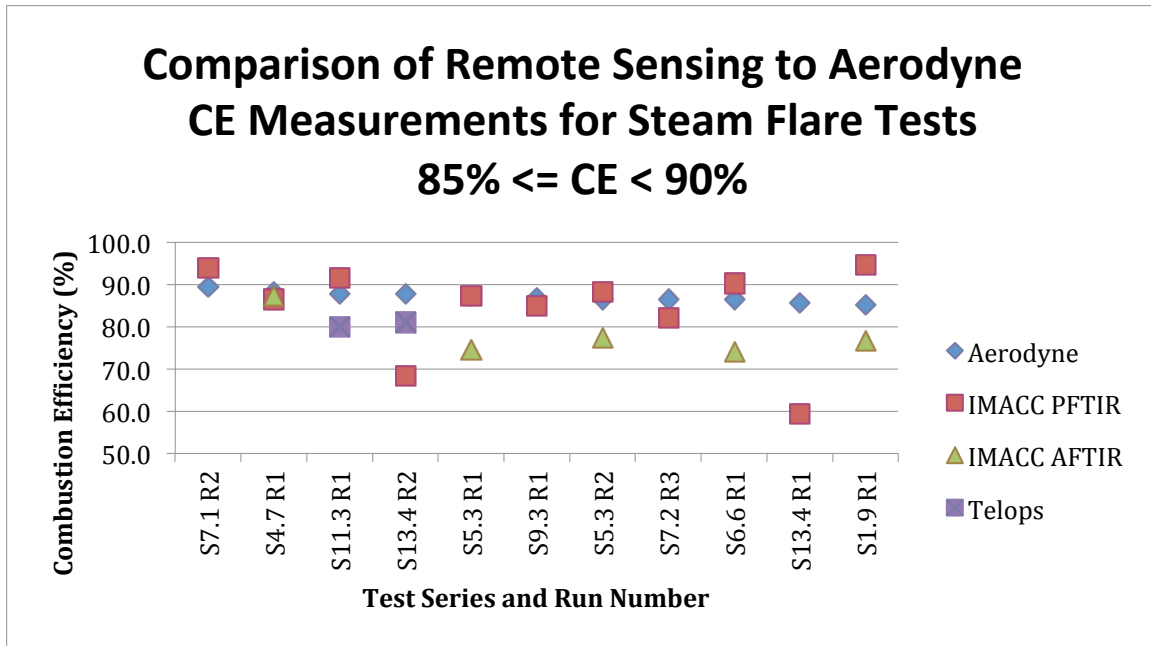


Figure 8-5. Comparison of All Remote Sensing Measurements Made to ARI Steam Flare CE Measurements  $85\% \leq CE_{ARI} < 90\%$

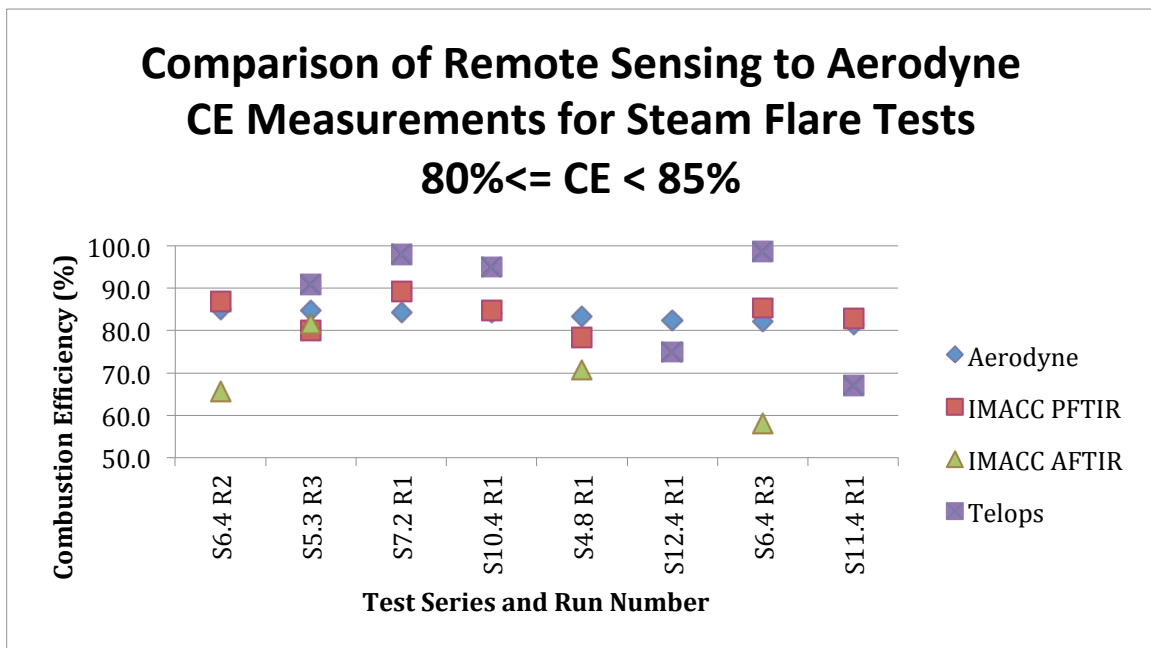


Figure 8-6. Comparison of All Remote Sensing Measurements Made to ARI Steam Flare CE Measurements  $80\% \leq CE_{ARI} < 85\%$

# DRAFT

In examining the data return in Table 10-1, the IMACC AFTIR was 100% in all four ranges, while the PFTIR was 100% in all ranges except  $90\% \leq CE_{ARI} < 95\%$ , where it was 95%. Data return for the Telops CE values was less than 45% for all ranges except  $80\% \leq CE_{ARI} < 85\%$ , where it was 88%.

## *Air Flare Tests*

The CE data for the four ranges are graphed in Figures 10-7 to 10-10. As shown in Table 10-1, the mean difference and the standard deviation of the CE differences for the IMACC PFTIR increase as the  $CE_{ARI}$  decreases. The IMACC AFTIR was not deployed for any of the air flare tests. In examining the CE differences in Table E-2, the data tend to be biased low relative to the  $CE_{ARI}$  values.

The number of Telops data points, five, for all four ranges of the air flare tests are too few to statistically develop trend data. Additionally, the data return for these four  $CE_{ARI}$  ranges did not exceed 15%. Therefore, no additional analyses will be performed on the Telops air flare data.

In summary, the IMACC PFTIR mean differences for the range  $CE_{ARI} \geq 90\%$  for both the air and steam flare tests averaged 2.0 percentage points, with an average standard deviation of the CE differences of 2.8 percentage points and average data return of 99%.

The IMACC AFTIR mean difference for the range  $CE_{ARI} \geq 90\%$  for the steam flare tests averaged 2.5 percentage points, with an average standard deviation of the CE differences of 3.2 percentage points and an average data return of 100%.

The Telops mean difference for the range  $CE_{ARI} \geq 90\%$  for the steam flare tests averaged 19.9 percentage points, with an average standard deviation of the CE differences of 57.8 percentage points and an average data return of 39%.

## *Data Processing*

All participants were required to submit their preliminary data within six weeks of completion of the field campaign. Telops was unable to do so. Their report explains some of the challenges they had in making measurements and processing the large volume of data generated by their sensor and the number of test points conducted in this study.

# DRAFT

## Comparison of Remote Sensing to Aerodyne CE Measurements for Air Flare Tests CE $\geq 95\%$

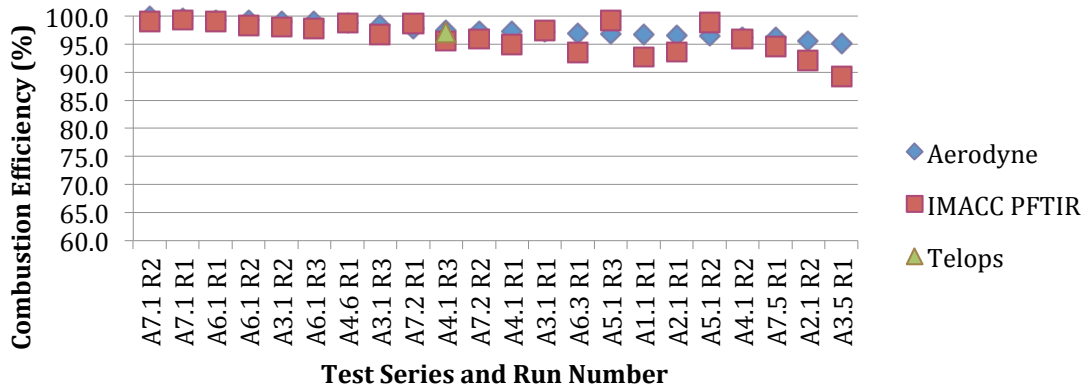


Figure 8-7. Comparison of All Remote Sensing Measurements Made to ARI Air Flare CE Measurements  $\geq 95\%$

## Comparison of Remote Sensing to Aerodyne CE Measurements for Air Flare Tests $90\% \leq CE < 95\%$

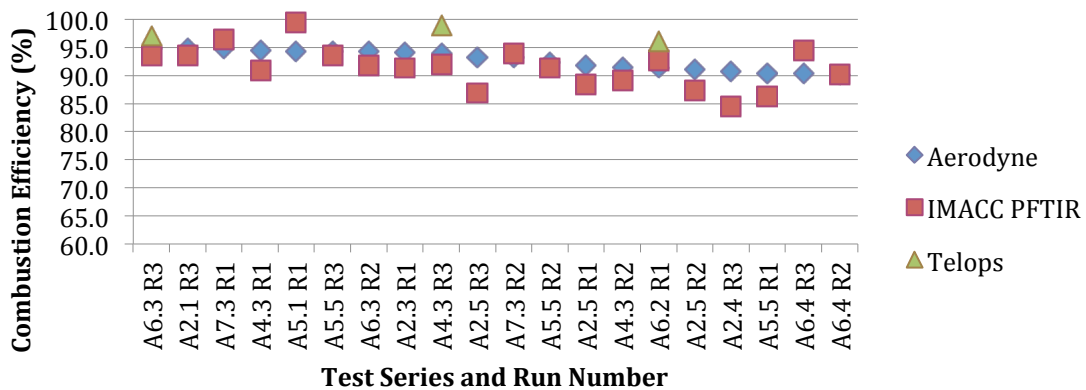


Figure 8-8. Comparison of All Remote Sensing Measurements Made to ARI Air Flare CE Measurements  $90\% \leq CE_{ARI} < 95\%$

# DRAFT

## Comparison of Remote Sensing to Aerodyne CE Measurements for Air Flare Tests 85% ≤ CE < 90%

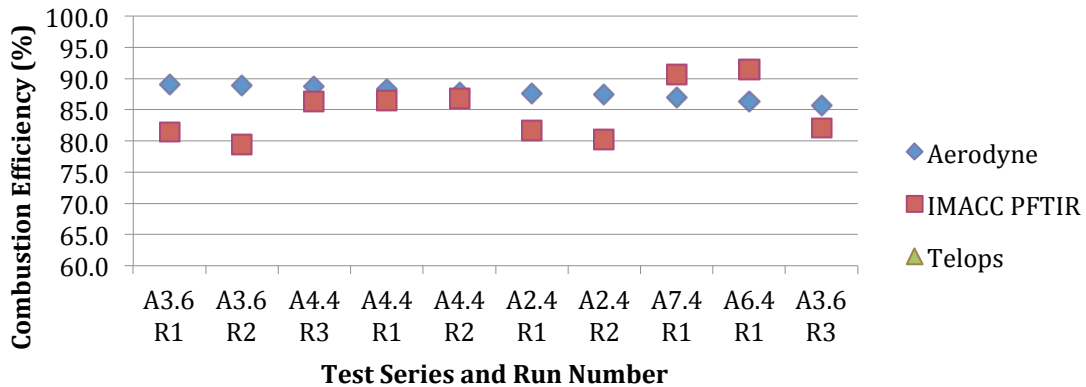


Figure 8-9. Comparison of All Remote Sensing Measurements Made to ARI Air Flare CE Measurements  $85\% \leq CE_{ARI} < 90\%$

## Comparison of Remote Sensing to Aerodyne CE Measurements for Air Flare Tests 80% ≤ CE < 85%

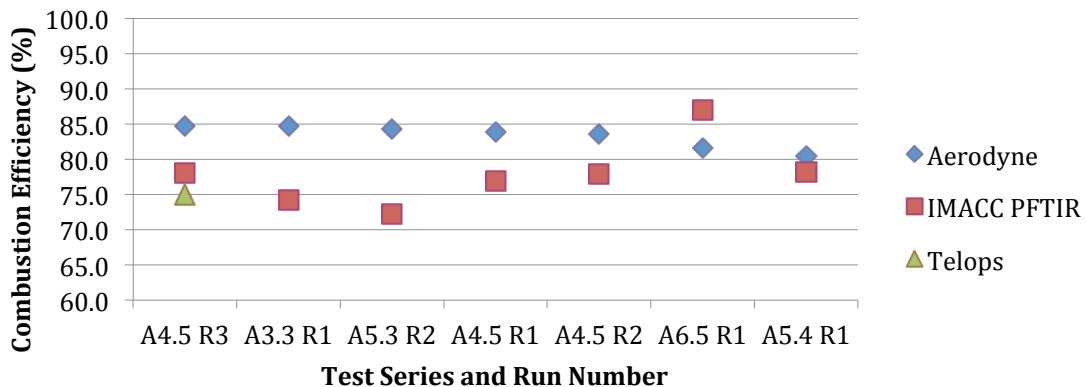


Figure 8-10. Comparison of All Remote Sensing Measurements Made to ARI Air Flare CE Measurements  $80\% \leq CE_{ARI} < 85\%$

# DRAFT

## 9.0 Comparison of Measured Emissions and Conventional Methods for Estimating Emissions

Conventional methods for calculating emission rates as prescribed by the TCEQ (Air Permit Division's *Technical Guidance for Flares and Vapor Oxidizers*, RG-109 Dated October 2000) and EPA's AP-42 (Table 13.5-1) assume a constant DRE for smokeless flares that are operated in compliance with 40 CFR § 60.18, i.e., greater than a minimum LHV of 300 Btu/scf and not in excess of the exit velocity criterion.

The tests in this study were conducted in compliance with all criteria of 40 CFR § 60.18. For propylene and propane, a DRE of 99% would be used to predict emissions for all the tests listed in Appendices D and E. As can be seen from the data, it was possible to achieve a 99% DRE for many conditions tested.

However, as can also be seen in the data, many operating conditions produced actual DREs of less than 99%. These operating conditions resulted in the production of propylene emissions multiple times greater than that that would be calculated using the above prescribed conventional estimation methods. Using the procedures from the TCEQ and EPA noted above, estimates of emissions for each test point were calculated and are tabulated along with the measured emissions in Appendix F, Tables F-4 and F-5. Although NO<sub>x</sub> was measured, it is not included in Tables F-4 and F-5. NO<sub>x</sub> was measured using a commercial chemiluminescence analyzer. This instrument did not meet the data quality objectives over all ranges of DRE observed.

A detailed explanation of the calculation procedure followed to estimate the emissions for each test point using the TCEQ and EPA methods is included in Appendix F. These methods consider only the vent gas constituents and flow rate used and assume a constant emission factor (for NO<sub>x</sub>, CO and THC emissions) or DRE (methane, ethane, and VOCs) in estimating the emissions. Consequently, for actual DREs less than those assumed, the estimates of emissions will be low. Also, the TCEQ conventional method for estimating speciated VOCs assumes the products of combustion to be the same in calculating the mass of emissions, i.e., 99% DRE for propylene results in 1% propylene emissions, when in reality the complex combustions process can result in propylene and other emissions. As an example, for the flare test conducted Table 6-1 lists the hydrocarbon species typically found during any of the propylene flare tests.

# DRAFT

Table 9-1. List of Hydrocarbons Typically Found in Plume During Propylene Flare Tests

Propylene  
Methane  
Formaldehyde  
Ethylene  
Acetaldehyde  
Acrolein  
Acetylene  
Ethane  
Propylene-oxide  
Methanol  
Acetone  
Propanol  
Butene isomers

Consequently, rather than attempting to examine emission results from every flare test, knowing that the conventional estimation procedure will provide the same results for many tests, a comparison of the emissions determined using the TCEQ and EPA estimation procedure with the measured emissions from steam and air flare tests with different DREs illustrates the different quantities and species of emissions

In Table 9-2, the emissions (lb/hr) for propylene, methane, total VOCs and THC's are tabularized by method along with the measured emissions for five steam and five air tests with DREs above 90%. As points of reference, the Test Point, Run Number and propylene flow rate (lb/hr) in the vent gas along with the DRE for the test point are also included with the estimates. The values in the table show that as the DRE decreases from 99.9% to 90%, the difference between the conventional estimate and the measured emissions increases. This is true for both the air and steam tests.

As an example, for test point S3.6R1, the conventional method estimated 1.89 lb/hr propylene and 1.89 lb/hr total VOCs, where the measured emissions were 0.13 lb/hr and 0.15 lb/hr, respectively. Measured emissions averaged only 7.4% of the amount estimated by the conventional method. At a DRE of 96.0% (S4.1R2), the conventional method estimated 4.84 lb/hr propylene and 4.85 lb/hr total VOCs, where the measured emissions were 19.21 lb/hr and 21.78 lb/hr, respectively. Measured emissions averaged 420% of the amount estimated by the conventional method. And finally at 90% DRE (S11.3R1), the conventional method estimated 2.97 lb/hr propylene and 2.98 lb/hr total VOCs where the measured emissions were 29.61 lb/hr and 32.46 lb/hr, respectively. Measured emissions averaged 1,043% of the amount estimated by the conventional method, more than 10 times the amount estimated. This trend is similar for the air flare.

# D R A F T

Table 9-2. Summary of Selected Emissions Estimated Using Conventional TCEQ and EPA Methods and Emissions Measured During the Flare Tests

Test Point	Run Number	Vent Gas Propylene lb/hr	TCEQ Conventional			EPA	Measured				ARI
			Propylene (99% DRE)	Methane (99% DRE)	Total VOCs	THC	Propylene	Methane	TVOC	THC	DRE
			lb/hr	lb/hr	lb/hr	lb/hr	lb/hr	lb/hr	lb/hr	lb/hr	lb/hr
S3.6	1	189.1	1.89	0.16	1.89	0.57	0.13	0.02	0.15	0.17	99.9
S8.1	1	509.9	5.10	0.45	5.11	1.55	9.92	1.31	11.25	12.66	98.1
S4.1	2	483.9	4.84	0.39	4.85	1.46	19.21	2.53	21.78	24.51	96.0
S5.6	2	312.2	3.12	0.28	3.13	0.95	18.43	2.43	20.20	22.82	94.1
S11.3	1	297.0	2.97	0.26	2.98	0.90	29.61	3.90	32.46	36.67	90.0
A6.1	1	117.8	1.18	0.10	1.18	0.36	0.34	0.05	0.41	0.46	99.7
A6.3	1	117.9	1.18	0.11	1.18	0.36	2.34	0.31	2.80	3.13	98.0
A4.3	3	297.7	2.98	0.27	2.98	0.91	12.23	1.61	13.88	15.61	95.9
A5.5	2	71.5	0.71	0.07	0.72	0.22	4.28	0.56	4.77	5.38	94.0
A6.4	1	118.1	1.18	0.11	1.18	0.36	10.84	1.43	12.09	13.63	90.8

The differences noted in the examples above are largely due to the difference in assumed DRE and the actual DRE. It is also important to note that the species included in the estimate of total VOCs for the conventional method is based on the components in the natural gas and not the actual products of combustion. Whereas Table 9-1 list the species actually measured during the actual flare tests. The actual VOCs produced are the result of the combustion chemistry and the flare operating conditions so an analysis attributing the VOCs to one or more of the constituents in the vent gas is beyond the scope of this project. It is simply important to note that if the specific VOCs that will be produced is important or the attribution of total VOCs produced to the vent gas components is desired, conventional estimation methods do not provide the information needed.

# DRAFT

## 10.0 Quality Assurance

Quality assurance for this study began with the development and approval of a Category 2 Quality Assurance Project Plan. This plan was followed during all phases of the testing from maintenance of certificates of conformance for gas standards and factory calibration of instruments, where appropriate, to initial calibration of instruments pre-test through daily calibration checks, most performed at least twice per day on critical measurement systems like the TRC and ARI instruments. An overview of the calibration activities and copies of the supporting documentation for field calibrations are included Appendix K by company.

### Data Quality Indicators

During a flare test, there were three parameters that provided indications of the quality of the data being collected. These four parameters were: the sample collector inlet gas temperature as measured by the three thermocouples at the inlet; the live video feed of the LSI visible, IR and two FLIR cameras used to position the collector and view the flare plume as it traveled to the sample collector; ratios of key combustion emission concentrations; and repeatability of results. Additionally, the degree of agreement in  $CE \geq 85\%$  between one of the remote sensing technology measurements and the extractive measurements made by ARI has provided further independent corroboration of the level of quality of the data from this study. Each will now be discussed.

#### *Average Sample Collector Inlet Temperature*

One of the most important criteria in obtaining a DRE and CE that reflects the all combustion that has occurred in the flare, is to ensure that emission measurements are made far enough downwind of the plume to ensure no further combustion is occurring in the plume. Since one product of combustion is heat, then an elevation of the plume temperature above the steam assist temperature would indicate some degree of combustion. Conversely, no or little combustion would result in a plume temperature at or below the steam assist temperature. So the anticipated steam temperature, approximately 250°F, was selected as an upper temperature limit for the collector inlet temperature. Indeed the steam temperatures ran in the range of 220°F to 300°F during the test series. On the lower end, the ambient temperature would be an indicator that the collector inlet could be outside the plume, i.e., any increase in temperature above ambient would certainly indicate thermal effects of the plume and therefore being in some portion of the plume exhaust.

But what if there was little or no steam assist as in the case of the air flare. Because the gauge used in the definition of the incipient smoke point involves distances two flame lengths from the flare tip, it was critical to always locate the sample collector inlet no closer in distance than this point in the plume. The first test point run was on the steam flare with all propylene. This was a “practice” test to allow all participants to acquaint their systems with the protocol to be used. It allowed us to fine tune positioning of the collector. This test showed that just past two flame lengths away, the average collector inlet temperature was in the range of 150°F to 170°F. If the collector were backed away to an average collector inlet temperature of about 105°F, the signal required by ARI to adequately measure emissions had not degraded sufficiently, i.e., greater dilution with ambient air, to adversely affect the accuracy of their measurement. So the

# DRAFT

temperature range of 105°F to 150°F was used for the steam-assisted flare tests as the average sample collector inlet temperature range where ARI measurements could be made that complied with the data quality objectives for their measurements of plume emissions needed to calculate DRE and CE. This assumed of course that that the collector was in a plume with a high level of combustion, i.e., strong thermal signal.

## *Four Way Video Camera Images*

In practice, it was learned that the flame could never be extinguished, i.e., snuff the flame, with the level of steam or air assist that Zink could provide. So the case of no combustion for the composition of the vent gas used never occurred in this test series. For the case of poor combustion or significant incomplete combustion, the UT Austin team depended on the two GasFind IR cameras, whose image of the plume actually improved with greater signal, i.e., when there were more unburned hydrocarbons in the plume.

Figure 10-1 is video image produced by LSI using the four cameras used during the field tests. The Sony visible light camera, aimed approximately perpendicular to the travel of the plume, produced the top left image. The GasFind IR-stationary camera, aimed looking approximately perpendicular to the travel of the plume, produced the bottom left image. The GasFind IR-mobile camera, aimed approximately coincident with the travel of the plume, produced the bottom right image. The thermal IR camera, aimed at approximately the same angle as the GasFind IR-stationary camera, produced the top right image. These four cameras were used to help find the plume when there was minimal flame or a plume that was invisible to the naked eye and to verify that the unburned products of combustion were traveling in the same path as the thermal products of combustion. The sample collector inlet would be positioned to intersect the largest portion of the plume. It was easy to line up the collector to intersect the plume if the wind direction was not changing rapidly. Fortunately for the study team, as can be seen in Appendix J, during the 7 to 10 minutes period of a test run, the wind direction did not change significantly, i.e.,  $\delta = X^\circ$ , during most of the test series. For those few runs where the wind direction was changing significantly, the collector would be repositioned frequently during the test to stay in the plume using the average collector inlet temperature, the real-time images of the four video cameras, and the ratios of concentrations of flare emissions in the plume measured by ARI. For these tests, longer run times were employed to obtain sufficient data to provide repeatable results.

# DRAFT



Figure 10-1. LSI Four-Way Video Images. LSI four-way video images were used to help position the sample collector. Top left, Sony visible light camera looking approximately perpendicular to plume travel; bottom left, GasFind IR-Stationary looking approximately perpendicular to plume travel; bottom right, GasFind IR-Mobile looking approximately coincident with plume travel; and thermal IR viewing at approximately the same angle as GasFind IR-Stationary.

### *Wind Speed and Direction Levels and Variation and Key Emission Concentration Ratios*

The duration of most test runs was in the range of 7 to 10 minutes, except as noted above when the wind was changing direction frequently during this period or if there was a request by TRC or ARI for additional time to their measurements. For most of the test runs, during these short periods of time, the wind direction changed on average  $X^\circ$ . The spatial impact of this change in wind direction is best examined with an example. If the collector were in line with the center of the plume and the wind direction changed  $5^\circ$ , at a distance of 20 ft from the flare, the centerline of the collector inlet would then be 1.8 ft from the line of travel of the plume in this new wind direction. With an effective draw of 2 ft in diameter, the centerline of the plume would be 0.8 ft from the edge of the effective draw of the collector. The collector would now be drawing from a section of the plume that was 0.8 ft from the center of the plume. As ARI was able to make measurements at a frequency of 1 Hz, they were able to monitor the change in emission measurements and key ratios as the direction of the wind changed. Key emission concentration ratios, e.g., propylene to carbon monoxide, methane to carbon monoxide, carbon dioxide to carbon monoxide, were an excellent indicator of the impact of the change in the relative position of the collector on the measurement of flare emissions. For a given test run and ambient wind conditions, these ratios should be a constant value representing the net result of the combustion reactions taking place in the flare combustion zone. If these ratios remain relatively constant as

# DRAFT

the wind direction changes, then representative measurements of the plume emissions are still occurring. If they all begin to change and there has been no change in the flare operating parameters, i.e., lower carbon dioxide to carbon monoxide ratio, and the ratios approach atmospheric ratios of these values, then the collector is not sufficiently in the plume and repositioning is needed. This approach was also employed if the wind direction were changing in a cyclic manner where repositioning of the collector would have been impractical. In this latter situation, the time period of the test run for collection of data would be extended until sufficient periods of data collection in the plume established repeatable emission concentration ratios representative of the combustion occurring for the test being conducted.

Similar to the case of the cyclic change in wind direction, small changes in wind speed were addressed in the same manner, i.e., the time period of the test run for collection of data would be extended until sufficient periods of data collection in the plume established repeatable emission concentration ratios representative of the combustion occurring for the test being conducted.

### *Repeatability of DRE and CE Results*

Another indicator to aid in evaluating the quality of the data is the repeatability of the data. Table 10-1 presents a summary the percent standard deviation of the DRE and CE for each test point where there were 3 repetitions of the flare test conditions and the average DRE for the three runs was greater than 60%. The percent (%) standard deviation is defined as follows:

$$\% \text{ Standard Deviation (DRE)} = \left( \frac{\text{Standard Deviation (DRE)}_{runs}}{\text{Average DRE}_{runs}} \right) \times 100 \quad \text{Eq. 10.1}$$

When calculating the % Standard Deviation (CE), then all terms on the right refer to CE values.

It can be seen from these data that the maximum % standard deviation (DRE) was 9.1% and in more than 73% of the cases it was less than 2%. This typically low % standard deviation indicates a high degree of repeatability in the test system and in the measurements providing greater confidence that the data are not random results.

### *Comparison with Independent Measurement of Remote Sensing Technology – IMACC PFTIR*

Not known during the field tests but upon analysis of measurements made by IMACC using their PFTIR spectrometer, in this study's range of greatest interest, i.e., CE ≥ 85%, these two independent measurement methods show very good agreement. As these measurements were made employing a single blind approach, this level of agreement provides additional independent confirmation of the study's data quality for the CE measurements.

Each of these five factors taken separately would not necessarily ensure a high degree of data quality. But taken together, they provide strong evidence to support the conclusion that the DRE and CE measurements made by the flare plume extractive sampling system are reliable data of high quality

# DRAFT

**Table 10-1. Repeatability of Test Results**

Test Series	ARI Extractive Sample Results			
	Average DRE	% Standard Deviation (DRE)	Average CE	% Standard Deviation (CE)
S2.1	99.2	0.8	98.6	1.4
S4.1	96.8	1.2	95.6	1.5
S4.2	98.7	0.4	98.2	0.5
S5.1	96.4	1.8	95.4	2.3
S5.3	88.9	1.3	86.2	1.8
S5.4	66.4	2.6	61.1	3.4
S5.6	94.5	0.8	93.0	0.9
S6.1	99.4	0.1	99.1	0.2
S6.3	97.5	0.1	96.2	0.1
S6.4	83.3	9.1	79.2	9.6
S7.2	87.9	4.0	87.4	4.0
A2.1	97.2	0.6	95.6	1.0
A2.4	93.0	1.6	88.6	2.1
A2.5	95.1	0.8	92.1	1.2
A3.1	98.9	0.8	98.2	1.0
A3.2	65.6	2.5	58.3	2.9
A3.4	76.8	0.4	71.3	0.4
A3.6	90.9	1.6	87.8	2.2
A4.1	97.9	0.5	96.9	0.7
A4.3	95.3	1.4	93.3	1.7
A4.4	91.3	0.5	88.2	0.5
A4.5	88.0	0.7	84.1	0.7
A5.1	96.4	1.5	95.9	1.4
A5.3	83.7	3.9	80.2	4.5
A5.5	93.9	1.7	92.3	2.2
A6.1	99.6	0.1	99.2	0.2
A6.3	97.1	0.8	95.3	1.5
A6.4	93.2	2.2	88.9	2.5

# DRAFT

## 11.0 Conclusions

1. At a vent gas LHV = 350 Btu/scf and flow rates of 0.1% and 0.25% of rated design capacity (propylene) for the John Zink Models EE-QSC-36" steam and LHTS-24/60 air flares, these flare models were able to achieve DREs (propylene) of > 99% and CE > 99%.
2. The most efficient operation, as measured by the DRE and CE, for the flare operating conditions tested, was achieved at or near the incipient smoke point. Higher efficiencies could have been achieved with steam or air assist slightly less than the ISP assist value but this condition, i.e., a smoking flare, would not have been in compliance with 40 CFR § 60.18.
3. At LHV = 350 Btu/scf and a nominal vent gas flow rate 937 lb/hr, the recommended steam assist rates of center = 500 lb/hr and upper = 750 lb/hr did not achieve a DRE (propylene) > 99%. At these conditions, a S/VG = 0.25 or less was required to achieve a DRE (propylene) > 99%, and the addition of only 100 lb/hr of center steam changed the DRE from 99.5% to 95.8%.
4. At these low vent gas flow rates (nominally 937 lb/hr and 2,342 lb/hr) and low LHVs (nominally 350 Btu/scf and 600 Btu/scf), the flare performance curve of DRE vs steam assist has a very short to non-existent "shelf" before the DRE falls off to less than 98%. Beyond this point, the DRE and CE decrease almost linearly as steam assist increases.
5. For nominal LHVs of 350 Btu/scf and 600 Btu/scf and vent gas flow rates of 359 lb/hr and 937lb/hr, air flare test data showed that an air-to-fuel ratio (lb/lb) of approximately 6.0 or less produced a DRE > 99%. Higher levels of air assist produced lower DREs in an almost linearly decreasing manner
6. Conventional emission estimation methods provide good estimates of emissions for DRE = 99%. However, flare performance was less than DRE (propylene) = 99% for many flare operating conditions tested during this study. For these operating conditions, conventional methods would have assumed DRE (propylene) = 99% and the actual emissions measured were greater than that estimated by the conventional methods.
7. The IMACC PFTIR and AFTIR mean differences between their values of CE and the ARI values of CE averaged 2.0 and 2.5 percentage points, respectively, and had average standard deviations of the CE differences of 2.8 and 3.2 percentage points in the range  $CE_{ARI} \geq 90\%$  for the air and steam flare tests. The PFTIR and AFTIR had average data returns of 99% and 100% in this range.
8. The Telops Hyper-Cam mean differences between their values of CE and the ARI values of CE averaged 19.9 percentage points, with an average standard deviation of the CE differences of 57.8 percentage points in the range  $CE_{ARI} \geq 90\%$ . The Telops Hyper-Cam had average data return of 39% in this range.

# DRAFT

## References

Baukal, Jr., Charles E. (2001). *The John Zink Combustion Handbook*, CRC Press, New York.

Environ International Corporation, (2009). *Control of HRVOC Emissions in Flares at Low Flow Conditions, Project 2009-53 (DRAFT Interim Report)*.

Green, Don W. and R. Perry, (2008). *Perry's Chemical Engineer's Handbook*, 8<sup>th</sup> Edition, McGraw-Hill, New York, 2008.

Ram A. Hashmonay, et al. Simultaneous Measurement of Vaporous and Aerosolized Threats by Active Open Path FTIR. <http://www.dtic.mil/cgi-bin/GetTRDoc?AD=ADA449529&Location=U2&doc=GetTRDoc.pdf> (accessed May 18, 2010).

Marathon Petroleum Company, LP, Detroit Refinery. Performance Test of a Steam-Assisted Elevated Flare with Passive FTIR – Detroit, Final Report. Detroit, Michigan, November 2010.

Marathon Petroleum Company, LLC, Texas Refining Division. Performance Test of a Steam-Assisted Elevated Flare with Passive FTIR, Final Report. Texas City, Texas, May, 2010.

National Physical Laboratory, *Measurement of VOC Emissions from Petrochemical Industry Sites in the Houston Area Using Differential Absorption Lidar (DIAL) During Summer 2007, Draft for Comment*. Texas Commission on Environmental Quality, February 2008.

Texas Commission on Environmental Quality, (2009). *Proposal for Grant Activities No. 582-8-86245-FY09-04, Comprehensive Flare Study, Tracking Number 2008-01, Amendments 1 & 3 (2010)*.

The University of Texas at Austin, (2010). *Quality Assurance Project Plan for Texas Commission on Environmental Quality Comprehensive Flare Study Project, PGA No. 582-8-862-45-FY09-04, Tracking No. 2008-81, Rev. 1*. The University of Texas at Austin, August 2010.

United States Government. *Code of Federal Regulations - Standards of Performance for New Stationary Sources, General Control Device and Work Practice Requirements, 40CFR § 60.18*. [http://edocket.access.gpo.gov/cfr\\_2009/julqtr/pdf/40cfr60.18](http://edocket.access.gpo.gov/cfr_2009/julqtr/pdf/40cfr60.18).

URS Corporation. *Passive FTIR Phase I Testing of Simulated and Controlled Flare Systems: Final Report*. Texas Commission on Environmental Quality, June 2004.